2014-08-26

Adsorption and Hydroprocessing of Water Soluble Asphaltenes

Manrique Porras, Luz Alejandra

UNIVERSITY OF CALGARY

Adsorption and Hydroprocessing of Water Soluble Asphaltenes

by

Luz Alejandra Manrique Porras

A THESIS

SUBMITTED TO THE FACULTY OF GRADUATE STUDIES

IN PARTIAL FULFILMENT OF THE REQUIREMENTS FOR THE

DEGREE OF MASTER OF SCIENCE

GRADUATE PROGRAM IN CHEMICAL AND PETROLEUM ENGINEERING

CALGARY, ALBERTA

AUGUST, 2014

ABSTRACT

Asphaltenes enriched heavy oil production is increasing worldwide, and consequently, an increase of these molecules is expected. The oil industry is challenged to explore new alternatives that allow converting asphaltenes into valuable products by economical feasible routes. The solubilization in water of asphaltenes has recently received attention due to the ease of mobilization and high level of dispersion of the resulting compounds. A first attempt to post-process this new water soluble material is here undertaken via selective adsorption followed by adsorbed molecules hydroprocessing. Different solids were screened at room temperature and batch conditions, and the asphaltenes uptake from water media was quantified. A packed bed reactor setup was built to investigate the adsorption of water soluble asphaltenes at various operating conditions, and subsequently, hydroprocessing tests were carried out using three NiMo catalysts supported on the adsorbent at 2 wt%, 5 wt% and 8 wt%. The 2% catalyst showed the highest selectivity towards liquid products, whereas the highest conversion was obtained in the 5% run. The last one yielded the lightest products, whereas the heaviest were obtained utilizing the 8% NiMo catalyst. From this research, a novel process implementing a battery of packed bed reactors could be proposed for development. This process could significantly improve distillate yields and liquid selectivity out of asphaltenes, which is an encouraging outcome of this thesis.

ACKNOWLEDGEMENTS

My sincere thanks to my supervisor, Dr. Pedro Pereira-Almao. This amazing journey is the result of his vision and his trust in me, and therefore I will always be indebted. Many thanks to NSERC/CNOOC-Nexen/AIEES, and the Chemical and Petroleum Engineering Department at the University of Calgary for the financial support.

My appreciation goes to all members of the Catalysis for Bitumen Upgrading group. In particular, thanks to Dr. Francisco López-Linares and Lante Carbognani-Ortega for their guidance and advise throughout this project. I would like to acknowledge Dr. Azfar Hassan, Dr. Gerardo Vitale, Dr. Héctor Guzmán, Dr. Carlos Scott, Dr. Monica Bartolini, Gustavo Trujillo and Jodi David for helping me in every stage of this research. Thanks to Dr. Josefina Pérez for sharing her knowledge and enduring the last months of my thesis without losing her sense of humor. My deepest appreciation and special gratitude are to David Gutiérrez, this project would not be possible without his experience, valuable feedback and constant support.

The personnel in the engineering stores are gratefully acknowledged: Larry Trudeau, Carl Houck, Gerald Downey, and Pat Walsh. Thanks to the Mandel technicians that constantly helped me with the analytical equipment, George Ruck, Derek Storrs and Andy Morrison.

Last but definitely not least, I wish to thank my backbone, my constant drive, my cheering team, my shoulder to cry on, my best friends. My family, without a doubt, this project is the result of your love, patience and encouragement to set and reach my goals. This is for and because of you.

TABLE OF CONTENTS

LIST OF TABLES

LIST OF FIGURES

LIST OF SYMBOLS, ABBREVIATIONS AND NOMENCLATURE

ATVR	Athabasca Vacuum Residue
BET	Brunauer-Emmet-Teller
BJH	Barret-Joyner-Halenda
BTEX	Benzene, Toluene, Ethylbenzene, Xylenes
CBU	Catalysis for Bitumen upgrading group
Cgas	Mass of carbon in the gas stream
Cinitial	Mass of carbon initially adsorbed on the catalyst
Cliquid	Mass of carbon in the liquid stream
C(t)	Total organic carbon concentration at time t
C/Co	Normalized total organic carbon concentration
D	Reactor diameter
Dp	Particle diameter
FTIR	Fourier Transform Infrared spectrophotometry
GAC	Granular Activated Carbon
GC	Gas Chromatography
H/C	Hydrogen-to-carbon atomic ratio
HCK	Hydrocracking
HDT	Hydrotreating
HTSD	High Temperature Simulated Distillation
IC	Inorganic Carbon
ICP	Inductively Coupled Plasma
L	Reactor length
MARS	Microwave Accelerated Reaction System
MCM-41	Mobil Composition of Matter 41
nC_5	n-pentane
nC_7	n-heptane

N/C	Nitrogen-to-carbon atomic ratio
O/C	Oxygen-to-carbon atomic ratio
OMM	Ordered Mesoporous Material
P	Pressure
PAC	Powder Activated Carbon
RFCC	Residue Fluid Catalytic Cracking
SARA	Saturates, Aromatics, Resins, Asphaltenes
SBA-15	Santa Barbara 15
SCCM	Standard cubic centimeters per minute
SOP	Standard Operating Procedure
std	Standard
t	Time
T	Temperature
TC	Total Carbon
TGA	Thermal Gravimetric Analysis
TNB	Temple-Northeastern-Birmingham
TOC	Total Organic Carbon
UV-vis	Ultraviolet visible
wt	Weight
WSA	Water Soluble Asphaltenes
X	Conversion
XRD	X-ray Diffraction
XPS	X-ray Photoelectron Spectroscopy
Y	Yield

1. INTRODUCTION

Asphaltenes, commonly referred to as “waste hydrocarbons”, are a solubility class defined as the most polar crude oil constituents insoluble in light paraffins and soluble in light aromatics (Nomura et al, 2005). When precipitated, these undesirable molecules cause many problems along the whole petroleum valorization process; they are responsible for well bore, equipment and pipeline plugging, as well as catalyst fouling and a tendency to coke formation (Nomura et al, 2005). However, asphaltenes could represent an opportunity if suitable processes are implemented to obtain valuable products by auxiliary treatments.

Nowadays, CNOOC-Nexen Northern Alberta facilities are facing a surplus production of asphaltenes (Carbognani, 2012). Heptane-precipitated asphaltenes constitute up to 12.5% of Canadian Athabasca bitumen and around 18% of Athabasca bitumen vacuum residue, according to SARA analysis results (Carbognani et al, 2010). If bitumen proved reserves in Alberta are approximately 1841 billion barrels, vast quantities of asphaltenes are anticipated within the province (Alberta Energy Resources Conservation Board, 2013). These numbers motivate to investigate economically feasible paths that yield profitable products utilizing bitumen’s most polar fractions.

For the past decades, different methods for extracting valuable products by processing asphaltenes have been studied. Catalytic steam gasification, hydrotreatment, cracking and adsorption of these heavy molecules and similar carbonaceous material, among other treatments, are some of the prospects that have been investigated (Heinemann et al, 1989; Pereira et al 1992; Byambajav et al, 2003; Ancheyta et al, 2005; Sosa et al, 2006; Nassar et al, 2011). An up-to-date industrial application is CNOOC-Nexen’s patented technology OrCrude^{TM} -Long Lake upgrader project-, where asphaltenes are removed prior to thermal cracking, and then gasified to produce synthetic gas (Alberta Energy Resources Conservation Board, 2013). A similar approach intended for refineries is the Texaco Gasification Process technology, an integrated gasification, hydroprocessing and power generation facility that converts asphaltenes to syngas, which can be transformed into hydrogen or fed to the integrated cogeneration facilities (Penrose et al, 1999).

Delayed coking is the preferred “bottom of the barrel” process installed in upgraders, in which the feedstock (usually vacuum residue, high in asphaltenes, resins, aromatics,

sulfur and metals content) is fed to the coker drums to produce lighter distillates -gases, gasoline and gas oils- and coke as by-product. However, unstable liquids and low value coke are obtained by means of current coking technologies (Speight, 2004); moreover, most oil sands coke recovered from the upgrading processes is stockpiled, and only a small amount is used to generate electricity (Alberta Energy Resources Conservation Board, 2013). These disadvantages encourage further studies in order to propose alternative treatments for bitumen heaviest fractions.

Then again, handling of solid-state asphaltenes has its own complications at many processing stages. One way to overcome these difficulties is to design an effective methodology to solubilize precipitated asphaltenes in water. Currently, the Catalysis for Bitumen Upgrading (CBU) group at the University of Calgary, is investigating asphaltenes oxidation as fundamental step to promote their solubilization in aqueous media. At present, this pioneering methodology is being under study to produce Water Solubilized Asphaltenes (WSA) under a wide range of conditions that, if proven successful, will provide mechanisms to facilitate asphaltenes manipulation.

This new procedure, combined with further processing of WSAs could provide visible economic advantages for dealing with waste hydrocarbons. In this work, a two stage process of adsorption and hydroprocessing of water soluble asphaltenes is studied aiming to provide better utilization of residual fractions and yield valuable light products. Hypothetically, by implementing an adsorption step prior to the hydroprocessing stage, light products could be obtained at less severe operating conditions compared with those in traditional hydroprocessing, while recovering the water used for solubilization of the asphaltenic compounds. The present study aims to prove this innovative concept by testing the selective adsorption of WSAs followed by hydroprocessing of the adsorbed material in a continuous setup.

This research is carried out in parallel with two PhD theses in the CBU group: one is intended to map optimal conditions for producing WSA, while the second one is focused in scanning direct hydroprocessing of WSA. These studies come together in the process scheme illustrated in Figure 1.1, in which the red box delimit the scope of this research and the yellow lines constitute other processing stages of the whole upgrading cycle.

The ultimate goal of the present study is to demonstrate the adsorption/hydroprocessing concept as an alternative route for heavy oil upgrading. The specific objectives of this work are:

1. To produce water soluble asphaltenes solutions to use as feedstock for adsorption and hydroprocessing experiments.

2. To select suitable materials to adsorb asphaltenes from aqueous streams and capable of holding catalytic active phases for hydroprocessing
3. To adsorb water solubilized asphaltenes on a selected surface in a packed bed reactor and test the effect of operating variables
4. To hydroprocess water soluble asphaltenes previously adsorbed on the surface of the material
5. To perform hydroprocessing reactions in continuous mode using different loads of catalyst

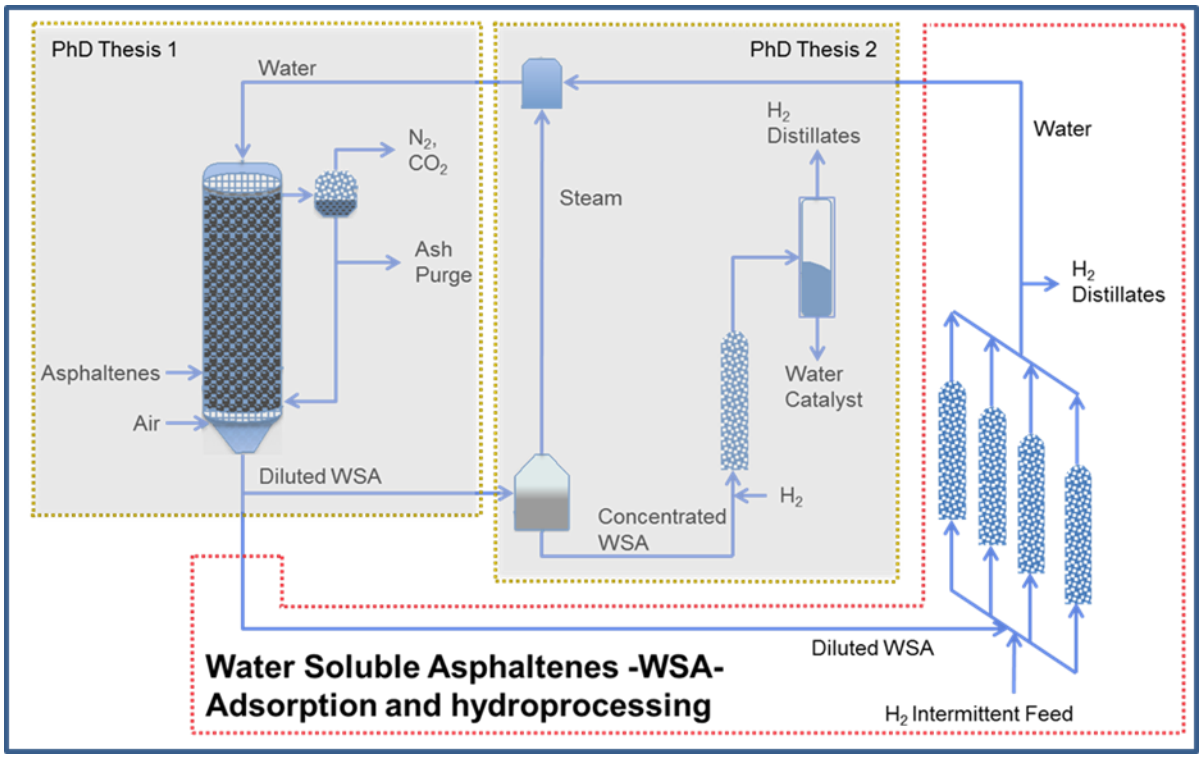

Figure 1.1. Water soluble asphaltenes processing cycle.

This document is divided in seven chapters addressing each one of the specific objectives (Figure 1.2). The first chapter explains the background, goals and main drive for this research. In the second chapter, pertinent terminology, fundamental concepts and relevant processes are examined. Chapter 3 contains a detailed description of the method to produce WSA and the effect of some variables on the final solution. In Chapter 4, methodology, tools and key parameters used for screening diverse adsorbents are described. Chapter 5 addresses the experimental procedure of adsorption in continuous mode, including experimental design, materials, pilot plant design, and evaluation of different operating conditions. The sixth chapter describes methodology, materials and results of hydroprocessing of pre-adsorbed WSA on Activated Carbon. Chapter 7 presents recommendations and global conclusions from

this work, and finally, appendices include catalysts characterization details, the standard operating procedure for the continuous setup and others.

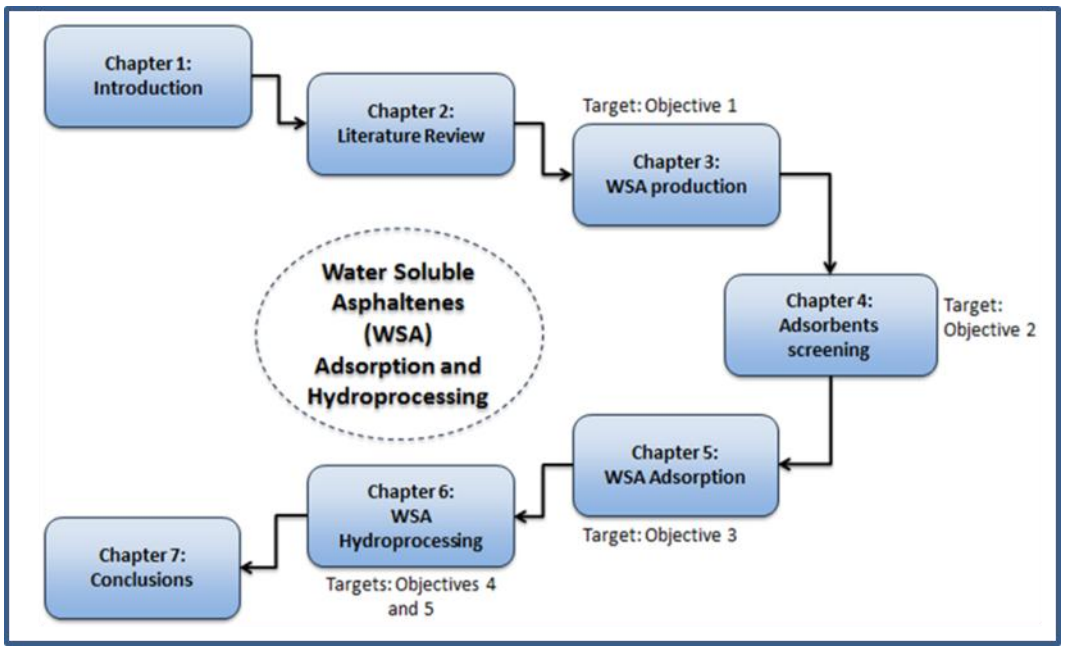

Figure 1.2. Structure of the Water Soluble Asphaltenes Adsorption and Hydroprocessing research thesis.

2. LITERATURE REVIEW

This chapter summarizes the most relevant aspects published in the open literature in relation to the research topic. First, discussions about asphaltenes and water soluble hydrocarbons are addressed. A brief humic substances chemistry review is made aiming to enrich posterior discussions within this document. Adsorption and adsorbent candidates are listed based on current practices in the waste water treatment industry. Concise remarks pertaining to heavy oil processing are described after which, hydroprocessing fundamentals are introduced. To finalize this section, catalysts, conditions and pertinent results from hydroprocessing studies with similar materials are explained.

2.1 Asphaltenes

Asphaltenes are polar crude oil components insoluble in light alkanes such as propane, n-pentane, iso-pentane and n-heptane. Conversely, they are soluble in liquids with a surface tension above 25 dyne/cm, such as pyridine, carbon disulfide, carbon tetra chloride and benzene (Speight, 2007).

This fraction has no definite melting point (Speight, 2007), and its molecular weight spans a wide range (Fahim et al, 2010), from 700 to 2,000 Daltons. Asphaltene structure contains fused aromatic rings bearing heteroatoms (O, N, S, Ni, V, Fe), linked to aliphatic chains with variable lengths (Nomura et al, 2005). Attempts to characterize asphaltenes in terms of chemical structure have been made, encountering differences depending on the origin of the crude oil and the method of extraction (Marczewski et al, 2002 and references therein). Figure 2.1 shows the asphaltene molecular structure proposed for Athabasca bitumen. Figure 2.2 shows asphaltene structures from a +510 Venezuelan residue in 2 and 3 dimensions. The 3D structure was drawn and optimized by Dr. Gerardo Vitale using Materials Studio Visualizer, and the minimization of the structure was done with DMol3, part of the Material Studio suite software.

Asphaltenes have a strong tendency to form aggregates, triggering precipitation inside the pores of rock formations, well heads and surface processing equipment (Fahim et al, 2010). These aromatic molecules inhibit catalyst activity, either by adsorption on its

active sites, by clogging the catalyst pores, or by promoting progressive deposition of coke on the catalyst surface.

To avoid these and other difficulties, a physical extraction process was implemented to separate asphaltenes from the oil to be converted. Solvent deasphalting is a physical carbon rejection process that typically uses three to ten volumes of solvent per volume of oil phase, and then the solvent is recovered under conditions that are as economical as possible (Le Page et al, 1992). Propane deasphalting process is a preferred practice in refineries while n-pentane and n-heptane are commonly used in laboratory scale (Ancheyta and Speight, 2007).

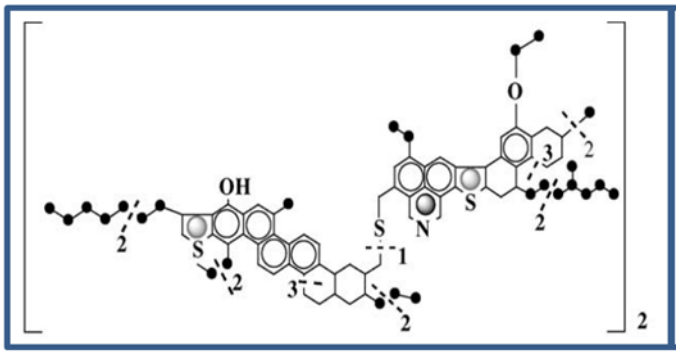

Figure 2.1 Hypothetical asphaltenes structure from Athabasca bitumen. (Suzuki et al, 1982)

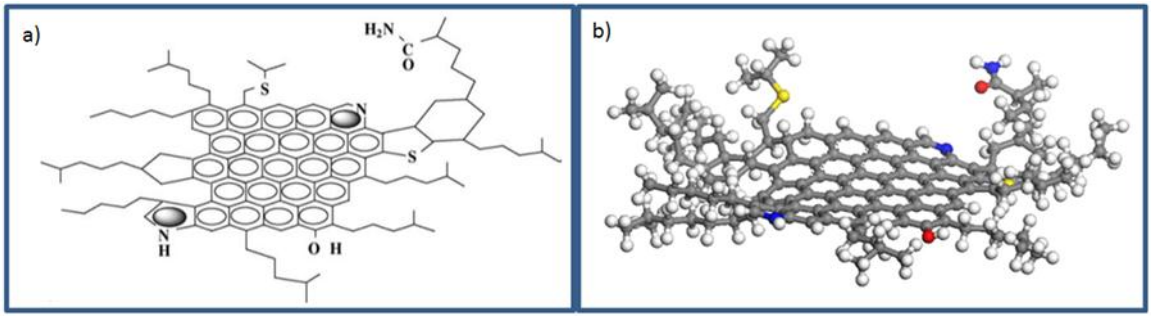

Figure 2.2. Hypothetical asphaltenes structure from Venezuelan crude oil proposed by Carbognani (1992): a) original 2D model, and b) Gerardo Vitale's optimized 3D model. Carbon atoms are represented in gray, nitrogen atoms in blue, sulfur atoms in yellow, oxygen atoms in red and hydrogen atoms in white.

It has been reported that quantity and composition of the precipitate changes with the solvent of choice. It is typical to indicate n-pentane (or nC_5) and n-heptane (or nC_7) asphaltenes in order to specify the precipitating medium. nC_7 asphaltenes have a lower hydrogen-to-carbon atomic ratio than the n-pentane precipitate; in other words, nC_7 asphaltenes have a higher degree of aromaticity. In the same way, nitrogen-to-carbon,

oxygen-to-carbon, and sulfur-to-carbon ratios are usually higher in the n-heptane precipitate (Speight, 2007).

2.2 Oxidation of asphaltenes and water soluble hydrocarbons

At present, the Catalysis for Bitumen Upgrading (CBU) group is developing a methodology to produce Water Soluble Asphaltenes via oxidation. Although WSA production is beyond the scope of this research, it is worth citing a few aspects since these constitute the feed for this project.

2.2.1 Catalytic and non-catalytic wet oxidation

Partial oxidation of heavy hydrocarbons has been widely studied in the past decades as a route to solubilize these materials into water. Severe oxidation leads to CO_2 production and water, whereas mild operating conditions (partial oxidation) result in highly oxygenated compounds, soluble in water. Both catalytic and non-catalytic processes have been used to oxidize asphaltenes, lignin, and coal, among others, using reagents such as air, oxygen, ozone, potassium permanganate, nitric acid, etc.. Catalytic oxidation studies using Thallium, Copper/Cobalt, Ruthenium and metal oxides have been previously published, as well as mechanistic features of this process (Carbognani, 2012 and references therein).

Two main stages of wet (in presence of water) oxidation have been identified: a physical stage followed by a chemical step. The first one involves transfer of oxygen from the gas phase to the liquid phase, where the only significant resistance is located at the gas/liquid interface. The chemical stage comprises reaction between the transferred oxygen and the organic compounds. Typical operating conditions for complete oxidation are 200°C-325°C, 725–2175 psi and 1 hour of residence time. High pressures are required to maintain reagents in liquid state and increase the concentration of dissolved oxygen in water (Debellefontaine et al, 1996).

2.2.2 Characterization of water soluble hydrocarbons

Researchers have made efforts to describe oxidized and water soluble hydrocarbons for many decades now. Filimonova et al (1976) studied the ozonolysis of asphaltenes, obtaining a product soluble in water, and a fraction soluble in acetone and alcohol but insoluble in benzene, aliphatic and chlorinated hydrocarbons. The water soluble portion was a mixture of carboxylic acids, scanned via Infrared –IR- Spectrophotometry; elemental analysis showed an increase in the H/C ratio, O/C and oxygen content compared to the initial asphaltenes. These trends in the water-soluble oxidized asphaltenes were also reported by Moschopedis (1971).

Curtis et al (1989) extracted nC_5-asphaltenes from oxidized asphalt at different levels of oxidation, and analyzed their adsorption behavior on silica, alumina, sandstone and limestone. They used infrared analysis as characterization technique to show the substantial increase in ketone and sulfoxide absorbances of oxidized n-C_5 asphaltenes. Similarly, formation of carboxyl and phenolic hydroxyl groups on water solubilized asphaltenes was tracked via IR spectrophotometry (Moschopedis, 1971).

Findings related to the size of water soluble hydrocarbons are worth pointing out. A patent assigned to Marathon Oil Canada Corporation claims that oxidized asphaltenes have an average molecular weight in the range from approximately 5% to 75% of the average molecular weight of the initial asphaltenes fraction (Duyvesteyn et al, 2010). In this process, catalytic oxidation performed at relatively mild temperature (25°C-95°C) and pressures near ambient, leads to breaking from around 2% to 50% of the aromatic rings in the original asphaltenes.

Hong (2006) patented an oxidation process of heavy hydrocarbons using ozone and supercritical fluids, and proposed a structure for asphaltenes, displayed in Figure 2.3. Associated products and reaction sequence were identified within his claims, utilizing ozone and a liquid solvent carrier such as CO_2, N_2O, NH_3, ethane, lower alkanes and combinations or mixtures at supercritical conditions.

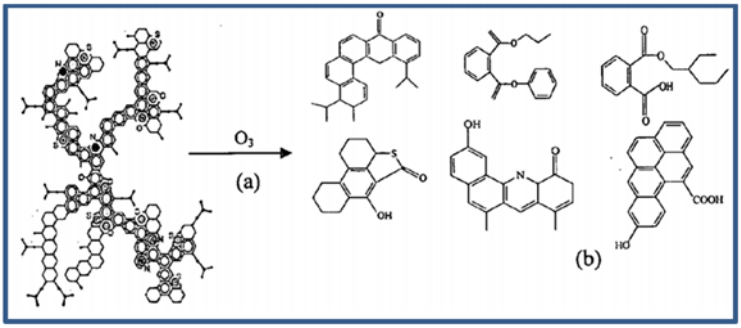

Figure 2.3. Asphaltenes and oxidation products from heavy hydrocarbons fragmentation upgrading process.
(Hong, 2006)

2.3 Humic acids

Humic acids remarkable resemble to WSAs obtained by wet air oxidation. Properties and characterization of humic matter are mentioned to provide a broader understanding of the chemistry and strategies used with these substances, which presumably are favorable to extend to the water soluble asphaltenes studies.

Humic substances, such as humic acids, fulvic acids and humin, are the largest component of soil and a sizeable part of the planet carbon pool (Humic Consortium for Carbon Sequestration, 2008). Based on their solubility in basic and acidic solutions, these substances are differentiated. Fulvic acids are the yellowish to brown fractions soluble in water; humic acids are the black fractions soluble in alkali that precipitate in acid, whereas humins are insoluble in alkali, acid and aqueous media (Tan, 2003).

Humic acids are the major fraction of humic substances, composed of carboxylic, phenolic, aliphatic, enolic-OH and carbonyl functional groups (Humic Consortium for Carbon Sequestration, 2008). These substances are prone to aggregate (Davies et al, 1997; Peña-Méndez, 2005), and have very high molecular weight ranging from several hundreds to thousands of daltons (Tan, 2003).

Despite origin, country or continent, the major elements in Humic Acids composition are carbon, hydrogen, oxygen, nitrogen and sulfur (Peña-Méndez, 2005). Humic acid elemental composition historical data was summarized by Tan (2003), displaying carbon contents of 53.8% to 58.7 wt%, hydrogen contents between 3.2% and 6.2 wt%, oxygen contents ranging from 33.6% to 43.5 wt% and nitrogen contents spanning from 1.2% to 5 wt%.

Computer modeling is the most recent tool to formulate the molecular structure for humic substances. As an example, Figure 2.4 displays the 3D structure of the lowest energy conformation for the Temple-Northeastern-Birmingham (TNB) Humic Acid building block $-C_{36}H_{30}N_2O_{15} \cdot xH_2O$-; conversely, Stevenson (1982) developed a humic acid 2D model structure, depicted in Figure 2.5.

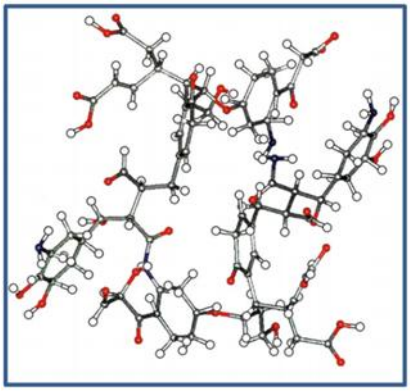

Figure 2.4. Temple-Northeastern-Birmingham (TNB) Humic Acid building block structure. Carbon atoms are represented in gray, nitrogen atoms in blue, oxygen atoms in red and hydrogen atoms in white (Davies et al, 1997).

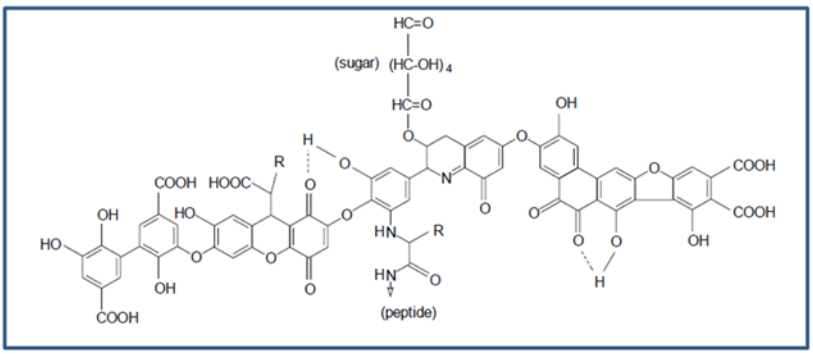

Figure 2.5. Model structure of humic acid.
R can be alkyl, aryl or aralkyl (Stevenson, 1982).

2.4 Adsorption fundamentals

Adsorption is the physical process by which a substance, originally soluble in one phase, is removed on a suitable interface by intermolecular forces of attraction, mainly Van der Waals forces (Fettig, 1999; Shon et al, 2006). Adsorption is one of the most popular water treatment processes and is known as an effective, efficient and economic method for water purification.

Adsorbent-adsorbate interactions are controlled by a number of factors in relation to the nature of the adsorbent, the nature of the adsorbate and the characteristics of the bulk solution. It is commonly accepted that high surface area and porosity are desirable characteristics of a good adsorbent (Shon et al, 2006; Zhang et al, 2012 and references therein). Similarly, mechanical strength proved to be vital when implementing adsorption fixed beds in industrial setups (Hansen and Davies, 1994). Other considerations for selecting appropriate adsorbents include their regeneration potential, adsorption capacity and cost (Rao et al, 2011).

In this perspective, research reports have demonstrated that pH, bulk ionic strength and the presence of specific divalent cations such as calcium, strongly affect the adsorption of humic matter from aqueous media (Fettig, 1999, and references therein). In particular, pH determines the adsorbent's preference for removal of neutral, negatively charged or positively charged species from aqueous solutions. Changes in solution pH led to presumable size and aromaticity changes of humic substances structure, meaningfully affecting their uptake from water streams (Fettig, 1999; Shon et al, 2006; Rao et al, 2011). In fact, some authors report that slightly acidic pH is favorable to deplete organic pollutants concentration from water streams by means of activated carbon adsorption (Grant and King, 1990; Choo and Kang, 2003).

2.5 Adsorbents in the waste water treatment industry

Water management is one of the challenges facing the oil sands mining industry, and adsorption is one of the treatment technologies applied to remove a wide array of pollutants associated with oilfield produced waters, most notably soluble organic carbon compounds, oil, grease and heavy metals. Solids used for this purpose include activated carbon, zeolites, clays, and synthetic polymers (Allen, 2008). Moreover, iron oxides were screened to test adsorption of highly aromatic moieties of residual organic material (Choo, 2003) and humic substances (Teerman and Jekel, 1999).

The following list comprises a number of currently available solids that, according to open literature, have proved successful in adsorbing organic compounds from aqueous streams. Among these materials, some were selected to be screened in the first part of this research, and their uptake performance will be described in the next chapters.

2.5.1 Activated carbon

Activated carbon has been by far, the most widely used adsorbent to remove a wide range of soluble hydrocarbons including BTEX (Benzene, Toluene, Ethylbenzene, Xylenes), some heavy metals, naphthenic acids, phenols, dyes, chlorinated hydrocarbons, and others (Hood, 1997; Allen, 2008). Its high surface area (from 500 to 1500 m^2/g), macroporous and microporous structure (average of 40% macropores, 20% mesopores and 40% micropores, depending on the raw material) and wide spectrum of surface functional groups, make this solid an effective adsorbent to clean pollutants from aqueous or gaseous media (Fettig, 1999; Rivera-Utrilla et al, 2011). Regeneration is often achieved by thermal methods, though chemical methods are also available. However, some authors have reported losses of substantial amounts of the carbon during each regeneration cycle, and reduction of the adsorption capacity in comparison with the virgin activated carbon (Hansen and Davies, 1994; Cooper and Burch, 1999; Gupta et al, 2009; Jiang and Ashekuzzaman, 2012); according to Grant and King (1990), phenolic compounds are specially difficult to remove and recover from activated carbons.

2.5.2 Zeolites

Zeolites (Figure 2.6) are a family of crystalline inorganic adsorbents which can be modified to provide hydrophobicity, affinity towards anionic species and BTEX, and other properties. Zeolites high cation exchange capacity is one of their most documented features (Choi et al, 2011). Clinoptilolite, a natural zeolite, has been studied for removal of BTEX compounds and metal-contaminated effluents with good results (Ouki and Kavannagh, 1997; Seifi et al, 2011). However, natural zeolites generally show

low surface areas, present pronounced microporosity and are naturally friable (Gupta et al, 2009; Hansen and Davies, 1994). Some zeolites are thermally stable up to 750°C, and others change in nature at 230°C-240°C (Güvenir, 2005 and references therein). An evaluation of natural zeolites adsorption qualities, concluded that zeolites having very high selectivity for a metal in a contaminated effluent, exhibit regeneration difficulties (Ouki and Kavannagh, 1997).

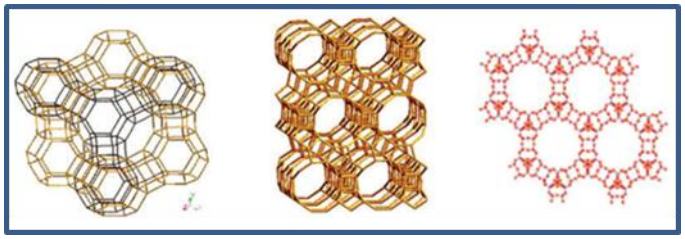

Figure 2.6. Examples of zeolite structures**:** a) Faujasite b) beta type and c) ITQ-33 type. (Aprile et al, 2008)

2.5.3 Clays

Clays, as zeolites, are modifiable structures by cation exchange. Hydrophobicity can be induced by replacing specific ions, enhancing their affinity to organic contaminants such as phenols. Surface modification of clays improves their intermolecular attraction towards both organic and inorganic contaminants, not without compromising its specific surface area (Jiang and Ashekuzzaman, 2012). A literature review of produced water treatment and hydrocarbon removal concludes that, at some extent, all organoclays adsorb organic compounds and some in potentially commercial quantities (Doyle and Brown, 2000). Their low cost and improved performance over conventional materials converts organoclays in emerging adsorbents being under study (Allen, 2008). In this context, bentonite (Figure 2.7) got the attention of many academics, yet kaolin, Fuller's Earth and other clays have also been topic of research on adsorption.

2.5.3.1 Bentonites and organobentonites

Organobentonites are synthesized to improve organic pollutant retention relative to conventional bentonite. Natural bentonite is an ineffective sorbent for non-ionic organic compounds in water (Shen, 2002). Yet, regeneration and ultimate disposal of spent organobentonites are limiting factors for their practical application. In addition, these organoclays are unlikely to endure high temperatures, and routine thermal reactivation methods probably destroy the sorbent. While bentonite degrades considerably around 500°C, major losses for organobentonites were seen between 200°C to 400°C (Zhu et al, 2005). In contrast, organobentonites exhibit an advantage when it comes to surface

area. A report made by Zhu, Tian and Shi (2005) states that modified bentonites have BET areas slightly above 500 m^2/g, in contrast to the virgin clay, with a measured area of 61 m^2/g.

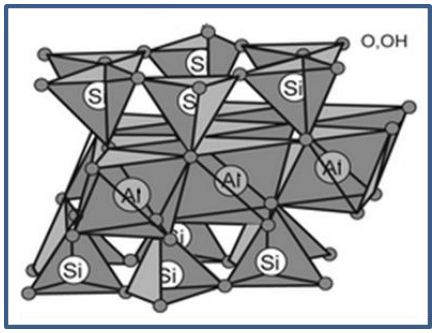

Figure 2.7. Diagrammatic illustration of the structural cell of montmorillonite, main component of bentonite.
(Adapted from Kindpac, 2012)

2.5.3.2 Fuller's Earth

Fuller's earth annual production in the United States was estimated to be 2.0 Mton in 2012, with 75% of it destined for adsorption processes (United States Geological Survey, 2013). Batch experiments were carried out for astrazon blue removal using this clay, displaying fast adsorption rates (within 1 hour), and uptakes as high as 1200 mg dye/g (Mckay et al, 1985). Fuller's earth was used as catalyst for conversion of lignite to gasoline back in 1929 by Eugene Houdry, testing its thermal stability at catalytic cracking temperatures of around 500°C (Sadeghbeigi, 2012).

2.5.4 MCM-41

MCM-41 (Figure 2.8), an inorganic mesoporous material developed by scientists at the Mobil Oil Corporation, offers structural and chemical characteristics such as narrow pore size distribution, mechanical stability, large pore volume and other attractive features for adsorption separation technologies (Serna-Guerrero, 2007). This material has reported areas between 900 and 1100 m^2/g, and its pore size can be tailored to target specific applications. It is considered an adsorbent with potential for the removal of organic pollutants from aqueous solutions, as found by Cooper and Burch (1999), who reported a large uptake (over 150 mg/g) of p-chlorophenol and cyanuric acid. Another study corroborates MCM-41 high adsorption capacity of volatile organic compounds (aromatic and chlorinated hydrocarbons) (X. S. Zhao et al, 1998; Serna-Guerrero, 2007).

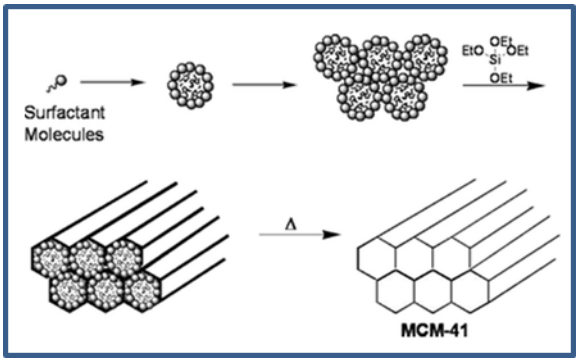

Figure 2.8. General formation mechanism of MCM-41.
(Aprile et al, 2008)

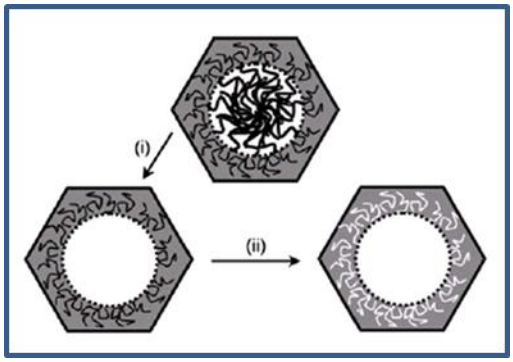

Figure 2.9. General formation mechanism of SBA-15.
a) With surfactant (top), b) after extraction of surfactants (left) and after calcination (right) (Zhang, 2008).

2.5.5 SBA-15

Santa Barbara 15, or SBA-15, was synthetized for the first time in 1998; the mesostructured silica displayed wider pores than MCM-41, higher pore volume and high hydrothermal stability (D. Zhao et al, 1998). As MCM-41, this mesoporous adsorbent is functionalized to enhance its adsorption capacity of phenol containing materials. Silanol and amino groups proved effective for the adsorption of organic compounds (Toufaily et al, 2013). Introduction of organic functional groups on SBA-15 demonstrated that cooperative effects lead to better adsorption performance of organic pollutants in water (Zhang et al, 2011; Koubaissy et al, 2011). Its generalized synthesis path is shown in Figure 2.9.

2.6 Heavy oil upgrading

The conventional approach for heavy oil and bitumen upgrading consists of implementing conventional refining processes to transform bottom of the barrel fractions, i.e. carbon rejection processes, thermal conversion processes and catalytic processes. This section is intended to provide a general idea of these technologies aiming to familiarize the reader with hydroprocessing concepts.

2.6.1 Carbon rejection processes

Carbon rejection results from a physical process of the extraction type or a chemical thermal cracking process. In both cases, technologies were designed to eliminate the most polar and highest molecular weight resin and asphaltenic compounds from the oil to be refined or converted (Le Page et al, 1992). As mentioned in previous sections, solvent deasphalting is a physical carbon rejection process whereas coking belongs to the second category.

Coking processes yield light components lower in sulfur, and principally coke, either formed from condensation of polynuclear aromatics, through condensation of olefins and butadiene with aromatics, or by many other reactions. Delayed coking, fluid coking and flexicoking are technologies in which moderate and severe temperatures are required; thereby, thermal cracking reactions are the core mechanism for upgrading heavy fractions. Typical delayed coking operations are 482°C-516°C at 90 psi, resulting in approximate coke yields of 30 wt% (Hsu and Robinson, 2006). Fluid coking and flexicoking need lower pressures (10 psi for temperatures ranging from 482°C to 566°C), produce higher yields of light ends and lesser coke formation. In fluid coking and flexicoking, reactions take place in fluidized beds with steam; on the contrary, delayed coking occurs in continuously cyclic-operated coke drums (Fahim et al, 2010).

2.6.2 Thermal conversion processes

Visbreaking was conceived to target reduction of the viscosity of vacuum residues by mild thermal cracking without carbon rejection. In this thermal conversion process, common operating conditions are 471°C-493°C at 50-200 psi, and there are two configurations available: heated coil or soaking drum. In the first case, high temperatures and short reaction times (from one to three minutes) are needed, while the soaking drum utilizes longer reaction times but lower furnace outlet temperatures. Although product yields and properties are similar, the soaker operation is preferred due to lower energy consumption (Gary and Handwerk, 2001).

Gasification is classified within the thermal conversion processes category. Gasification consists of the conversion of any carbonaceous fuel to a gaseous product with a usable heating value, in particular by means of partial oxidation (Higman and van der Burgt, 2008). Normally, synthetic gas is generated at temperatures above 1000°C in presence of pure oxygen, air and/or steam. Texaco Gasification Power Systems (TGPS) is a technology that converts coal, petcoke, vacuum residue and asphaltenes into syngas, power and steam in any combination. Integrated with hydroprocessing and power generation facilities, the company ensures an economical alternative to heavy oil processing for both refinery and oil field applications (Penrose et al, 1999). However, gasification of coal material has shown un-controlled selectivity; despite its low SOx and NOx emissions, this process has received comparatively less attention than other upgrading processes (Rana et al, 2007). At present, a combination of visbreaking and asphaltenes gasification is used at CNOOC-Nexen Long Lake upgrader facilities to avoid coke production and natural gas usage.

2.7 Catalytic Hydroprocessing

As mentioned before, hydroprocessing is a catalytic upgrading process designed to convert petroleum and nonpetroleum feeds to commercial fuels (Furimsky, 2013). Hydroprocessing is a term used to denote Hydrotreating (HDT) and Hydrocracking (HCK) together - coupled to reduce the boiling range of the feedstock as well as to remove substantial amounts of impurities such as metals, sulfur, nitrogen, and high carbon forming compounds (Gary and Handwerk, 2001; Hsu and Robinson, 2006). These reactions can be carried out in different types of catalytic reactors, require hydrogen and active catalysts, and usually yield more liquid fractions than thermal processes (Furimsky, 2007).

Residue hydrotreating and hydrocracking demand hydrogen partial pressures of 2000–3000 psig; as a general rule, the heavier the feedstock, the more severe conditions are needed. In hydrotreating, residue conversion varies between 5% and 15%, whereas 15% to 25% residue conversion is achieved by hydrocracking (Hsu and Robinson, 2006). Temperatures in the range 360°C-425°C and residence times of 2-4 hours are typical for these processes (Speight, 2004). An old patent claimed hydroprocessing of carbonaceous feedstocks containing up to 90 wt% in asphaltenes, under a wide range of conditions: 315°C-454°C, pressures from 500 to 5000 psi, hydrogen flow rates of 2000 to 20000 standard cubic feet per barrel of feed, and a slurry hourly space velocity in the range of 0.1 to 10 $hours^{-1}$ (Kuehler, 1983).

In the following sections, key parameters will be discussed in detail, including reactions, catalysts, type of reactors and results from previous works on hydroprocessing of oxygenated feeds. Though hydrotreating and hydrocracking reactions are in separate sections for organizational purposes, it is worth mentioning that at one extent or another, all the chemical reactions explained in the following sections occur in hydrotreaters and hydrocrackers (Hsu and Robinson, 2006).

2.7.1 Hydrotreating Fundamentals

The main goals in Hydrotreating (HDT) consist of: a) removing impurities (sulfur, nitrogen, oxygen, metals) and b) saturating olefins and their unstable compounds. High pressures and high flow rates of hydrogen are preferred, due to the fact that these conditions reduce coke formation and enhance removal of sulfur and nitrogen compounds. As well, high space velocities are chosen to maintain low coke formation, low conversion and low hydrogen consumption. In contrast, excessive temperatures will lead to thermal cracking and are usually avoided in HDT (Fahim et al, 2010). Operating conditions for residua are summarized in Table 2.1.

Table 2.1. Process parameters for residua hydrotreating.
(Adapted from Fahim et al, 2010)

Operating Temperature	360 – 380 ^{o}C
Hydrogen pressure	1700 – 2300 psi
Hydrogen consumption	1.5 – 2.0 wt%
Liquid Hourly Space Velocity –LHSV-	0.15 – 0.3 h^{-1}
H_2 / Hydrocarbon ratio	12 – 24 std m^3 / m^3

2.7.1.1 HDT Reactions

The highly exothermic HDT process includes hydrodesulfurization, hydrodenitrogenation, hydrodemetallization and hydrodeoxygenation reactions. Likewise, isomerization and saturation of aromatics and olefins are present in HDT. Minimal carbon carbon bond breaking reactions, summarized by Hsu and Robinson (2006), are displayed in Table 2.2.

Hydrodesulfurization is one of the most important reactions in hydroprocessing, where removal of sulfur is targeted and H_2S is produced. Sulfur compounds in residue are mainly sulfide and thiophenic compounds, the last one being decomposed only by catalytic means (Morel and Peries, 2001). Hydrodesulfurization of dibenzothiophene has been widely investigated in the past, and results showed that this reaction occurs via

two major pathways, direct hydrodesulfurization (Figure 2.10) and indirect hydrodesulfurization (Figure 2.11).

Table 2.2. Hydrotreating reactions and enthalpies.
Conventions are: R for alkyl, M for metal, A for metals-adsorbing material (Hsu and Robinson, 2006).

Reaction type	Illustration	Reaction Enthalpy (KJ/m^3 H_2 consumed)
Hydrodesulfurization	$R\text{-}S\text{-}R' + 2H_2 \Rightarrow RH + R'H + H_2S$	-2.5 to -3.0
Hydrodenitrogenation	$R{=}N\text{-}R' + 3H_2 \Rightarrow RH + R'H + NH_3$	-2.5 to -3.0
Hydrodeoxygenation	$R\text{-}O\text{-}R' + {}^5/_2H_2 \Rightarrow RH + R'H + H_2O$	-2.5 to -3.0
Hydrodemetallization	$R\text{-}M + {}^1/_2H_2 + A \Rightarrow RH + M\text{-}A$	-3.0
Saturation of aromatics	$C_{10}H_8 + 2H_2 \Rightarrow C_{10}H_{12}$	-3.0
Saturation of olefins	$R{=}R' + H_2 \Rightarrow HR\text{-}R'H$	-5.5

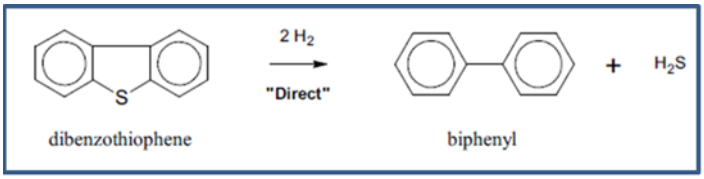

Figure 2.10. Direct hydrodesulfurization pathway of dibenzothiophene.
(Hsu and Robinson, 2006)

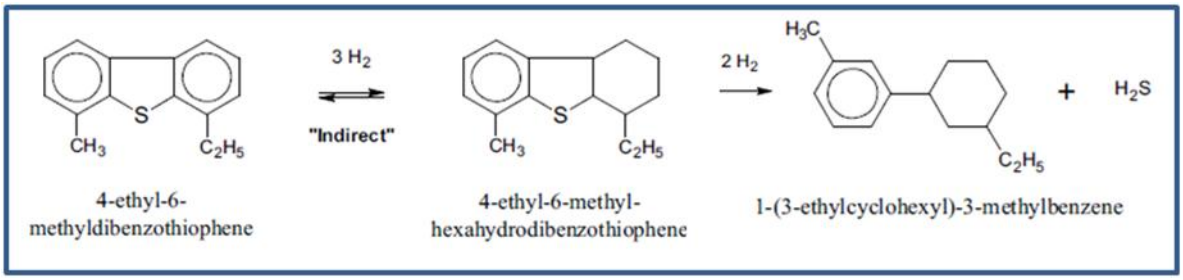

Figure 2.11. Mechanism for hydrodesulfurization of a hindered dibenzothiophene.
(Hsu and Robinson, 2006)

Hydrodenitrogenation is considered to be more demanding than hydrodesulfurization. Removal of nitrogen in heavy petroleum fractions is quite complex because most of the nitrogen is present in heterocyclic compounds (mainly five or six member rings, nearly all unsaturated). Nitrogen is removed after the ring containing this atom is hydrogenated and then, hydrogenolysis of the carbon-nitrogen bond occurs producing ammonia (Ancheyta and Speight, 2007). Quinoline has been frequently used to study the

kinetics of hydrodenitrogenation, and one of the proposed mechanisms illustrating this process is illustrated in Figure 2.12.

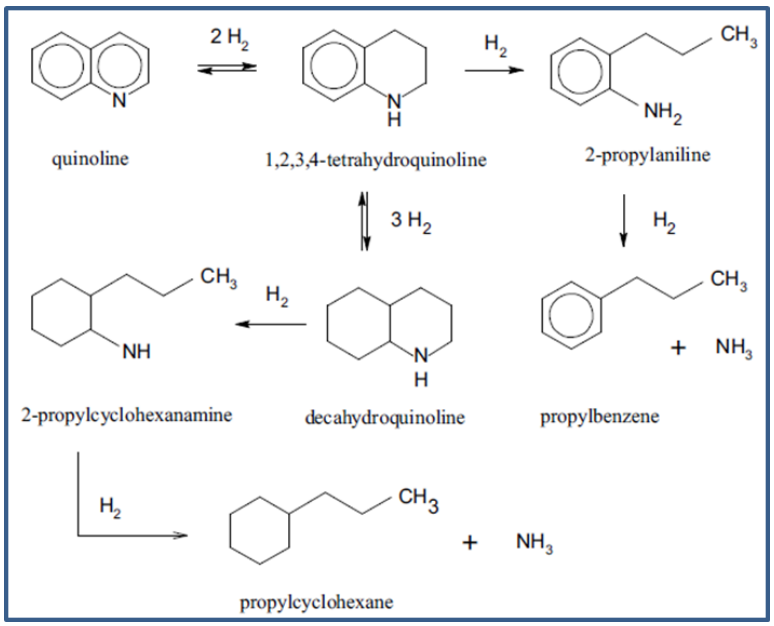

Figure 2.12. Hydrodenitrogenation of quinoline.
(Hsu and Robinson, 2006)

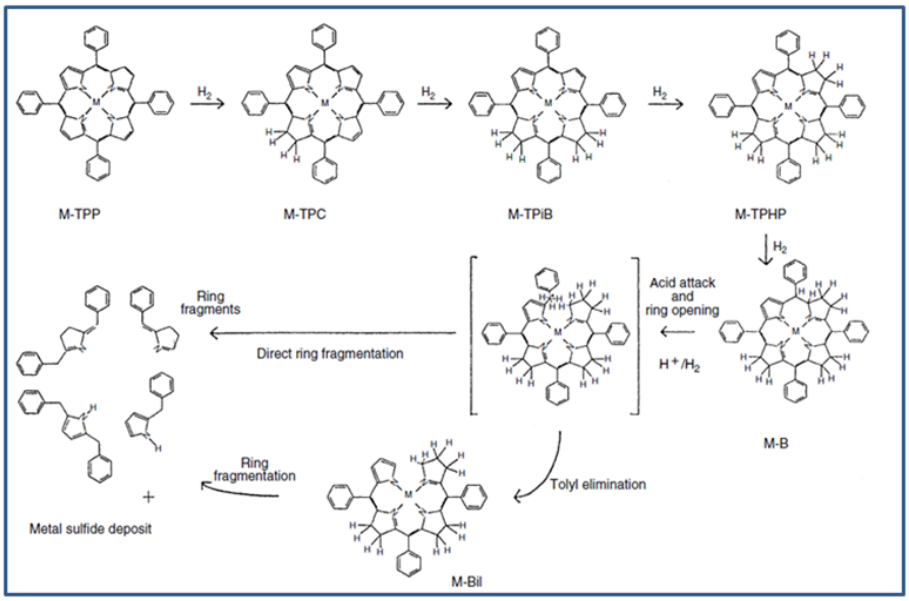

Figure 2.13. Hydrodemetallization mechanism of metallo-porphyrins.
M stands for Ni or V (Janssen et al, 1996).

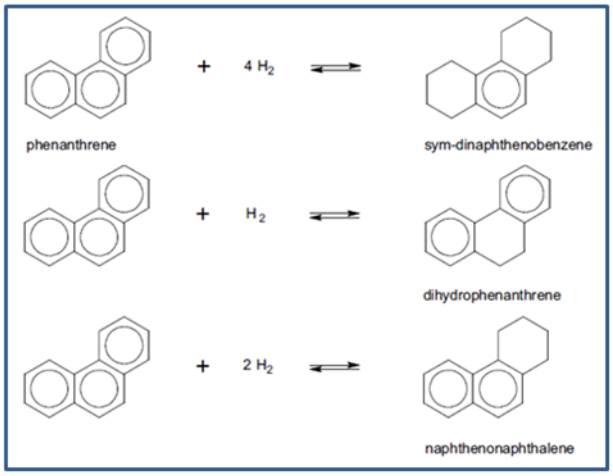

Figure 2.14. Hydrogenation of phenanthrene.
(Hsu and Robinson, 2006)

Hydrodemetallization aims to eliminate metals from petroleum crudes, in particular Ni and V because they are predominant in heavy oils and bitumen derived from tar sands. These substances are mainly present in porphyrin type structures; their removal involves hydrogenation of the organic compound to reduce the stability of the organo-metallic complex, followed by a cleavage of a metal-N bond (Ancheyta et al, 2005). Figure 2.13 displays the complete reaction mechanism for hydrodemetallization of metallo-porphyrines.

Saturation of aromatics is a reversible path favored by high hydrogen partial pressures and low operating temperatures: maximum aromatic reduction is observed between 370^{o}C and 400 ^{o}C (Gary and Handwerk, 2001). Breaking of the C=N bonds in the aromatic nuclei and heterocycles becomes a crucial step for other HDT reactions. In most cases, saturation of aromatics stage governs the overall conversion rate in HDT process (Le Page et al, 1992). Figure 2.14 exemplifies the mechanism of saturation of phenanthrene.

2.7.2 Hydrocracking Fundamentals

Hydrocracking –HCK- is classified as a flexible, destructive process characterized by the rupture of carbon-carbon bonds and hydrogen saturation of the fragments. By convention, HCK requires high temperatures (normally above 350°C), and high hydrogen pressures to minimize coke formation. In this process, hydrogenation accompanies cracking and the overall result is usually a change in the quality and character of the products (Ancheyta et al, 2007). Catalytic cracking mechanisms and HCK mechanisms are quite similar, but HCK technologies involve concurrent hydrogen flow rates (Ancheyta and Speight, 2007). Conventional HCK operating conditions are provided in Table 2.3.

Table 2.3. Process parameters for high conversion HCK.
(Scherzer and Gruia, 1996)

Operating Temperature	350 – 450°C
Hydrogen pressure	1200 - 3000 psi
Hydrogen consumption / hydrocarbon ratio	210 - 590 std m^3 / m^3
Liquid Hourly Space Velocity –LHSV-	0.5 – 2.5 h^{-1}
H_2 / Hydrocarbon ratio	1760 std m^3 / m^3

There are multiple configurations for HCK: single-stage, once-through, two-stage, separate-hydrotreat, among others. In all cases, cold hydrogen quench injection is necessary to control reactor temperatures due to the exothermicity of the reactions taking place (Ackelson, 2004). In commercial service, the two-stage flow scheme is the better suited for heavy feedstocks (Scherzer and Gruia, 1996).

2.7.2.1 HCK Reactions

As shown in Table 2.4, hydrocracking reactions are slightly exothermic. Simultaneous hydrogenation of aromatics and cracking are exothermic processes, while cracking reactions are endothermic; nevertheless, the net energy balance in HCK gives a negative reaction enthalpy value. In heavy fractions, more than half of the carbon atoms might be found in polyaromatic hydrocarbons, thus, the feedstock nature adds complexity to the whole HCK process (Hsu and Robinson, 2006).

Table 2.4. Hydrocracking reactions and enthalpies.
Conventions are: R for alkyl, Φ for aromatic (Hsu and Robinson, 2006).

Reaction type	**Illustration**	**Reaction Enthalpy (KJ/m^3 H_2 consumed)**
Dealkylation of aromatic rings	$\Phi\text{-}CH_2\text{-}R + H_2 \Rightarrow \Phi\text{-}CH_3 + RH$	-1.3 to -1.7
Opening of naphthene rings	Cyclo-$C_6H_{12} \Rightarrow C_6H_{14}$	-1.3 to -1.7
Hydrocracking of paraffins	$R\text{-}R' + H_2 \Rightarrow RH + R'H$	-1.3 to -1.7

Researchers defined a reaction sequence for vacuum gas oils and other +345°C material: the first step is saturation of an aromatic ring, followed by the opening of the resulting naphthenic ring, ring dealkylation and isomerization of paraffins and naphthene-aromatics as final step (Qader and McOmber, 1975; Lampinas et al, 1991). Typical hydrocracking reactions and reaction enthalpies are displayed in Table 2.4. The first two reactions are represented in Figure 2.15.

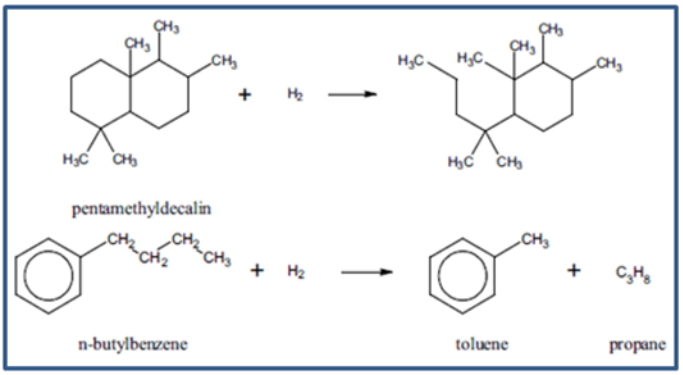

Figure 2.15. Naphthene ring opening and ring dealkylation reactions.
(Hsu and Robinson, 2006)

2.7.3 Hydroprocessing reactors

Residue hydroprocessing is strongly influenced by the method of feed introduction, the arrangement of catalyst, and mode of operation of reactors. Consequently, a variety of reactor technologies has been developed over the past decades, generally classified in fixed bed, moving bed, ebullated bed and slurry phase processes (Ancheyta and Speight, 2007). Innovative designs considering feedstock flow, catalyst utilization, or online removal, continue to be the focus of hydrocracking of heavy feedstock researches (Speight, 2011). Schematics of reactor types are presented in Figure 2.16.

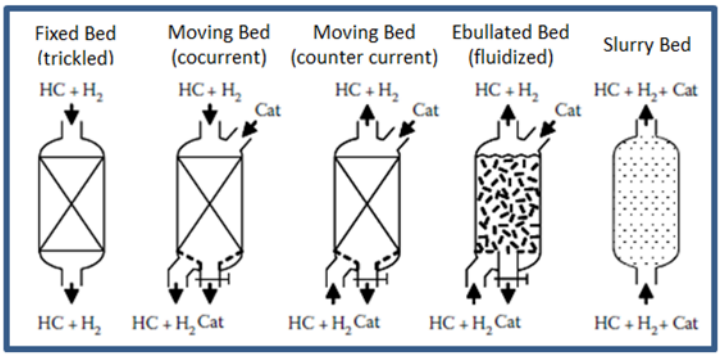

Figure 2.16. Reactor technologies for hydroprocessing of heavy oils.
(Ancheyta and Speight, 2007)

Light and medium oils are typically hydroprocessed in reactors containing fixed beds of catalyst, and heavier fractions are usually fed to other reactor systems with different hydrodynamics (Bridge and Hamilton, 2004). By 2007, Ancheyta and Speight reported that fixed bed reactors were the most popular configuration for petroleum residua hydroprocessing at that time. Frequent shutdowns to have the catalyst changed and high pressure drops are major drawbacks of this type of reactors (Gary and Handwerk,

2001). These problems can be alleviated by utilizing a proper catalyst particle size, and implementing a guard reactor or several reactors connected in series. Multi-beds reactors have been investigated and patented with good overall results (Furimsky, 2007). RCD Unibon process, ABC process, RHC Residue Hydroconversion process, Isocracking process and MAKfining process are examples of technologies that utilize fixed bed reactors, the last two working with multibed systems (Speight, 2011).

H-Oil and LC-Fining are two successful commercial technologies that rely on ebullated (or expanding bed) reactors to process residual oils. In these systems, fresh catalyst is added and spent catalyst is removed continuously, minimizing shut down of the units in comparison to fixed bed reactors (Hsu and Robinson, 2006). Uniform temperatures and almost inexistent plugs inside the reactor are advantages of these technologies; however their operability complexity increases, in particular during the catalyst renewal operation (Fahim et al, 2010).

Other licensed technologies are Hycon, OCR, MRH and Veba Combicracking; the first two utilize moving bed processes, whereas MRH and Veba Combicracking implement slurry bed technologies (Ancheyta and Speight, 2007); yet, these processes have not been installed in a commercial scale.

2.7.4 Hydroprocessing catalysts

Catalysts for hydrotreating and hydrocracking of heavy oils and residua have been the subject of investigation of researchers and industry for many years now. Designing catalysts for hydroprocessing of heavy feeds takes into account the presence of high molecular compounds, heteroatom containing structures and metals (Furimsky, 2007). The materials most commonly used to prepare these catalysts are shown in the following table.

Table 2.5. Support and active metals used in hydroprocessing catalysts. (Adapted from Hsu and Robinson, 2006)

Material	Type	Major Use
ɣ-Al_2O_3	Support	HDT
Amorphous aluminosilicates	Support	Distillate-selective HCK
Zeolites	Support	High-stability HCK
CoMo	Active metals	Hydrodesulfurization
NiMo	Active metals	Hydrodenitrogenation, HCK
NiW	Active metals	Hydrodenitrogenation, HCK
Pd, Pt	Active metals	HCK

Hydrotreating catalysts consist of a hydrogenation component dispersed on a porous, fairly inert material. Hydrocracking catalysts serve dual functions, containing both hydrogenation and cracking sites, the last ones usually as a result of using porous supports of acidic nature (Bridge and Hamilton, 2004). A balance of hydrogenation and hydrocracking functions has to be made to synthetize the optimal catalyst to target a specific product distribution. The concentration by weight of the metals is usually 1-4% for Co and Ni, 8-16 % for Mo and 12-25% for W (Topsøe et al, 1996).

The ideal combination of chemical composition and physical properties of the catalyst depends on many factors. Size and shape of catalyst particles must be matched with properties of the feed and the type of catalytic reactor. For heavy feeds, mechanical strength is critical to ensure a smooth operation of a catalyst bed, especially in fixed bed reactors (Furimsky, 2007). Typically, heavy oil processing catalysts require large pore volumes for high efficiency, to provide tolerance to metals and to minimize diffusion constrains. Less porous, high surface area catalysts have a higher hydrotreating activity, however, they are more susceptible to deactivation through pore-mouth plugging (Speight, 2004).

Cracking behaviour of asphaltenes utilizing an iron catalyst supported on SBA-15 was studied by Byambajav and Ohstuka (2003); they reported an increase in asphaltenes conversion as the pore diameter of the catalyst increased. Leckel (2006) evaluated the performance of NiMo and NiW on ɣ-Al_2O_3 catalysts in severe hydroprocessing of tar oils and tar products resulting from coal gasification. He found that the maximum deoxygenation activity was achieved with the NiMo catalyst, having a maximum pore size distribution in the range of 110 Å–220 Å; conversely, the NiMo catalyst with smaller pore sizes (35 Å-60 Å) displayed lower hydrogenation activity.

2.7.4.1 Carbon supported catalysts

There are a number of authors who have investigated hydroprocessing of diverse feeds utilizing carbon supported catalysts. Vit and Zdražil (1989) evaluated the performance of Ru, Rh, Pd, Ir and Pt over carbon for the simultaneous hydrodenitrogenation of pyridine and hydrodesulfurization of thiophene at 280°C, 290 psi and 3-6 hours of reaction. They concluded that the carbon supported sulfides were better hydrodesulfurization and hydrodenitrogenation agents than commercial NiMo/alumina and CoMo/alumina catalysts. Another paper presented the overall results from the hydrodenitrogenation of pyridine by Mo and NiMo over activated carbon catalysts (Calafat et al, 1996). In this study, a fixed bed reactor was used at 435 psi and 350°C to demonstrate that Ni and high concentrations of H_2S in the feed promoted conversion of pyridine and piperidine to C_5 hydrocarbons.

A comparative study of alumina and carbon-supported catalysts for hydrogenolysis and hydrogenation of model compounds (dibenzothiophene, quinoline, butenes, naphthalene and others) was made back in 1986 by Groot and coworkers. The team proved that carbon supported catalysts were more active than the alumina supported ones, when working at pressures below 725 psi of H_2 and temperatures ranging from 380°C to 430°C. Similar outcomes were reported by Hillerová and Zdražil (1991), who evidenced more catalytic activity using the NiMo/C catalyst compared to the NiMo/Al_2O_3 reference catalyst, regardless of hydrogen pressure. However, researchers also found much higher selectivity of alumina-supported catalysts compared to carbon-supported ones for the hydrodenitrogenation and hydrodesulfurization of pyridine and thiophene at 290 psi and 320°C in a packed bed reactor (Hillerová et al, 1991).

A patent assigned to Standard Oil Company states that fossil fuels containing polynuclear aromatics are effectively hydrotreated at elevated temperatures (from 399°C to 454°C) and hydrogen partial pressures in excess (2200 to 4000 psig), including a catalyst made of activated carbon and metallic components (Wennerberg and Frazier, 1974). However, they reported that catalysts used to hydroprocess resids became irreversibly deactivated, even though these were tested with different metallic loads and numerous formulations using metals from groups VI and/or VIII.

2.8 Advances on hydroprocessing of oxygenated feeds and others

Two key areas are worth addressing: advances on hydroprocessing in water media and current practices for hydroprocessing of oxygenated feeds. These topics have been reviewed and developed in the past, and the next section is intended to show the highlights of these, in particular the ones more related to this research.

2.8.1 Hydroprocessing in water media

A review of hydroprocessing in aqueous phase revealed that non-petroleum high oxygen content substances (i.e. lignin) and petroleum residues have been hydroprocessed in an aqueous phase. Lignin containing feeds may be used for hydroprocessing in water either directly or as the source of a bio-oil after upgrading (Furimsky, 2013).

In the case of residual feeds, a number of studies state that hydroprocessing in aqueous phase is successful if carried out under supercritical conditions with diverse catalysts (Furimsky, 2013 and references therein). However, Chadwick, Oen and Siewe (1996) demonstrated that water was a mild kinetic inhibitor for tetralin hydrogenation with a PNiMo/alumina catalyst at 1000 psi and 330°C. A review of hydrotreating of pyrolysis

bio-oil and oxygen-containing model compounds reported some study cases where water inhibited hydrotreating reactions by competitive adsorption on active sites (Wang et al, 2013).

Catalytic reforming of lignin in aqueous alkaline medium was recently addressed by testing several Ru and Ni over activated charcoal catalysts; lower molecular weight structures like guaiacol, 4-ethylphenol and 3-ethylphenol were obtained after 7 hours at 300°C and 2900 psi in a packed bed reactor (Kudo et al, 2013). Another recent study (Nimmanwudipong et al, 2014) described a high pressure plug flow reaction system for guaiacol hydroprocessing. In this case, Pt/ɣ-Al_2O_3 yielded smaller hydrocarbons at 250°C, 1000 psi and 46.4 g/h of organic reactant solution per gram of catalyst.

2.8.2 Hydroprocessing of lignin in non-aqueous phase

Deutsch and Shanks (2012) investigated the hydrodeoxygenation of lignin model compounds over a copper chromite catalyst at mild conditions (less than 300°C, 750 psi), observing reduction of hydroxymethyl groups of trifunctional phenolics at temperatures as low as 150°C. Another study by Mochizuki and coworkers (2014) showed the effect of different catalysts (including Ni/SiO_2 and Co/SiO_2) on the hydrodeoxygenation of guaiacol and woody tar, at temperatures between 300°C-350°C and H_2 pressures in the range of 145-750 psi.

A patented process (Shabtai et al, 2003) is in the demonstration stage, in which lignin is treated to form and extract phenols. Then, extracted substances are hydrotreated, obtaining high yield to hydrocarbons by use of a transition metal catalyst and 750 psi of hydrogen (Green Car Congress, 2009). In another process, the same authors claim that using sulfided CoMo, NiMo and NiW over alumina, depolymerized lignin can be hydroprocessed at 350°C-385°C yielding reformulated hydrocarbon gasoline (Shabtai et al, 1999).

3. PRODUCTION OF WATER SOLUBILIZED ASPHALTENES

As indicated in the first chapter, the Catalysis for Bitumen Upgrading (CBU) group is currently targeting the optimal conditions to solubilize asphaltenes in aqueous media. In the present study, the basic methodology for preparation of Water Soluble Asphaltenes (WSA) is described, as well as characterization of WSA and parent asphaltenes. Findings on the effect of temperature during WSA production on the final solution quality are included in this chapter.

3.1 Basic methodology for production of WSA

3.1.1 Materials

nC_5 asphaltenes from Athabasca Vacuum Residue (ATVR) were obtained by a standard refluxing n-pentane precipitation procedure (Institute of Petroleum, 1985), using a relation of 15-20 mL of pentane (98.0%, reagent grade from BDH) per gram of residue. The mixture of alkane and vacuum residue was poured into a round bottom flask and placed over a heating mantle, in which the voltage diverter was set to 40% of 110V maximum output voltage. After refluxing for half an hour, the mixture was cooled down and ultrasonicated. Asphaltenes were recovered by filtration and repeatedly washed with fresh portions of pentane until the filtrate was resins free. Finally, asphaltenes were dried overnight in a vacuum oven (-25 mm Hg, 70°C) and posteriorly crushed to powder.

Ultra-high purity grade oxygen (99.993%, purchased from Praxair) was selected as the oxidation reagent. A 5N NaOH solution in water from Sigma Aldrich was used to neutralize the acidity produced during the oxidation process, aiming to prevent severe corrosion and to increase asphaltenes solubility in water (Eldood et al, 2010).

3.1.2 Methodology

The following methodology is the basis of the procedure utilized to: a) produce WSA as feedstock for different experiments, and b) to examine the influence of temperature on WSA quality; variables such as stirring speed, qualities and quantities of the reagents described below, remained unchanged for all tests performed to produce WSA.

4 grams of crushed nC_5 asphaltenes, 156 mL of water and 8 mL of NaOH solution were poured into a 500 mL stainless steel batch reactor from Parr instruments. 1000 psig of oxygen was injected to the reactor and its stirring speed was set to 1000 rpm. The system was heated up to the target temperature and reaction took place for a period of time. Afterwards, the reactor was cooled down to room temperature using an in-house fabricated copper water coil cooler. Produced gases were injected into a Gas Chromatograph (GC) from SRI (multiple gas configuration, model 8610C) for mass balance and yield calculations. The resulting WSA solution was filtered and unconverted solids were dried overnight and weighed for mass balances and conversion calculations.

3.1.3 Techniques for WSA and nC_5 asphaltenes characterization

3.1.3.1 Total organic carbon

The Total Carbon (TC) technique was chosen to quantify the amount of asphaltenes dissolved in water as asphaltenes are the only source of carbon during the oxidation process. However, other oxidation products like CO_2, may solubilize in the WSA solution and also contribute to its carbon content. Therefore, a distinction between Total Organic Carbon (TOC) and Inorganic Carbon (IC) is made in order to quantify asphaltenes concentration in the aqueous stream. The TC content corresponds to the sum of TOC and IC contributions.

TC, TOC and IC measurements were made in a TOC-CPH analyzer from Shimadzu. For TC analysis, the sample is heated to 680°C in presence of an oxidation catalyst, transforming all carbon components to carbon dioxide. CO_2 is monitored by a non-dispersive infrared gas analyzer and peak areas are related to the TC concentration of the sample. IC quantification is made by injecting HCl to the sample and calculating the CO_2 produced; once again, signals detected by the infrared gas analyzer are matched to the IC concentration of the sample. TOC content is determined by subtracting the IC concentration from the TC concentration. The TOC apparatus is configured to inject every sample three times into the combustion tube and to calculate an average value, providing results within 3% accuracy in relation to the TC, IC and TOC content.

3.1.3.2 Fourier transform infrared spectrophotometry

Fourier Transform Infrared spectrophotometry (FTIR) analyses were used to characterize parent asphaltenes and their oxidized products. The infrared technique relies on infrared light absorption causing vibrational excitation of chemical bonds, each one at a characteristic frequency; hence, absorption bands at determined frequencies can be used to identify specific functionalities. FTIR spectra were recorded in a Nicolet 6700 FT-

IR spectrometer, equipped with a diffuse reflectance cell for KBr dispersed solid samples and a transmission cell for liquid samples.

3.1.3.3 Elemental analysis

Elemental analyses of Athabasca vacuum residue asphaltenes and WSA were carried out in a LECO 628 CHN elemental analyzer for carbon, hydrogen and nitrogen determination. In this equipment, samples are introduced into a combustion chamber where CO_2, NO_2, and water are produced and monitored with thermal conductivity detectors. By means of calibration curves, water, CO_2 and NO_2 signals are matched to the hydrogen, carbon and nitrogen content in the sample, respectively. The equipment is able to provide results with accuracy of around 5% of relative error.

Sulfur composition was determined with an Antek 9000 SN Elemental Analyzer. After injecting samples into the combustion chamber, SO_2 was detected by an UV-fluorescent detector which matched signals with calibration curves that were created with reference standards and reference bitumen samples. The apparatus, which is able to detect concentrations down to ppb (European Virtual Institute for Speciation Analysis, 2010), provided sulfur content with relative errors below 5%.

3.1.3.4 Metal analysis

Metals quantification procedure consists in two steps: a) sample digestion and b) analysis by Inductively Coupled Plasma spectroscopy (ICP). Digestion was carried out in a Microwave Accelerated Reaction System (MARS) from CEM Corporation following a methodology developed by the CBU group, in which 0.5 grams of each sample (weighed to the nearest milligram) are placed in vessels and mixed with 10 mL of a 70 wt% HNO_3 solution, 1 mL of an 85 wt% H_3PO_4 solution and 23 mg of a 1,000 ppm cobalt standard solution. Next, vessels are introduced in the MARS apparatus; temperature was increased to 210°C and the system dwelled for 50 minutes. Then, vessels were cooled down to room temperature and their contents were diluted to 25 mL using deionized water. Afterwards, digested samples were analyzed in an ICP-atomic emission spectroscopy apparatus (IRIS Intrepid II XDL, from Thermo-Instruments Canada Inc.), in which the prepared dilution is injected to a nebulization area inside the machine, converted in aerosol or vapor and ionized inside the plasma. Metal content was quantified using calibration curves and known standard solutions.

3.2 Characterization of parent asphaltenes and WSA

The elemental analysis technique was used for ATVR nC_5 asphaltenes and a WSA solution prepared at 250°C and 2 hours of residence time, using the methodology described in section 3.1.2. The WSA column in Table 3.1 corresponds to water-free based calculations, as water was evaporated from the solution to carry out elemental analyses on oxidized/solubilized asphaltenes.

Metals were quantified by metal analysis (section 3.1.3.4), whereas oxygen composition, both in virgin asphaltenes and WSA, was determined by subtracting the carbon, hydrogen, sulfur, nitrogen, and metals concentration from 100%. Values from the NaOH solution (second column in the table below) correspond to computed stoichiometric quantities of the 5M solution used in the WSA synthesis.

Table 3.1. Elemental composition of ATVR nC_5 asphaltenes and WSA produced at 250°C and 2 hours of residence time.

	Virgin asphaltenes	**NaOH solution**	**WSA (after drying)**
Carbon	80.9 wt%	0.00 wt%	31.2 wt%
Hydrogen	8.6 wt%	9.4 wt%	2.5 wt%
Sulfur	7.1 wt%	0.00 wt%	3.8 wt%
Nitrogen	1.4 wt%	0.00 wt%	0.6 wt%
Oxygen	1.7 wt%	79.1 wt%	36.5 wt%
Nickel	0.03 wt%	0.00 wt%	0.02 wt%
Iron	0.19 wt%	0.00 wt%	0.01 wt%
Vanadium	0.06 wt%	0.00 wt%	0.04 wt%
Potassium	0.03 wt%	0.00 wt%	0.01 wt%
Sodium	0.00 wt%	11.5 wt%	25.3 wt%
H/C atomic ratio	1.3	-	1.0
S/C atomic ratio	0.03	-	0.05
N/C atomic ratio	0.01	-	0.02

There are two main aspects worth noting from Table 3.1: the hydrogen-to-carbon atomic ratio and oxygen concentration. The H/C ratio decreased in the oxidized asphaltenes products, most probably due to cracking of small chains from the original structure, and consequently increasing the aromaticity of water soluble asphaltenes. Even though mechanisms are not part of the scope of this project, it is evident that carbon atoms of cracked chains have converted into CO_2 and methane, as shown in the next section.

Substantial amounts of oxygen and sodium are transferred to the WSA solution. In particular, oxygen composition increases by 35% and obviously, major changes in the

soluble asphaltenes structure are expected. FTIR spectrophotometry analyses were performed to identify how the oxygen is anchored in the WSA structure (Figure 3.1); the red spectrum corresponds to WSA and the green one relates to nC_5 parent asphaltenes.

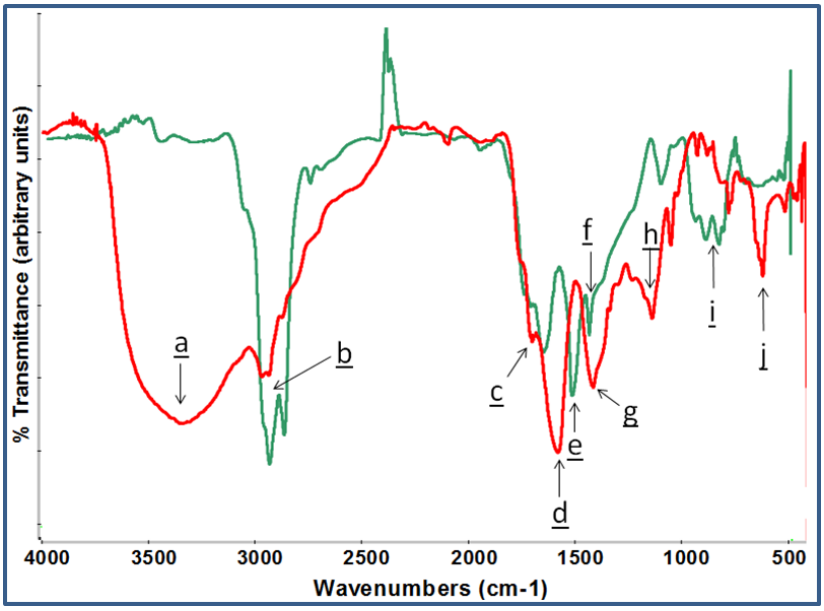

Figure 3.1 FTIR spectra of WSA produced at 250°C and 2 hours of residence time (in red) and ATVR nC_5 asphaltenes (in green).

Relevant zones and peaks of the resulting spectra have been labelled. Inverted peaks indicate infrared light absorption at a specific wavenumber, evidencing the existence of a particular functionality depending on the wavenumber at which light is absorbed. Zone a and peak c correspond to the signal emitted by RCOOH moieties; the inverted peaks in these regions show the presence of carboxylic acids in the WSA sample, which are not seen in the nC_5 parent asphaltenes as demonstrated by the flat spectrum between 3600-3100 cm^{-1}. The alkyl functionalities in ATVR asphaltenes, identified in zone b, are lost when asphaltenes are oxidized and solubilized in water. Similarly, inverted peaks e and f show alkyl moieties only in the nC_5 asphaltenes spectrum. Around 1600 cm^{-1} (denoted by letter d), carboxylate anions or $RCOO^-$ are identified in the red signal; in region g carboxylate anions are recognized, as an inverted peak is displayed in the WSA sample. Sulfonic acids are evidenced in peaks h and j, which are not present in the parent asphaltenes but generated after the oxidation process. Aromatics (region i) provide a strong signal in nC_5 asphaltenes but a weaker one for the WSA sample.

3.3 Effect of temperature on WSA production

This section explains results from different batches of produced WSA at different temperatures (and in a single experiment, residence time was also changed), exploring changes in TOC, IC and TC content. Generated gases were analyzed by gas chromatography and liquid samples were filtered and characterized in the TOC apparatus.

The experimental plan consisted on performing wet air oxidation of asphaltenes following the methodology described in section 3.1.2, quantifying unconverted solids and assessing gas and liquid streams qualities. Stirring speed was set to 1000 rpm, and ATVR nC_5 asphaltenes (4 grams), water (156 grams), NaOH 5N (8 mL) and ultra-high purity oxygen (1000 psig) quantities remained unchanged for all the experiments. Residence time was adjusted in one experiment, and temperature was changed as displayed in Table 3.2. Conversion (X) and yields (Y) were calculated employing the next equations:

(Equation 3.1) $$Conversion\ (\%) = \frac{4.0\ g - g\ of\ unconverted\ asphaltenes}{4.0\ g} \times 100\%$$

(Equation 3.2) $$Carbon\ Yield\ (\%) = \frac{Carbon\ in\ products\ (g)}{Carbon\ in\ nC_5\ asphaltenes\ (g)} \times 100\%$$

Table 3.2. Experimental plan for assessment of WSA production.

Test	Temperature	Residence time	Conversion
A	220°C	1.5 hours	57.3 ± 2.5 %
B	220°C	3 hours	69.3 ± 1.1 %
C	230°C	3 hours	80.4 ± 0.6 %
D	240°C	3 hours	91.9 ± 1.1 %

In equation 3.1, g of unconverted asphaltenes relates to the amount of solids remaining after reaction, which were recovered from the reactor, filtered and dried at room temperature for 24 hours before they were weighed. The amount of carbon in the products in equation 3.2, was quantified by adding the carbon contribution from both liquid and gas streams, determined by means of TOC and GC analyses, respectively.

Each set of experiments was repeated 5 times to ensure reproducibility with an overall carbon mass balance of 96.4 ± 4.1%. This value is entirely attributed to experimental errors knowing that the volume of reactor (500 mL) surpass by far the amount of asphaltenes to oxidize (4 grams). Even though the reactor was cleaned between each test, asphaltenes might have been trapped in any of the joints between the reactor and the pressure gauge, the impeller and/or the thermo well. As asphaltenes initial quantity

is not large, every 0.1 grams represents 2.5% of the total solids to be handled, thus, the smallest amount of lost powder contributes to the experimental error percentage.

Average results obtained at conditions described in Table 3.2, are presented in the following diagrams. Although not easily seen in many of the plotted points in Figure 3.2, error bars for each yield value were incorporated, some being so small that are barely noticed. Figure 3.3 zooms in on the soluble inorganic carbon and CH_4 yields, in which error bars are drawn in black and green, respectively. TOC values reported in Table 3.3 show that reproducibility is achieved in terms of WSA quality, where standard deviations don't exceed 6%.

Table 3.3. Liquid and gas analyses during WSA preparation at different temperatures.

Test	Conversion	Liquid Stream		Gas Stream	
		TOC (mg/L)	IC (mg/L)	CO_2 v/v%	CH_4 v/v%
A	57.3 %	7638 ± 152	734 ± 18.0	1.31 ± 0.07	0.06 ± 0.02
B	69.3 %	9048 ± 139	411 ± 66.2	2.64 ± 0.01	0.15 ± 0.01
C	80.4 %	9804 ± 596	64.0 ± 12.5	4.95 ± 0.15	0.28 ± 0.25
D	91.9 %	8200 ± 93	6.31 ± 0.2	8.48 ± 0.36	0.50 ± 0.04

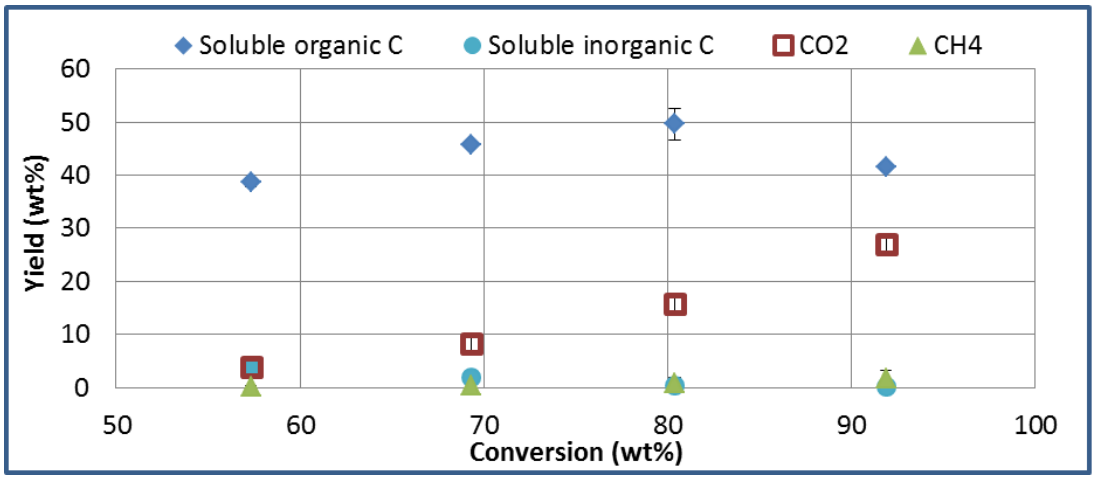

Figure 3.2. Products yield from wet air oxidation of Athabasca vacuum residue nC_5 asphaltenes.

As demonstrated in Figure 3.2, production of CO_2 is promoted as the severity of the oxidation reaction increases. At the highest conversion studied, CO_2 yield is almost 30%, soluble organic carbon yield is 41% and water soluble inorganic carbon yield is practically zero. Under these operating conditions, WSA solution is constituted by 8,000 ppm of organic carbon (i.e. solubilized asphaltenes), and it can be generalized that TC = TOC.

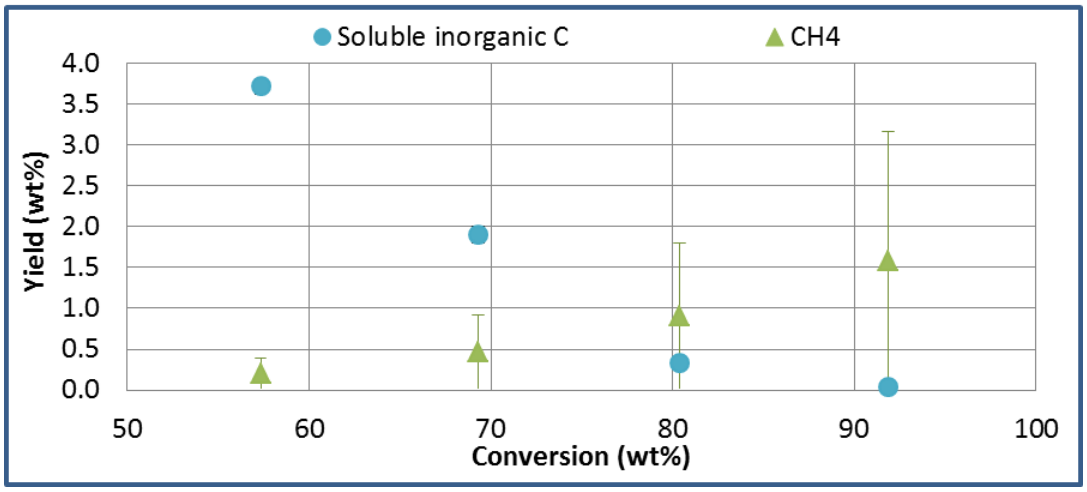

Figure 3.3. Soluble inorganic carbon and methane yields from wet air oxidation of Athabasca vacuum residue nC_5 asphaltenes.

This is not the case when the reaction is carried out at 220°C and 1.5 hours, because 10% of the TC content of the WSA produced corresponds to inorganic constituents, specifically CO_2 and sodium carbonates. At these operating conditions, the strict relation of TC = TOC + IC must be followed and the asphaltenes composition in the aqueous solution has to be only related to the TOC content.

When conversion is 80.4%, a local maximum of organic carbon dissolved in water is achieved. Almost 10,000 ppm of asphaltenes were dissolved in the liquid stream and the amount of inorganic carbon in the resulting solution is less than 1% of the TC content. These conditions seem most appropriate to maximize asphaltenes solubilization without a significant contribution from CO_2 in the oxidized solution. However, carbon yields in the generated gas reach a value of 16.5%, whereas at X = 69.3%, this value drops down to less than 10%, yet a substantial portion of asphaltenes are solubilized (more than 9,000 ppm TOC). At these last severity conditions, 220°C and 3 hours residence time, IC content in WSA solution still remains low enough (less than 5% of TC).

In summary, partial conclusions originate from the previously reported information: first, temperature has a pronounced effect on CO_2 production from the oxidation process of nC_5 asphaltenes in aqueous media. As well, residence time is a key factor in the oxisolubilization of asphaltenes, as demonstrated by the increase in conversion from X = 57.3% to X = 69.3% in experiments A and B after the residence time was doubled in test B. Under the studied range the conditions, an optimum operation is found at 230°C and residence time of 3 hours, at which the TOC content was the largest obtained and IC contributions were less than 0.7% of the TC concentration in the solution. At higher temperatures, carbon in the parent asphaltenes is transformed into gaseous CO_2 at a

higher extent in comparison to carbon solubilization, and trends suggest that CO_2 and soluble organic carbon lines cross at nearly complete conversion; this tendency agrees with studies of wet oxidation of asphaltenes previously developed by the CBU group employing the same reactor vessel (Eldwood et al, 2010).

4. ADSORBENTS SCREENING

Adsorbents screening was the first step taken to prove the global concept of this project: solubilization of asphaltenes, adsorption of WSA and hydroprocessing of pre-adsorbed WSA. Ten adsorbents were evaluated in order to select the best-ranked solids in terms of water soluble asphaltenes uptake. Five adsorbents were chosen from current practices in the waste water treatment industry. The remaining five are synthesized in-house adsorbents, which were also screened and compared to commercial solids. This chapter comprises methodologies for characterization of these adsorbents and results from screening tests.

4.1 Selected adsorbents for screening tests

Based on the literature review (refer to section 2.5), solids representing each family of commercial adsorbents were selected to be tested for WSA uptake. Activated carbon was the obvious first pick due to its extensive application on water purification. Fuller's earth and bentonite were selected for screening due to features previously summarized. Similarly, MCM-41 and SBA-15 are the benchmark materials that seemed necessary to explore. Five adsorbents, named Ordered Mesoporous Material (OMM), were conceived and designed by Dr. Gerardo Vitale and synthetized at the CBU facilities located in the University of Calgary.

4.1.1 Commercial and in-house materials

Bentonite, Fuller's earth and Powdered Activated Carbon (PAC) were purchased from Sigma Aldrich and used as received. Both SBA-15 and MCM-41 were synthetized using reagents quality and procedures described elsewhere (Meynen et al, 2009).

The in-house silicate based adsorbents OMM-20, OMM-21, OMM-40, OMM-86 and OMM-88, were designed to provide mesoporous nature and hydrophobicity. Although their syntheses at present are confidential and cannot be discussed in detail, preparation includes mixing of templates, sulfuric acid, alcohol, a neutralizing agent and other materials purchased from Sigma Aldrich. Once all of the components are homogenized, solids are filtered and subsequently washed with alcohol and water. After drying the solid at 100°C for 20 hours, the adsorbent is calcined at 550°C under ambient atmosphere (air).

The difference among OMMs resides in the incorporation of different metals in their structures and the templates used for their syntheses. Both OMM-40 and OMM-86 are silicate-based adsorbents without metals in their structure, yet the last one is the pore expanded version of OMM-40. Likewise, OMM-88 is the pore expanded version of OMM-20, but these two are iron based materials. The last in-house adsorbent tested, OMM-21, has copper in its structure.

4.1.2 Solids characterization

Textural properties were monitored using a Micromeritics Surface Area and Porosity System Analyzer, model Tristar II 3020. Each sample was degasified prior to textural analysis by leaving the adsorbent at 150°C with a controlled flow of nitrogen for 12 hours. Then, solids were introduced in the Tristar apparatus to measure Brunauer-Emmet-Teller (BET) surface area, and pore size distribution, pore volume and average pore diameter determined by the Barret-Joyner-Halenda (BJH) method. Nitrogen adsorption measurements were performed at -196°C to quantify BET surface areas, and to identify mesoporosity (from 20 Å to 500 Å) and macroporosity (beyond 500 Å) in solids. Table 4.1 shows measured textural properties of screened adsorbents.

Table 4.1. Textural properties of screened adsorbents.

Adsorbent	**BET Surface Area (m^2/g solid)**	**BJH average pore size (Å)**
Bentonite	87.6	268
Fuller's earth	87.6	274
PAC	1335	68.9
SBA-15	645	72.9
MCM-41	1318	31.8
OMM-40 (SiO_4)	930	44.4
OMM-86 (pore expanded SiO_4)	1174	39.8
OMM-20 (Fe-SiO_4)	480	168
OMM-88 (pore expanded Fe-SiO_4)	572	99.6
OMM-21 (Cu-SiO_4)	1006	41.8

It is worth recalling that reported BJH pore size values correspond to averages, and pore distribution is needed to assess the mesoporosity of each material. At first sight, it may appear that OMM-88 and OMM-86 syntheses were not successful since their average pore sizes are actually smaller than those in OMM-20 and OMM-40, respectively. Further assessments on this matter had to be made by looking at pore distribution charts, shown in Appendix A.

Both OMM-40 and OMM-86 have bimodal pore size distributions in the mesoporous area. OMM-40 surface confirms pore widths of 21 Å and 39 Å, while OMM-86 shows two peaks at 23 Å and 37 Å. Average pore sizes indicated in Table 4.1 are larger than widths of identified pores because these averages take into account macroporosities that are not displayed in these charts (refer to Appendix A). Evidently, the template used to prepare OMM-86 accomplished two key things: opened pore widths by 2 Å for the smaller pores and increased the total contribution of mesopores.

Likewise, OMM-21 has a bimodal pore distribution, with pore sizes of 24 Å and 36 Å. As for the iron-silicate based adsorbents, it appears that only one pronounced peak is located at 34 Å for OMM-20, and at 38 Å for OMM-88. The last adsorbent holds a larger total mesopores contribution; however, the trend in OMM-20 chart suggests an array of pores with diameters of 200 Å and larger.

Pore distribution charts for commercial solids are also available in Appendix A. SBA-15 and MCM-41 exhibit pores of 55 Å and 22 Å, respectively. PAC, fuller's earth and bentonite surfaces have a broad distribution of pore widths. PAC's maximum peak is located at 26 Å but significant contributions are seen from 77 Å width pores. Regarding evaluated clays, bentonite displays a broad array of pore sizes of > 40 Å, with the strongest signal peak identified at 328 Å. Fuller's earth surface has an assortment of pore sizes ranging from 50 Å to the highest end of the mesoporous region. In this solid, the maximum peak is found at 298 Å pore width.

4.2 Adsorbents screening: Qualitative analysis

A simple, fast methodology was implemented to scan the adsorption performance of selected solids. This qualitative procedure relies on the Q-ratio technique, a popular index used for characterization of humic substances. Subsequent paragraphs explain the adapted procedure to qualitatively evaluate the adsorption uptake of WSA by each solid.

4.2.1 Characterization techniques: Q-ratio and UV-vis spectroscopy

The color of humic substances is a physical property that has been widely investigated; many scientists believe that the intensity of light absorption is characteristic for the type and molecular weight of humic substances. The color ratio, or Q-ratio, is an index that expresses the degree of humification in terms of rate of light absorption in the visible range (Tan, 2009). Two selected wavelengths, commonly 400 nm and 600 nm, are employed to compute Q-ratios of humic substances by implementing the following equation:

(Equation 4.1) $$Q - ratio = \frac{Absorbance\ at\ 400\ nm}{Absorbance\ at\ 600\ nm}$$

A high color ratio is usually observed for fulvic acids or humic acids of relatively low molecular weights. On the other hand, a low Q-ratio is exhibited by humic acids and other related compounds with high molecular weights (Tan, 2009). The Q-ratio has also been employed in the pharmaceutical field as a simple, sensitive, rapid and accurate method for estimation of combined pharmaceutical drugs in tablet dosage form (Gowamil et al, 2012; Sharma and Shaa, 2012).

Q-ratio can be utilized as a qualitative tool for assessing adsorption of similar substances by tracking solutions color change. For instance, if a WSA solution is in contact with a particular solid for a period of time, WSA adsorption can be recognized if the WSA solution has a lighter colour after a determined time frame. These "extinctions" of asphaltenes in the WSA solution can be estimated by visible light spectrophotometry, calculating Q-ratios of WSA solutions before and after being in contact with the adsorbent. For this purpose, the percentage of qualitative WSA adsorption was defined as follows:

(Equation 4.2) $$Qualitative\ WSA\ uptake = \frac{Qbefore - Qafter}{Qbefore} \times 100\%$$

In the previous equation, Qbefore corresponds to the Q-ratio of the WSA solution prior to the adsorption experiment, in other words, the color ratio of the WSA solution. Qafter stands for the Q-ratio of the WSA solution measured at the end of the adsorption experiment.

Ultraviolet-visible (UV-vis) light spectrophotometry is a characterization tool employed to quantify the concentration of a compound present in a sample by measuring light absorbance following the Beer-Lambert law: absorbance varies linearly with concentration at a given range. Therefore, if the compound is more concentrated, more light will be absorbed. WSA solutions spectra were recorded in a Cary 4E UV-vis spectrophotometer from Varian, using quartz spectrophotometer cells of 4.5 mL capacity and 1 cm path length.

4.2.2 Materials and methodology

A batch of WSA (10,000 ppm by weight) was prepared at 250°C and 2 hours of residence time in a high pressure-temperature autoclave from PARR Instruments. After the assessment described in section 3.3, the last conditions (250°C and 2 hours of residence time) seemed inappropriate for WSA production. However, it must be clarified that adsorbent screening tests were completed before studying the effect of temperature on

WSA production. Results from these tests were not known at the time the WSA solution was produced because the sequence of the experiments doesn't match the order of this document. Regardless, this batch was used for the first part of the project because it was available and ready to use, saving valuable processing time.

The WSA batch under consideration was highly concentrated and impossible to analyze via visible light spectrophotometry due to the darkness of the sample solution. In consequence, a diluted solution of 500 ppm by weight was prepared and employed for WSA qualitative uptake analysis. A sample from the WSA diluted solution was placed in a quartz cell for scanning by UV-vis spectrophotometry. The blank sample (in other words, WSA without adsorbent) spectrum was recorded from 200 to 800 nm, programmed to scan each 10 nm. Q-ratio was quantified and denoted as Qbefore.

0.2 grams of each adsorbent were accurately weighed and placed in 20 mL glass vials. 8 mL of 500 ppm by weight solution were added to all vials and allowed to stay at room temperature for 72 hours (refer to Figure 4.1). Then, solutions in vials were filtered and poured into quartz cells to measure absorbance by UV-visible light spectrophotometry. Wavelengths from 200 to 800 nm were recorded and Q-values were computed for each adsorbent (Qafter). Finally, percentages of qualitative WSA uptake were calculated using equation 4.2.

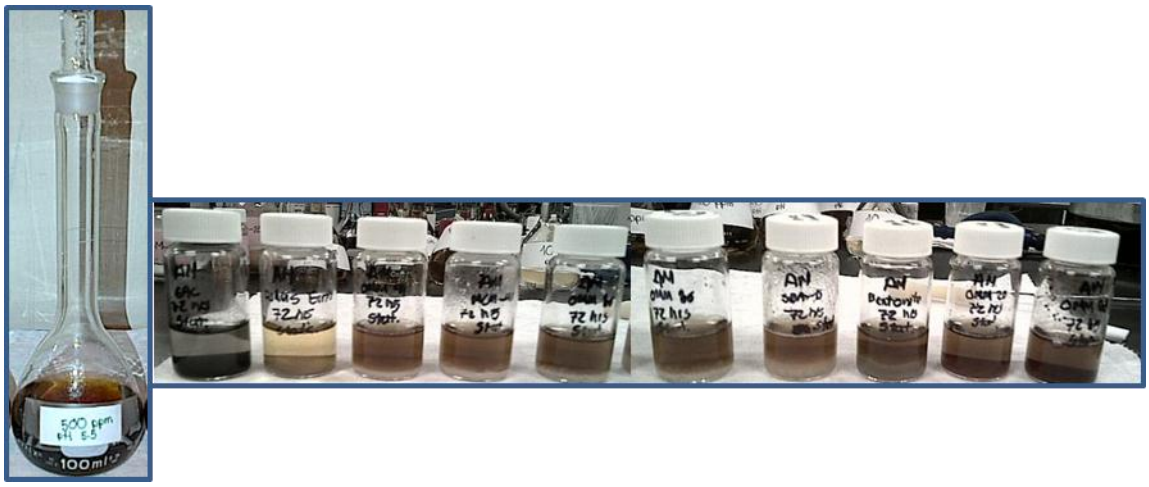

Figure 4.1. Diluted 500 ppm WSA solution and vials after qualitative uptake experiments.

There were two variations made during the qualitative evaluation: static and dynamic conditions. Static conditions refer to tests in which vials stayed in the same spot and position (without agitation) for the length of the experiment; conversely, during dynamic experiments, vials were placed in shakers and constantly agitated.

4.2.3 Results

Qualitative uptake experiments were performed three times for each adsorbent at static and dynamic conditions. Q-ratios standard deviations were from 1% to 20% (only half of the experimental results had less than 5%), demonstrating significant reproducibility difficulties. There was the need of a more reliable method, therefore, a quantitative approach was designed to improve reproducibility of screening tests and to ensure proper adsorbents assessment; nevertheless, results obtained from these tests are shown in Table 4.2.

Table 4.2. WSA adsorption results from qualitative screening tests.

Adsorbent	**Percentage of Qualitative WSA uptake**	
	Static conditions	**Dynamic conditions**
Bentonite	41.7 ± 20.4%	13.0 ± 11.7%
Fuller's earth	-4.0 ± 3.2%	46.0 ± 2.7%
PAC	95.9 ± 3.6%	89.5 ± 0.1%
SBA-15	12.1 ± 0.1%	42.3 ± 18.5%
MCM-41	17.7 ± 7.4%	48.5 ± 8.5%
OMM-40 (SiO_4)	16.6 ±1.6%	59.7 ± 5.4%
OMM-86 (pore expanded SiO_4)	20.9 ± 3.2%	54.3 ± 6.4%
OMM-20 (Fe-SiO_4)	54.0 ± 17.5%	61.8 ± 3.6%
OMM-88 (pore expanded Fe-SiO_4)	50.2 ± 6.0%	56.3 ± 4.1%
OMM-21 (Cu-SiO_4)	36.1 ± 3.5%	58.5 ± 2.0%

Negative percentages can be interpreted as if there was no WSA adsorption at all. Under this scenario, qualitative evaluation suggests that fuller's earth didn't retain any WSA on its surface at static conditions. This percentage is considerably improved when tests are carried out by continuously shaking testing vials, evidencing important diffusional limitations. The same analysis in regards to diffusional constrains applies to almost all the other adsorbents, with the exception of bentonite and activated carbon. During experiments carried out using bentonite, there were some difficulties at trying to reproduce calculated Q-ratios; for this particular solid, tests had to be performed 5 times and error percentages still exceeded 10%. In addition, its small particle size made it difficult to filter after the experiment, causing erroneous absorbance measures due to suspension of fine particles. The trend exhibited by PAC could also be attributed to fine carbon powder suspended in the liquid; similarly, the WSA solution was challenging to filtrate after adsorption experiments with activated carbon. Regardless, this solid displayed the largest uptake in terms of percentage of qualitative adsorption both in static and dynamic conditions.

Even though results reproducibility for some solids was difficult to achieve, partial conclusions can be derived from qualitative uptake percentages. If only dynamic conditions are taken into account, the solid that adsorbed the most WSA was PAC, followed by solids belonging to the OMM family and subsequently, benchmark materials (MCM-41 and SBA-15). The most probable cause for experimental errors was the suspension of fine particles in the WSA solution after adsorption experiments. Other errors that may have been incurred include temperature fluctuations and variation of shaking intensity, though it is suspected that the extent of these factors is no greater than the cause analyzed before. There is no doubt that a more accurate, reliable procedure had to be implemented; as a result, a quantitative methodology was conceived to select the appropriate solid to test in the adsorption/hydroprocessing continuous setup. Details are addressed in the following sections.

4.3 Adsorbents screening: Quantitative analysis

4.3.1 Methodology

A 500 ppm by weight WSA solution was diluted from the batch obtained at oxidation conditions of 250°C and 2 hours of residence time (section 4.2.2). Other diluted samples below 500 ppm by weight were prepared and scanned in the UV-vis spectrophotometer and the TOC analyzer. In all cases, the maximum absorption intensity peak was seen at 400 nm and IC content from diluted samples didn't exceed 5% of the Total Carbon content. With data from both techniques, a calibration curve was created as shown in the next figure.

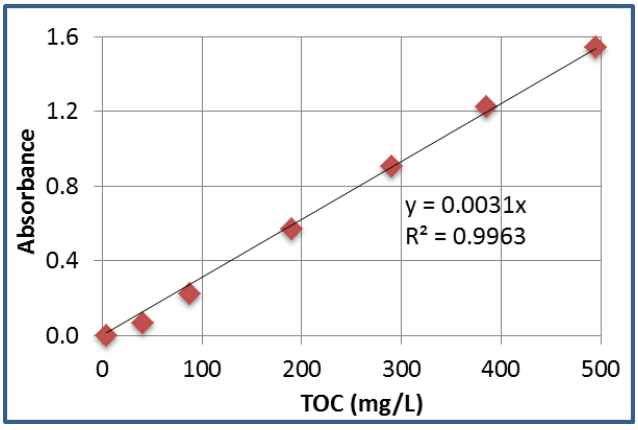

Figure 4.2. UV-vis spectrophotometer calibration curve @ 400 nm.

0.1 grams of adsorbent (weighed to the nearest milligram) and 500 ppm by weight WSA were mixed in a quartz cell, maintaining a ratio of 40 mL asphaltenes solution per gram

of solid. Immediately after, the cell was placed in the UV-vis spectrophotometer in which spectra were generated every 5 minutes for 2 hours, scanning every 10 nm in the range of 200 nm to 800 nm. Quantitative uptake (in mg WSA/g adsorbent) was computed by converting absorbances read at t=0 min and t=120 min into concentrations, and using these values in the following equation:

(Equation 4.3) $$WSA\ uptake = (Co - Cf) \times 0.04$$

Where Co is the initial total organic carbon concentration (at minute 0) in mg/L, and Cf is the final total organic carbon content after two hours (at minute 120) in mg/L.

4.3.2 Results

The following figures were plotted using adsorption uptakes calculated by the quantitative method. Figure 4.3 displays WSA uptakes as function of the solid in relation to surface areas, and Figure 4.4 shows WSA adsorption related to average pore sizes for every solid.

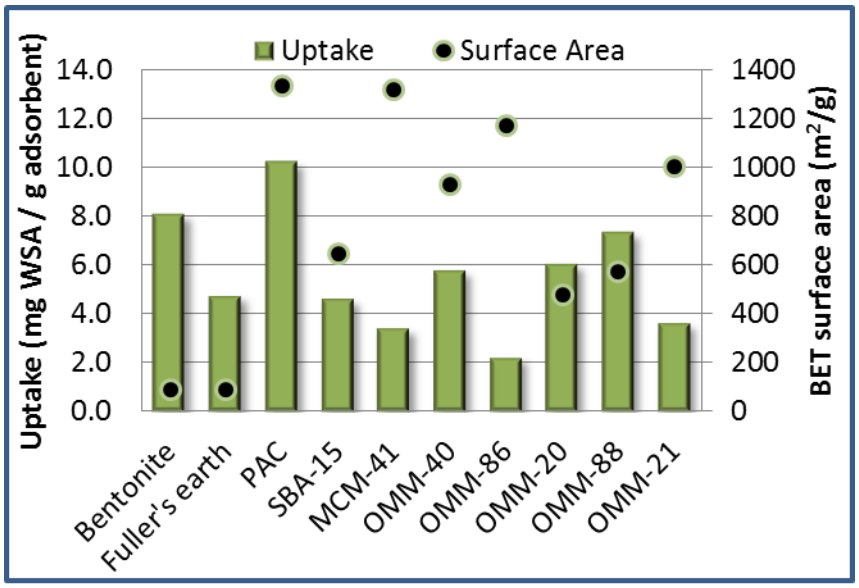

Figure 4.3. WSA quantitative uptake and adsorbents surface areas. Adapted from Manrique et al, 2013.

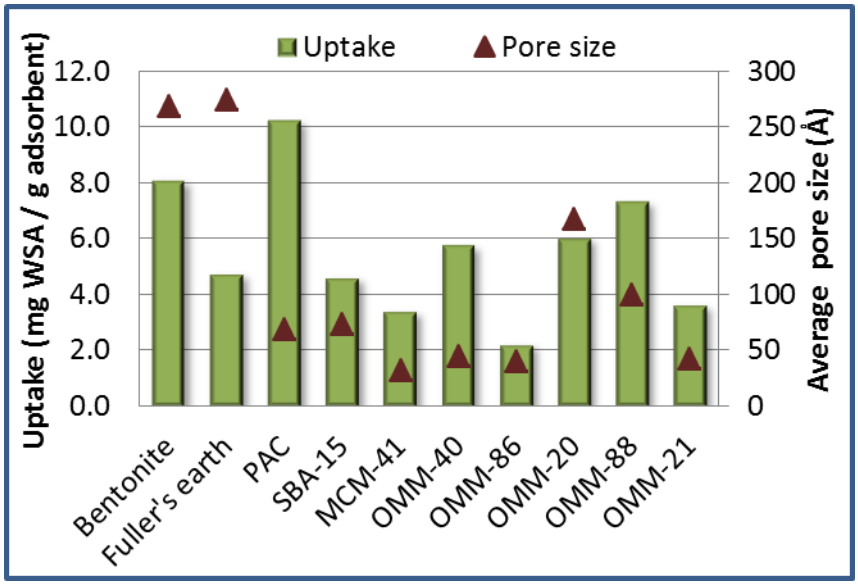

Figure 4.4. WSA quantitative uptake and adsorbents average BJH pore sizes. Adapted from Manrique et al, 2013.

Quantitative tests were performed by triplicate for each adsorbent, with a maximum deviation of 15% for bentonite and MCM-41 and less than 6% for the other studied solids. Once again, these errors can be attributed to the powder nature of both adsorbents which can float from the bottom of the spectrophotometer cell even with the slightest movement, leading to errors in the equipment.

PAC was confirmed to have the strongest affinity towards WSA, compared with the other studied materials, adsorbing 10 mg WSA per gram of solid. In a time frame of two hours, this solid was the only one that adsorbed the total amount of asphaltenes solubilized in the aqueous solution; just after 50 minutes, absorbance readings were zero. Activated carbon fast adsorption rate and adsorption capacity makes it a strong adsorbent/catalyst candidate for testing WSA adsorption in continuous mode, and potentially for scaling up the process to an industrial level in which contact times and concentrated asphaltenes solutions are key parameters.

Figures 4.3 and 4.4 show that the next best-ranked solid is bentonite, closely followed by the iron silicate materials (OMM-88 and OMM-20) and OMM-40. In both qualitative and quantitative evaluations, iron silicate materials showed better uptakes than those obtained with OMM-40 and OMM-86, suggesting that iron could promote WSA adsorption. There are a number of studies that reported the favorable effect of iron on adsorption capacities in the waste water treatment industry. Just to name a few, an investigation on modified clays reported improved adsorption capacity with iron addition on these materials for removal of organic and inorganic compounds in aqueous

media (Jiang and Ashekuzzaman, 2012). Methyl orange adsorption was also explored by Asuha et al (2011) using mesoporous maghemite, a solid able to adsorb up to 90% of the initial methyl orange concentration contained in a waste water stream within a few minutes. Adsorption on iron oxides is also reported as an alternative for waste water treatment (Choo and Kang, 2003).

The assumption of high surface areas directly leading to large adsorption capacities has to be discarded as evidenced in quantitative tests outcomes. This property cannot be considered as the only indication of WSA adsorptivity since for example, MCM-41, a solid with 1300 m^2/g, exhibits one of the lowest performances in terms of asphaltenes uptake. Similarly, OMM-86 shows poor affinity towards WSA despite of its high surface area. The templating agent used for synthesizing OMM-86, even though it was removed during the calcination step, could have inhibited asphaltenes adsorption due to significant differences seen in WSA uptake between OMM-40 and OMM-86.

Likewise, pore size and WSA uptake don't seem to have a direct proportional relationship. Even though examined clays displayed an array of pores of large widths in the mesoporous region, their uptakes are comparable to those obtained with solids of much smaller average pore sizes, OMM-88 and SBA-15 respectively. Once again, textural properties alone cannot be chosen as indicators of WSA adsorption capacities for any particular solid. Uptakes have to be assessed by combining a number of factors: textural properties, wetting properties, kinetics, WSA properties and adsorption rates.

4.4 Adsorption isotherms

Isotherms are useful representations to thermodynamically analyze adsorption phenomena between species. Isotherms were plotted to study WSA adsorption on some surfaces using concentrated and diluted oxidized asphaltenes solutions. WSA uptakes are presented as function of the adsorbate concentration measured at the end of the experiment, denoted as Equilibrium concentration. These concentrations are computed in terms of TOC content (in mg/L) in all isotherms. WSA uptakes are quantified in mg/g of adsorbate, relying on TOC contents of the samples. Further information is discussed within this chapter.

4.4.1 Materials and methodology

Specific solids were chosen to create adsorption isotherms: PAC, OMM-20, OMM-40, OMM-21 and MCM-41. The adsorption isotherm using activated carbon in granular form

was also addressed; this solid was tested with different concentrations of WSA, and using solutions derived from potassium salts of humic acid.

Granular Activated Carbon (GAC) was purchased from Sigma Aldrich with a specific particle size ranging between 20 to 40 mesh (420 µm to 841 µm) in order to meet specifications required for the continuous setup. Solid potassium humate obtained from Angostura Humics C.A. was solubilized in water at different concentrations spanning from 10 ppm by weight to 10,000 ppm by weight. Likewise, several WSA solutions in the range of 10 ppm to 9,000 ppm by weight were prepared by diluting the concentrated batch referred in section 4.2.2. Once prepared, WSA and potassium humate solutions were analyzed in the TOC apparatus.

0.5 grams of each solid (weighed to the nearest milligram) were put in several glass vials, and 20 mL of WSA solutions at different concentrations were added to each one. Then, vials were placed in the shaker for 72 hours at room temperature, allowing enough time to reach equilibrium. At the end of this time frame, solutions were filtered and their organic carbon content was assessed. The same procedure was repeated using GAC and potassium humate solutions at different concentrations.

4.4.2 Results

Subsequent isotherms are grouped to compare adsorption dynamics of activated carbon in powder and granular form, and differences between WSA solutions and potassium humate solutions using the same adsorbent. GAC, OMM-20 and MCM-41 isotherms are presented in one chart for adsorbent families' comparison, as well as synthetized representatives of OMM types. Equilibrium concentrations are displayed in terms of TOC content (in mg/L) in all graphics below, and uptake was assessed in terms of mg of TOC per gram of adsorbent.

Isotherms for GAC and PAC (Figure 4.5) practically overlap in the low equilibrium concentrations region (1,000 mg/L and lower), in which ≤ 3,000 ppm by weight WSA solutions were used. Up to this point, prepared solutions were 6 times more concentrated than those used for quantitative and qualitative analyses, and asphaltenes uptake went up 5 times in relation to the amount adsorbed using the 500 ppm solution.

At more concentrated regions, PAC and GAC display dissimilarities in terms of uptakes and equilibrium concentrations. However, it is crucial to understand that concentrations measured at equilibrium are not necessarily related to the same initial WSA concentration for both activated carbons. For instance, the last point in the PAC isotherm (5,110 mg/L; 157 mg/g) was obtained using the 10,000 ppm by weight WSA solution. Using the same batch and composition, equilibrium concentration for the

activated carbon in granular form was 4,400 mg/L and quantified uptake was almost 200 mg/g. In this perspective, it is possible to think that GAC improves the overall water soluble asphaltenes adsorption compared to the powdered solid at high WSA concentrations.

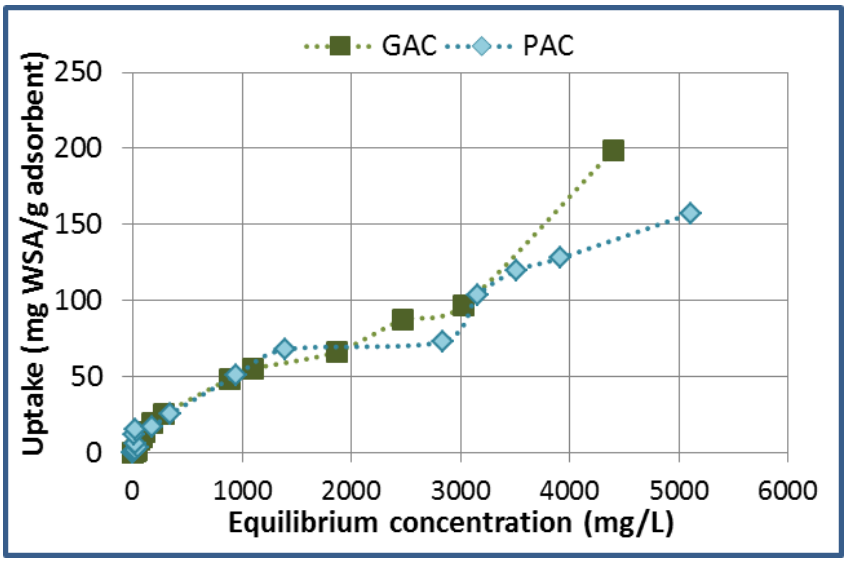

Figure 4.5. WSA adsorption isotherms (at room temperature) on GAC and PAC.

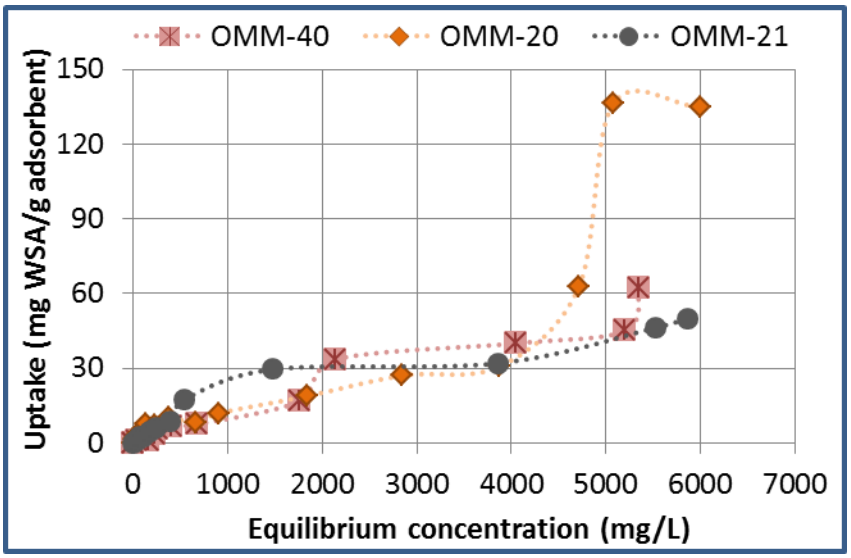

Figure 4.6. WSA adsorption isotherms (at room temperature) on Ordered Mesoporous Materials.

The shape of the PAC curve suggests a type IV adsorption isotherm, where multilayer adsorption occurs. As for the GAC isotherm, it might be the same type displayed for PAC; however, the plateau is not as evident as the one seen for PAC within the range of 1,400

mg/L – 3,000 mg/L equilibrium concentration. More points are needed to unquestionably define the type of WSA-solid interaction, particularly for GAC. However, WSA solutions of organic content beyond 10,000 ppm were not used at any point of this research, consequently, full assessment of isotherms at higher WSA concentrations could not be carried out.

In Figure 4.6, in-house adsorbents isotherms at room temperature exhibit multilayer adsorption, characteristic of mesoporous materials. Plateaus identified in OMM-20 and OMM-40 curves designate these particular isotherms as type IV. WSA-OMM-21 interaction curve could be recognized as a type IV isotherm, with a second layer beginning to form at equilibrium concentrations larger than 4,000 mg/L.

Experiments carried out using the most concentrated WSA solutions (10,000 ppm by weight), resulted in concentrations measured at equilibrium of around 6,000 mg/L TOC for OMM-20 and OMM-21. Yet, the iron-silicate based material adsorbed more than two times the copper-silicate solid uptake, with a final adsorbed quantity of 135 mg WSA/g. Overlapping between OMM-20 and OMM-21 is also seen at an equilibrium concentration of 3,900 mg/L and WSA uptake of 30 mg/g; however, the points were obtained using a WSA solution of 5,000 ppm by weight in the case of OMM-21, and a 6,000 ppm by weight WSA solution for OMM-20. These values illustrate OMM-20's affinity towards WSA, found stronger than that of the copper based material.

The adsorption capacity of OMM-20 is also demonstrated at the last point in the OMM-40 curve (5,300 mg/L; 62 mg/g). The uptake obtained with the 10,000 ppm by weight initial WSA solution, was the same achieved with OMM-20 at a less concentrated WSA solution of 6,500 ppm by weight. Data and analyses support previous hypothesis about adsorption enhancement by incorporation of iron in the ordered mesoporous materials.

As for MCM-41, it proved to be the less effective material for adsorption of WSA at high concentrations (Figure 4.7). Not only was the equilibrium concentration the highest with the most concentrated WSA solution, but the final uptake was less than 50 mg/g adsorbent. Figure 4.7 is plotted with an uptake scale that prevents identification of the benchmark material isotherm. With proper zooming, this isotherm is identified as type IV and the first layer is formed at equilibrium concentrations below 100 mg/L, corresponding to prepared WSA solutions of ≤ 200 ppm by weight.

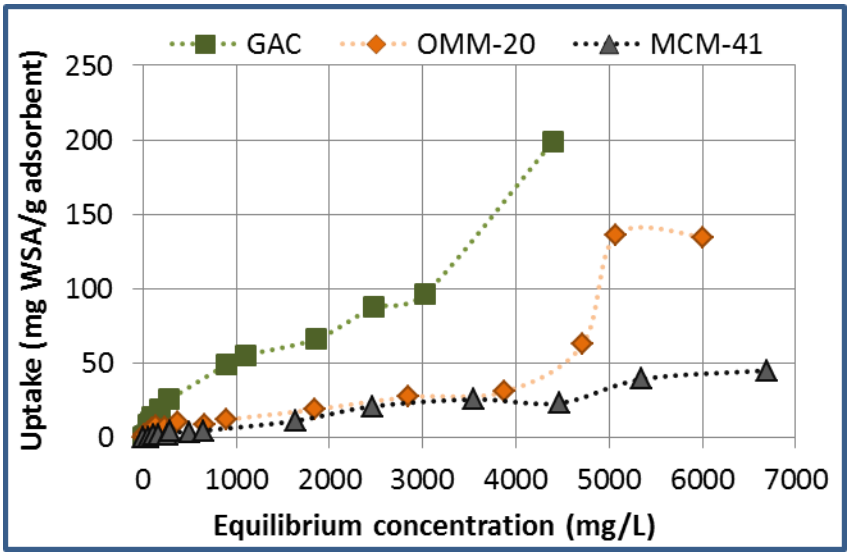

Figure 4.7. WSA adsorption isotherms (at room temperature) on GAC, iron-silicate based OMM and benchmark MCM-41.

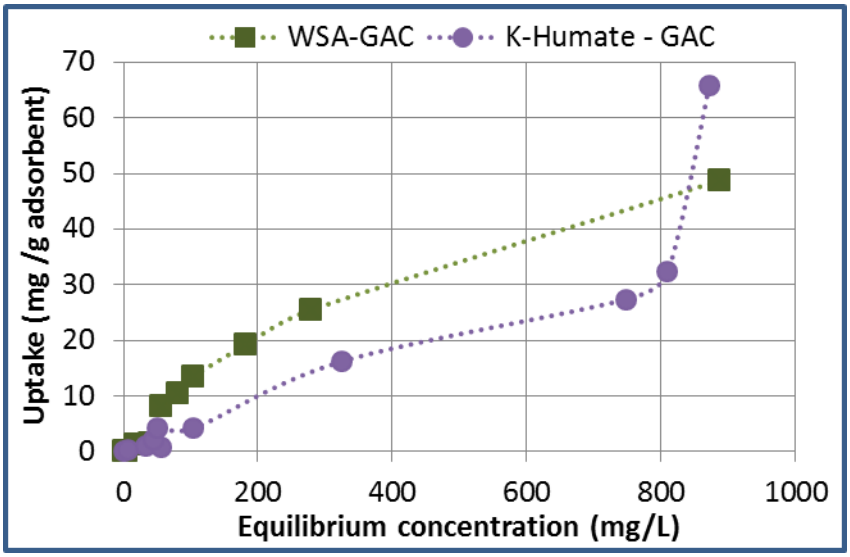

Figure 4.8. WSA and Potassium humate adsorption isotherms (at room temperature) on GAC.

The last figure shown in this chapter provides interesting information in regards to WSA – humic acids similarity. In order to facilitate visual comparison, WSA-GAC isotherm is plotted only within the same range of equilibrium concentrations reached using the potassium humate solution.

Experiments for the 10,000 ppm by weight potassium humate solution ended up in a measured equilibrium concentration of around 880 mg/L organic carbon. The same equilibrium concentration was obtained utilizing GAC with an initial WSA concentration

of 2,500 ppm by weight. The highly concentrated potassium humate solution (10,000 ppm by weight) had an initial TOC content of 2,500 mg/L, and the calculated uptake on GAC was 66 mg C/g. The 6,000 ppm by weight WSA solution had an initial TOC concentration of around 2,470 mg/L, however, the adsorption capacity of GAC after 72 hours was 89 mg C/g, exceeding potassium humate uptake by 35%.

Results discussed above indicate that prepared humic acid solutions are not exactly comparable to WSA in terms of carbon content, which imply differences in molecular size and/or functionalities. Differences in 10,000 ppm by weight WSA and potassium humate solutions indicate that the amount of soluble organic carbon in the last one is less than half compared to the TOC content of oxidized asphaltenes. Even with equal total organic carbon concentrations in both solutions, WSA exhibited more affinity towards activated carbon than that of humic acids. Multilayer adsorption was also seen in the potassium humate experiment, with the second layer presumably formed after equilibrium concentrations of 7,200 mg/L (6,500 ppm by weight initial solutions). Yet, at the same carbon concentrations in the WSA solution, there is no indication of pores saturation.

5. CONTINUOUS WSA ADSORPTION STUDIES IN A PACKED BED REACTOR

Chapter 5 deals with all items related to water solubilized asphaltenes adsorption in continuous operation, including pilot plant design considerations, experimental plan, adsorbent characterization and evaluation of different operating conditions. Granular activated carbon was chosen to pack the reactor as a result of its effective adsorption performance and other features that made it suitable to modify as a catalyst for hydroprocessing experiments.

5.1 Bench-scale unit design

A bench unit was designed and built to fulfil both adsorption scale-up purposes and hydroprocessing of the adsorbed material. Several types of reactors are employed for hydroprocessing, but fixed bed reactors are a convenient bench configuration for hydroprocessing of petroleum residue. Specifically for this project, a packed bed reactor was selected to test adsorption/hydroprocessing of WSA; its easy operability, undemanding building and straight forward assembling make this system preferable compared to ebullated or moving bed processes.

Some basic parameters were defined at the beginning of the process design; reactor size was the most important one, specified to provide a 5 grams capacity of adsorbent/catalyst. As previously mentioned, activated carbon in granular form was chosen to fill the reactor. The range of operating conditions was another key parameter in consideration as it defined materials and parts in the bench unit, especially valves packing.

Once the reactor capacity was defined, the bench plant scheme was designed. Appendix B presents the Piping and Instrumentation Diagram for the unit as built, incorporating comments from the HAZOP study (Appendix C), and other modifications that took place while constructing the unit. A block diagram presenting main sections of the unit is shown in Figure 5.1. The Standard Operating Procedure (SOP) for this setup is attached in Appendix D.

5.1.1 Unit overview

The adsorption/hydroprocessing unit consists of five major zones: feed section, adsorption/reaction zone, liquids pressurization and sampling zone, hydrogen injection

zone and hydroprocessing products separation zone; each section is highlighted in Figure 5.1 by black, orange, purple, green and red doted squares, respectively.

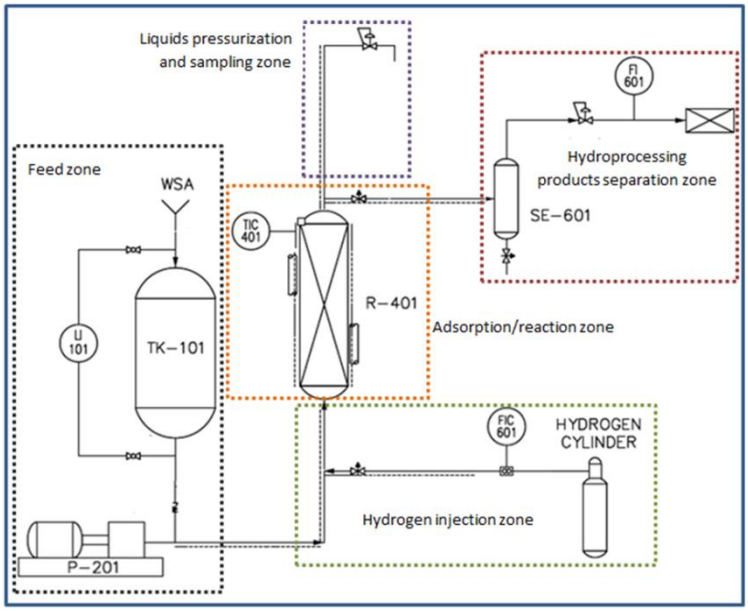

Figure 5.1. Adsorption/hydroprocessing unit block diagram.

Adsorption experiments were carried out utilizing the feed zone, the reactor and the liquids pressurization and sampling zone. First, the WSA solution was loaded in the pump and then sent to the reactor through heated, insulated lines, passing through the packed bed at a specific temperature. The reactor effluent was routed to the liquids pressurization and sampling zone in which liquids were collected in glass vials for further analyses.

Once asphaltenes are adsorbed, hydroprocessing of the adsorbed WSA is achieved by injecting pre-heated hydrogen to the reactor at the specific flow rate delivered by the mass flow controller. Hydroprocessing took place in the reactor while generated products were sent to the separation zone. In there, gases were splitted and aligned to a gas chromatograph for online analysis. On the other hand, liquids were accumulated in the separation vessel and collected at the end of the hydroprocessing run.

With just a few exceptions, all connecting lines were built in 1/8” stainless steel tubing purchased from Swagelok; likewise, the feed tank, the separation vessel, the pump cylinder and all valves are made of stainless steel. Equipment and instrumentation details are discussed shortly.

5.1.2 Feed section

This zone covers the feed tank TK-101, the positive displacement pump P-201, the pressure relief valve PSV-201, blocking valves, check valves and others. Table 5.1 lists all valves comprised in the feed section, as well as their maximum operating conditions and design conditions given by the manufacturer. Despite the rated pressures exceeding by far the maximum operating pressure, PSV-201 was set to 200 psig due to low operating pressures conceived for this particular zone.

Table 5.1. Valves and operating conditions of the feed zone.

Valve	Service	Type	Max. operating conditions		Manufacturer Rating	
			T (°C)	P (psig)	T (°C)	P (psig)
V-101	WSA to feed tank valve	Ball	Room	50	148	2500
V-102	Tank block valve	Ball	Room	10	148	2500
V-103	Tank drain valve	Needle	Room	10	232	3435
V-104	WSA to pump suction valve	Ball	Room	10	148	2500
V-105	Pump suction check valve	Lift	Room	10	482	3820
V-106	Bypass pump suction check valve	Ball	Room	10	148	2500
V-107	Level indicator valve	Plug	Room	10	204	1000
V-108	Level indicator valve	Plug	Room	10	204	1000
PSV-201	Pressure relief valve	Spring	120	200	121	350
V-201	Pump discharge check valve	Lift	120	80	482	3820
V-202	Pump discharge block valve	Ball	120	80	148	2500
V-203	Pump discharge drain valve	Needle	120	80	232	3435

A heating tape (120 Volts, HTS/Amptek) was installed at the pump discharge line for pre-heating, controlled by the temperature read at the surface of the stainless steel line (TIC-201). The fluid temperature was measured with the thermocouple TI-201 and read in a local temperature indicator from Omega Instruments.

TK-101 is a 300 mL vessel purchased from Swagelok, rated at 426°C and 930 psig, or 1800 psig at room temperature. A level indicator (LI-101) and a pressure gauge (PI-101) were attached to the tank inlet for monitoring WSA loading and suction operations. The SOP attached in Appendix D explains these and all other operational procedures.

P-201 is a high pressure Teledyne ISCO syringe pump model 500, with 507.4 mL of cylinder capacity and a minimum delivered flow rate of 1 µl/min. It has a pressure indicator used as the pressure gauge PI-201 backup, installed before the block valve V-202.

5.1.3 Adsorption/Reaction zone

This section consists of an upflow packed bed reactor (R-401) and associated instrumentation. Based on past experiences in the CBU pilot plant, reactor diameter was set to 3/8" nominal size. GAC particle size was chosen to meet chemical reactors design criteria established by Rase (1977), in which reactor length (L), catalyst particle diameter (Dp) and reactor diameter (D) are key parameters taken into account to compute the following ratios:

1. L/Dp must be greater than 100 for gases in packed beds and greater than 200 for liquids in packed beds; these values assure that axial dispersion is negligible.
2. Dp/D must be below 0.1 in order to avoid bypassing (channeling).

From commercially available activated carbons, the one selected had a particle size between 420 µm to 841 µm, conveniently small to meet the second criterion but sufficiently large to minimize pressure drops. GAC apparent density value was used to calculate an approximate reactor length to hold 5 grams of adsorbent, and with this computed value (L = 26 cm), the first criterion was also satisfied. Once GAC was purchased, trials were made to check the required reactor dimensions and finally, the reactor length was fixed at 25 cm. Mesh-300 rings and a metallic porous washer were used, custom-fitted to the reactor inner diameter to hold the bed together (Figure 5.2).

Figure 5.2. Mott porous metal and Mesh-300 rings washers.

Reactor heating was provided by a 120V heating tape, controlled by a thermocouple installed on the middle of the reactor's wall (TIC-401). Inlet and outlet connections to the reactor were insulated using fiber glass materials, and a tailored jacket supplied insulation to the setup core. A local temperature indicator (TI-401) showed the fluid temperature at the reactor's outlet. Two pressure gauges were placed at the reactor exit; one read pressures within the range of 0-200 psig (PI-401A) and the other one measured from 0 psig to 600 psig (PI-401B). Needle valves V-401A and V-401B allowed choosing the most appropriate instrument for each step of WSA processing.

The adsorption/reaction section was designed in such a way that it could be operated under a wide range of conditions without compromising the integrity of the unit. The

reactor R-401 was able to handle temperatures up to 400°C and pressures up to 800 psig, even though maximum operating conditions were not that severe (350°C, 600 psig)

5.1.4 Liquids pressurization and sampling section

This zone is delimited by a high temperature valve (V-501) that separated the high temperature section from this zone, in which much lower adsorption temperatures were used. Valve V-504 controlled the reactor upstream pressure, monitored through the gauge installed at the entrance of the back pressure valve (PI-501). A segment of this section was wrapped in a heating tape (120 Volts, HTS/Amptek), insulated by synthetic materials and temperature-controlled by the TIC-501 system; a local temperature indicator (TI-501) helped during the operation of the unit. Details of valves and intended operating conditions are listed in the following table.

Table 5.2. Valves and operating conditions of the liquids pressurization and sampling zone.

Valve	Service	Type	Max. operating conditions		Manufacturer Rating	
			T (°C)	P (psig)	T (°C)	P (psig)
V-501	High temperature block valve	Needle	380	600	648	1715
V-502	Liquid sampling block valve	Ball	100	80	148	2500
V-503	Liquid sampling drain valve	Needle	80	80	232	2500
V-504	Liquid back pressure valve	Back Pressure	80	80	200	250

5.1.5 Hydrogen injection zone

This zone delivered a constant flow rate of hydrogen during WSA hydroprocessing. Ultra-high purity hydrogen of 99.999% from Praxair was connected to the setup through a pressure regulator which allowed setting the delivered pressure to the preferred value. Hydrogen was injected to the mass flow controller FIC-301 (Brooks Instruments, model 5850S), which provided a maximum flow rate of 100 SCCM at a fixed pressure drop of 50 psig. Line heating was supplied by 120 Volts heating tapes, controlled by the tubing external wall temperature through the TIC-301 system. The local temperature indicator TI-301 was strategically mounted as close to the reactor inlet as possible, in which injected gas temperatures were constantly monitored. Heated sections were insulated with fiber glass materials to prevent heat losses.

The pressure sensor PI-301 was located before the heated segment of the hydrogen line and enabled pressure readings downstream the flow controller. The pressure relief valve PSV-301 was adjusted to activate at 1000 psig and discharged to the enclosure exhaust. Specifics on valves in this section are summarized in Table 5.3.

Table 5.3. Valves and operating conditions of the hydrogen injection zone.

Valve	Valve Service	Type	Max. operating conditions		Manufacturer Rating	
			T (°C)	P (psig)	T (°C)	P (psig)
PSV-301	H_2 overpressure relief	Spring	Room	1000	135	1500
V-301	H_2 cylinder regulator	Self-Actuated	Room	710	80	3600
V-302	H_2 Flow Controller	Needle	Room	710	232	3435
V-303	H_2 Flow Controller bypass	Needle	Room	710	232	3435
V-304	H_2 check valve	Poppet	380	600	482	3820
V-305	H_2 reactor inlet	Needle	380	600	648	1715
V-306	Depressurization	Needle	250	600	315	3130

5.1.6 Hydroprocessing products separation zone

Gas and liquid products from hydroprocessing reactions were aligned to this section; its main features include a biphasic separator (SE-601), a gas flow rate meter and an online gas chromatograph. Table 5.4 summarizes valves, rated and operating conditions of the hydroprocessing products separation zone.

The segment closer to the blocking valve V-601 was provided with a heating system similar to those already described for other sections of the unit. TI-601 displayed the temperature measured by a thermocouple contacting hydroprocessing products while flowing through the insulated tubing. A non-insulated section was deliberately conceived upstream the separator SE-601 in order to condensate volatile material and adequately split the incoming mixed flow.

The separator vessel was made of 6.5 cm long 3/8” stainless steel tubing installed before the back pressure V-604. This valve and the pressure gauge PI-601 maintained and monitored the reactor pressure at the desired values. A digital flow meter from Omega Instruments (model FMA-4001) quantified the gas stream flow rate within the range of 0.1 SCCM to 10 SCCM. The instrument included local display and data acquisition system that recorded flow rate values in the computer. A condensate trap was installed upstream the flow indicator to prevent liquids from entering the instrument.

A three way valve (V-608) allowed aligning the gas stream to the GC or to the safe depressurization system. The last one consists of a line that ends into a KOH solution glass container, in which produced gas was bubbled through and then vented to the enclosure exhaust. The same valve was used to route the gas stream through the gas chromatograph, an SRI multiple gas analyzer model 8610, calibrated to detect

combustion products (CO, CO_2), light hydrocarbons from C_1 to C_5, and sulfur-containing components such as SO_2 and H_2S.

Table 5.4. Valves and operating conditions of the hydroprocessing products separation zone.

Valve	Valve Service	Type	Max. operating conditions		Manufacturer Rating	
			T (°C)	P (psig)	T (°C)	P (psig)
V-601	High temperature block valve	Needle	380	600	648	1715
V-602	Gas stream block valve	Ball	80	600	148	2500
V-603	Liquids drain valve	Needle	80	600	315	3130
V-604	Gas back pressure valve	Back pressure	60	600	200	3000
V-605	Condensates trap valve	Needle	30	600	232	3435
V-606	Flow meter block valve	Needle	30	600	232	3435
V-607	Flow meter bypass valve	Needle	30	600	232	3435
V-608	Gas three way valve	Ball	30	600	148	2500

Table 5.5. Valves and operating conditions of the pressurization system.

Valve	Service	Type	Max. operating conditions		Manufacturer Rating	
			T (°C)	P (psig)	T (°C)	P (psig)
V-701	N_2 cylinder regulator	Self-Actuated	Room	600	80	3600
V-702	Gas check valve	Poppet	Room	50	482	2185
V-703	Liquids check valve	Lift	Room	50	232	3820
V-704	N_2 to feed tank	Needle	Room	50	232	3435
V-705	N_2 to top of reactor	Needle	Room	10	232	3435
V-706	N_2 to bottom of reactor	Needle	Room	50	148	3435
V-707	N_2 three way valve	Three way	Room	800	400	2500
V-708	N_2 flow control valve	Needle	Room	800	190	2000
V-709	N_2 gas check valve	Poppet	Room	800	148	2185
V-710	N_2 three way valve	Three way	Room	800	190	2500

5.1.7 Pressurization system

The bench-scale plant is equipped with a pressurization system not shown in the block diagram, yet displayed in the P&ID (Appendix B). It consists of a nitrogen cylinder that supplied the gas to different places by an array of needle valves placed in tactical spots. This system delivered nitrogen to the feed tank TK-101 to contribute to the pump suction head, as well as it helped pressurizing the unit at the beginning of adsorption runs. It was also used as a purging agent after packing sulfided catalysts (refer to

Chapter 6 for more details) and as a cleaning carrier at the end of both adsorption and hydroprocessing steps. Valves V-707, V-708, V-709 and V-710 were arranged to provide quenching during hydroprocessing of pre-adsorbed asphaltenes when required. Specifications and service of each instrument that conform this system are explained in

Table 5.5.

5.2 Adsorption experiments procedure

The bench-scale setup was assembled aiming to study WSA adsorption in a continuous mode. For this purpose, temperature and WSA flow rate were the operating parameters chosen to evaluate their impact on the adsorption of oxidized asphaltenes, using packed GAC.

5.2.1 Materials

5.2.1.1 GAC

GAC attributes have been discussed in preceding sections of the document; however, its textural properties and others are listed in Table 5.6. Textural properties were measured using the same general procedure previously discussed in Chapter 4 (section 4.1.2): degasified GAC was placed inside the Micromeritics Surface Area and Porosity System Analyzer for BET surface area and average pore size evaluations.

Table 5.6. Granular activated carbon characterization.

GAC Property	Value	Comments
BET surface area	615 m^2/g solid	Nitrogen physisorption
Average pore size	72.9 Å	BJH desorption method
Mass loss from 200°C to 700°C	86 wt%	Thermal Gravimetric Analysis

Remarkably, GAC has half of the total surface area compared to PAC (1300 m^2/g), the solid utilized in batch experiments. This is a major hint indicating that the nature of the granular solid is not completely identical to the activated carbon in powder form, and therefore, differences in adsorption uptakes are anticipated.

Thermal Gravimetric Analysis (TGA) was employed to analyze the decomposition temperature of activated carbon and its thermal stability at hydroprocessing conditions. This technique tracks mass loss as a function of increasing temperature, and in this project it was used as an indication of foreign species present in the adsorbent. TGA analysis was performed in a SDT Q600 system from Thermal Analysis Instrument

Company, in which 6.5 mg of GAC weighed to the nearest 0.005 mg were placed in a ceramic holder and introduced in the apparatus chamber. The instrument was programmed to increase the chamber's temperature to 900°C at a heating rate of 10°C/min, utilizing 100 mL/min of high purity nitrogen to pyrolyze the sample.

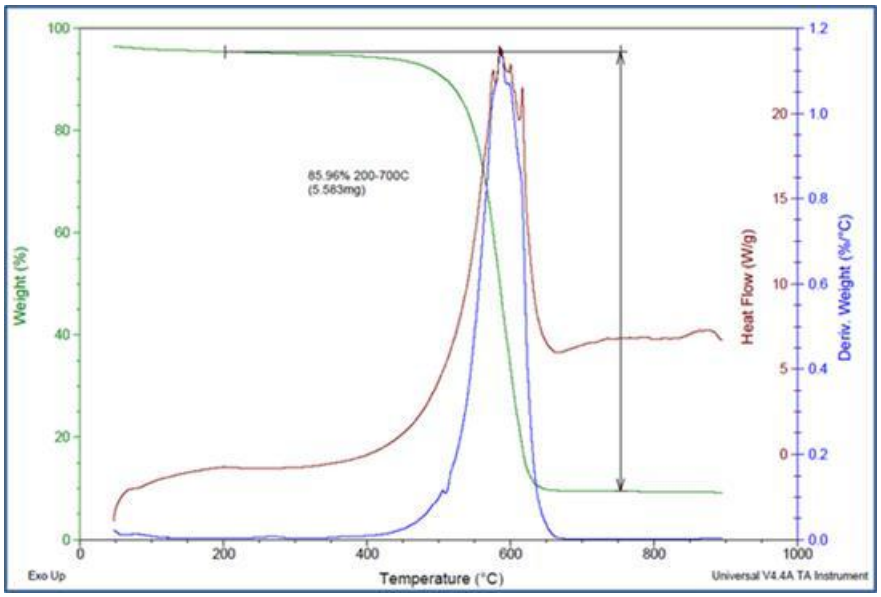

Figure 5.3. Thermogravimetric Analysis of granular activated carbon.

TGA results shown in Figure 5.3 demonstrated that after 650°C, 14% of mass didn't pyrolyze under the nitrogen environment. X-ray Photoelectron Spectroscopy (XPS) and X-ray Diffraction analyses will be addressed in the next chapter to detect any minerals crystalline materials that may be on the activated carbon surface. Metal analysis of the GAC sample showed just a few amount of metals in the bulk (less than 0.2 wt%); based on these quantities, the remaining material could only be microcarbon residue and mineral species.

On the other hand, Figure 5.3 provides information in regards to the thermal stability of the adsorbent. It is inferred that GAC is a stable material below 500°C since 5% mass loss is displayed at temperatures slightly above this value. This temperature was critical for determining the most severe condition under which hydroprocessing experiments were performed, and as stated in previous paragraphs, the maximum hydroprocessing operating temperature was set to 350°C.

Methodologies and materials used for WSA production were already described in Chapter 3. The solution used in the following experiments was a blend of batches prepared at 220°C, 230°C and 240°C using 3 hours of residence time for each temperature. The final mixture had the properties shown in Table 5.7.

Table 5.7. Characterization of WSA solution for adsorption in continuous operation tests.

WSA property	Value	Comments
TOC content	8,892 ± 40 mg/L	Std. deviations given by the TOC analyzer
IC content	103 ± 5.5 mg/L	Std. deviations given by the TOC analyzer
pH	8.4	At room temperature

5.2.2 Methodology

WSA adsorption in continuous mode was evaluated by changing two operating conditions: asphaltenes solution flow rate and adsorption temperature. However, the amount of GAC packed in the reactor (5 grams) and the WSA solution initial concentration (denoted as Co, ≈ 9,000 mg/L) were fixed parameters for all adsorption experiments. It is important to mention that the adsorbent was placed in the vacuum oven for overnight drying (-25 mm Hg, 70°C) before packing the reactor to remove moisture and possible adsorbed gases.

Adsorption tests began by loading enough WSA in the pump, taking into account dead volumes and the duration of the experiment. Then, the system was pressurized with nitrogen to the desired value by manipulating valve V-504. The CN616 temperature controller software (Omega Instruments) allowed setting pre-heated lines temperature to 3°C above the selected adsorption temperature, whereas the reactor temperature was specified between 5°C to 10°C above. Wall temperatures were monitored through the controller software and once the set points were reached, temperatures were held for 30 minutes to stabilize the system. After this period, the pump switch was turned on and began pumping WSA at the indicated flow rate. Aliquots were collected at the exit of the back pressure valve at different time intervals, according to the WSA flow rate. At the end of the experiments, the pump switch was turned off, the system was depressurized and cooled down, and liquids still remaining in the setup were collected and quantified for mass balance purposes. Samples were assessed in the TOC-CPH analyzer from Shimadzu, in which each sample was injected three times to the combustion tube to compute an average of its TOC content. Once the setup was cooled down to room temperature, the packed bed was removed, dried overnight in the vacuum oven (-25 mm Hg, 70°C) and weighed the next day. Specifics on operating procedures are attached in Appendix D.

The experimental plan for WSA adsorption assessments is presented in Table 5.8. When the temperature effect was evaluated, a WSA flow rate of 3 cc/min was kept constant for 100 minutes in every test. Depending on the operating temperature, enough pressure was provided to assure that water soluble asphaltenes remained in liquid state

and didn't vaporize. In regards to the flow rate influence on WSA adsorption, conditions were 120°C and 70-80 psig for each velocity, and time frames were 300, 120 and 80 minutes for WSA rates of 1 cc/min, 3 cc/min and 5 cc/min, respectively.

Table 5.8. Experimental plan for WSA adsorption evaluation in dynamic operation.

Adsorption Conditions	WSA Flow rate		
	1 cc/min	3 cc/min	5cc/min
Room temperature, 10-15 psig		X	
80°C, 30-40 psig		X	
120°C, 70-80 psig	X	X	X

5.3 Results of WSA adsorption in continuous mode

Breakthrough curves were obtained by plotting normalized TOC concentrations (C/Co) versus time. Normalized concentrations were computed by dividing the TOC content of the aliquot at a given time (C) over the initial TOC content of the WSA solution (Co ≈ 9,000 mg/L, refer to Table 5.7). Average TOC values were reported by the TOC apparatus, with resultant standard deviations lesser than 2% of TC content. It is worth mentioning that IC content was negligible and TOC composition was taken as the sample TC composition.

Reproducibility tests were carried out by evaluating the same conditions (5 grams GAC, 120°C, 70-80 psig, 5 cc/min and Co≈ 9,000 mg/L) in three different days. Results shown in Figure 5.4 proved that the setup was reliable and experiment outcomes were reproducible. Obtained aliquots had to be filtered with hydrophilic nylon syringe filters (0.45 µm, Whatman) to remove fine powders suspended in the samples; even though suspended solids quantities were negligible, they could potentially damage the TOC apparatus and had to be removed before analytical procedures.

Every adsorption run closed with mass balances above 99%. Calculations considered dead volumes, amount of WSA loaded to the system according to pump readings, quantities of effluent aliquots and the weigh difference between the (dry) packed bed at the beginning and at the end of the experiment. In this case, WSA density was specified as 1 g/cc, but even if this property was set to 1.06 g/cc or 0.95 g/cc, mass balances still closed above 95%. These outcomes, along with reproducibility tests, confirmed the reliability of the system.

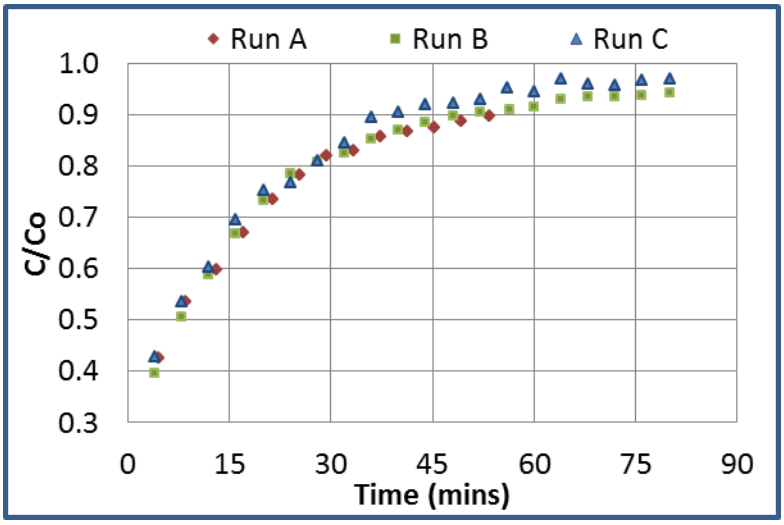

Figure 5.4. Adsorption reproducibility tests carried out at 120°C, 70-80 psig, 5 cc/min and WSA Co ≈ 9,000 mg/L.

5.3.1 Breakthrough curves of WSA adsorption at different WSA flow rates

Figure 5.5 displays the breakthrough curves for WSA adsorption at different flow rates and operating conditions illustrated in Table 5.8. "Saturation" of GAC occurred at the moment when C/Co ratio stabilized, in other words, didn't change with time. Results show that the bed was saturated after 300 minutes using a concentrated asphaltenes solution (about 0.9 wt%) at the slowest evaluated flow rate. When WSA was pumped at 5 cc/min, C/Co ratio was held constant after 70 minutes of contact time, whereas saturation was reached after 90 minutes utilizing a flow rate of 3 cc/min. These values showed that the adsorption process is relatively fast, considering the small amount of GAC in the packed reactor (5 grams).

Saturation times decreased when flow rate increased as the WSA residence time in the bed is reduced at higher flow rates. Adsorption equilibrium concentration may not be reached and consequently, asphaltenes are not adsorbed at the column potential extent and the effluent concentration increase faster. Expectably, breakthrough curves steepness rose up at higher flow rates since the rate of mass transfer increases at faster velocities. In other words, the column mass transfer zone was broadened when operated at lower WSA flow rates and effluent concentrations increased at a slower proportion. These results are in agreement with other dynamic adsorption studies in packed columns reported in the literature (Zeinali et al, 2010; Gupta and Babu, 2010; Yahaya et al, 2011; Hosseini and Fatemi, 2013).

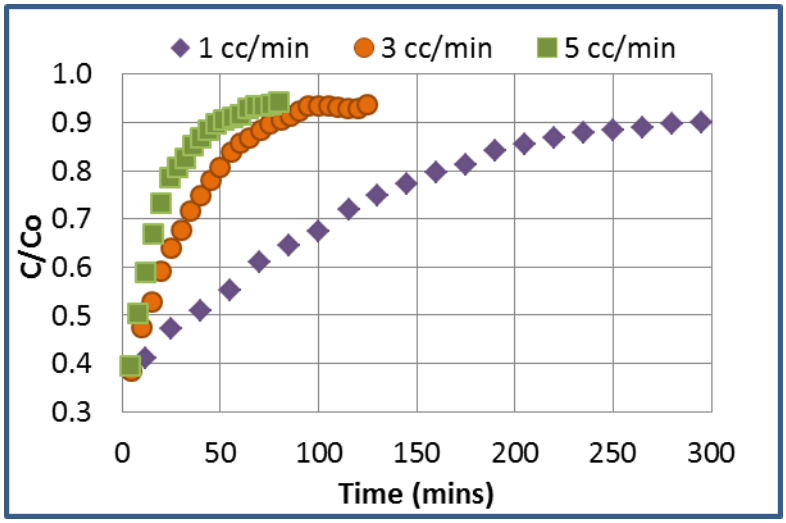

Figure 5.5. WSA adsorption on 5 grams of GAC at 120°C, 70-80 psig, and different WSA flow rates.

It is important to bring up to discussion the fact that C/Co ratio was not larger than 0.92 in the green and red curves, and likewise, the trend shown by the purple diamonds line seems to increases very slowly that is hardly recognizable. Theoretically, saturation (or exhaustion) time is ideally defined when C/Co values reach 1.0, but generally beds saturate at 0.9-0.95. This has been the case for several studies in packed bed reactors, such as biosorption of metals (Oliveira et al, 2011), removal of Cr(VI) and Cu(II) from aqueous solutions (Gupta and Babu, 2009; Salmani et al, 2013)), among many others. In particular for activated carbon, researchers have reported exhausted packed beds at C/Co < 0.95 for dichloromethane adsorption from aqueous phase (Zeinali et al, 2010), adsorption of organic components from oil refinery wastewater (Hosseini and Fatemi, 2013), Cu(II) removal from water using rice husk based activated carbon (Yahaya et al, 2011), and natural organic matter adsorption from groundwater on GAC (Fettig, 1999). These outcomes were attributed to short experimental time frames, in which the provided contact time between the adsorbent and the adsorbate was not sufficient, and the driving force (concentration gradient) was not enough to fully exhaust the bed. Adsorbate-adsorbate parallel interactions could also be involved in the delayed saturation of the GAC bed.

5.3.2 Breakthrough curves of WSA adsorption at different temperatures

Adsorption tests were carried out at room temperature, 80°C and 120°C for 100 minutes at a constant asphaltenes flow rate of 3 cc/min. As explained in section 5.2.2, GAC was dried overnight at vacuum conditions before packing the reactor. Adsorption pressures were fixed according to the guidelines provided in the experimental plan (page 61), and

the WSA initial concentration was the same for every test (Co≈ 9,000 mg/L). At the end of each experiment, the overnight dried bed (at -25 mm Hg and 70°C) was weighed and WSA uptake was computed by the difference between the initial and the final weight of the packed bed. Breakthrough curves are shown in Figure 5.6 and asphaltenes uptakes are presented in Table 5.9.

Table 5.9. Asphaltenes uptakes after dynamic adsorption experiments at different temperatures.

Temperature	Asphaltenes uptake (mg/g)
Room	139
80°C	202
120°C	175

The lowest asphaltenes uptake corresponds to the room temperature test. At 80°C, asphaltenes uptake is improved and almost 20% in weight of asphaltenes, with respect to the adsorbent weight, were adsorbed at these conditions. As for the highest temperature, WSA adsorption is still better than the one exhibited at room temperature, and it is somehow similar to that calculated at 80°C; even though WSA uptake at 120°C (175 mg/g adsorbent) is not the best observed, the same conclusion regarding the beneficial effect of temperature is derived. This outcome, in which an optimum adsorption point is observed at an intermediate temperature, was reported for toluene adsorption (in gas phase) on activated carbon fibers by the team of Das et al (2004).

Figure 5.6 evidenced that room temperature was the least favorable condition studied because the bed was exhausted quicker in relation to higher temperatures. Bed saturation was only observed in the room temperature test; probably higher temperatures became beneficial in terms of kinetic energies which increased asphaltenes diffusivity to the surface of the solid. Association or multilayer adsorption could also explain this behavior, perhaps the adsorbate-adsorbate weaker interactions between the first and subsequent layers contributed to the overall uptake as if physisorption was taking place. Adsorption at room temperature could resemble a chemisorption process in which stronger interactions between the adsorbate and the adsorbent were formed, but limited to only one layer, reducing the overall WSA uptake.

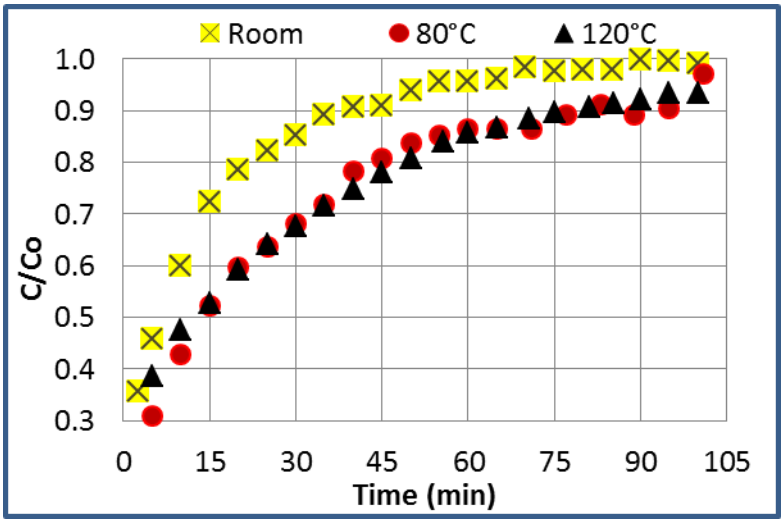

Figure 5.6. WSA adsorption on 5 grams of GAC at room temperature, 80°C and 120°C, at constant WSA flow rate of 3 cc/min.

The red dots and black triangles suggest trends with less steep curves compared to the room temperature experiment, indicating a slight adsorption enhancement. The 80°C and 120°C curves overlapped in some sections, yet the difference in asphaltenes uptake was showcased during the first 15 minutes of the experiment.

5.3.3 Additional remarks

Breakthrough curves in this study advise that longer columns and lower flow rates would have resulted in more detailed breakthrough curves before the onset point, and normalized concentrations below 0.4 could have been achieved. However, lower flow rates meant longer experimental operation times and this would limit the number of experiments that could have been ran. In addition, 12 mL was the minimum aliquot volume required to analyze the TOC content of a sample, a manufacturer constrain that cannot be modified. If only small amounts of sample are available, dilution would cause more problems related to accuracy and addition of systematic errors would be inevitable.

Small particles retrieved in the effluent stream did not became a major concern because these didn't impact overall mass balances or pressure drops in the reactor. However, the nature of these solids had to be identified in order to determine their potential influence on adsorption and hydroprocessing. The origin of these powders was believed to be either dragged activated carbon being pulverized during the dynamic adsorption experiments, or precipitated asphaltenes from the WSA solution due to changes in the solution pH. Therefore, FTIR analyses were carried out on different samples: the filtered solid from the column effluent, an insoluble particle retrieved during WSA production,

and asphaltenes from a solubilized solution. Generated spectra were recorded by the equipment described in page 28.

To validate the first hypothesis, GAC spectrum (in blue) was compared to the adsorption column effluent spectrum (in red) as shown in Figure 5.7. Clearly, peaks in the whole range of wavenumbers are different for both samples, demonstrating that suspended solids in the column effluent are not activated carbon powders caused by adsorbent attrition. To set an example, the peak in the red spectrum between 1600 cm^{-1} and 1700 cm^{-1} is completely inexistent in the activated carbon; this strong signal seems to be the contribution of carboxylic acids (RCOOH), carboxylate anions ($RCOO^-$), and aromatics. Not only this peak but the overall difference in spectra suggests that these solids are not similar in nature.

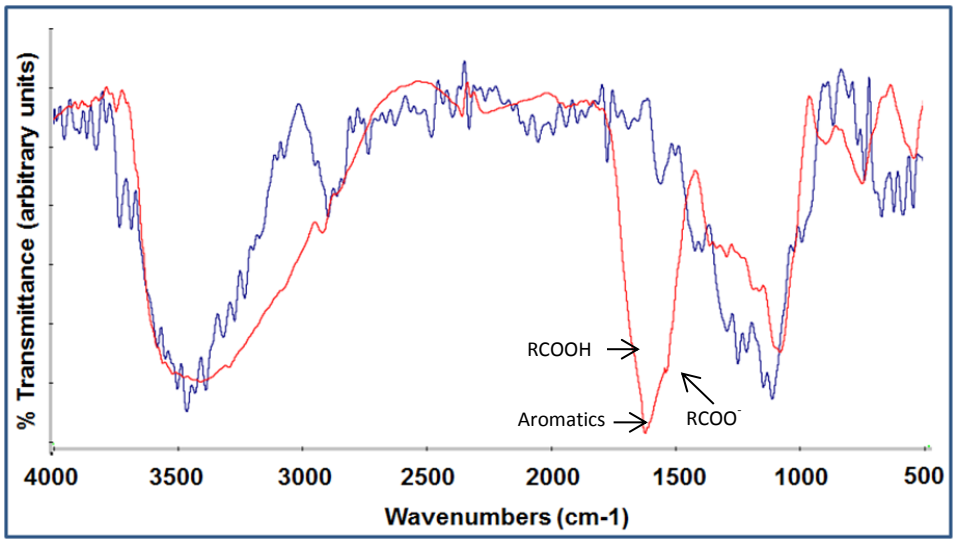

Figure 5.7. FTIR spectra of GAC (in blue) and adsorption column effluent (in red).

The effluents pH was recorded for two adsorption experiments carried out at 80°C, 3 cc/min, utilizing 5 grams of GAC and a WSA solution of initial organic carbon concentration around 9,000 ppm. Measurements are plotted in Figure 5.8.

Evidently, pH jumped down in both runs during the first 15 minutes of the dynamic adsorption run, but then it increased 0.5 beyond the initial pH and slowly stabilized down to the original value. These variations indicate that ionic interactions took place in the reactor; as pH is lowered, RCOO- protonation could be favored, thus, precipitating insoluble carboxylic acids. FTIR spectrophotometry was used once again to compare the recovered powder particles to the oxidized/solubilized asphaltenes. Insolubles

recovered from a WSA production batch at 300°C and 3 hours of residence time, were also scanned in the FTIR apparatus.

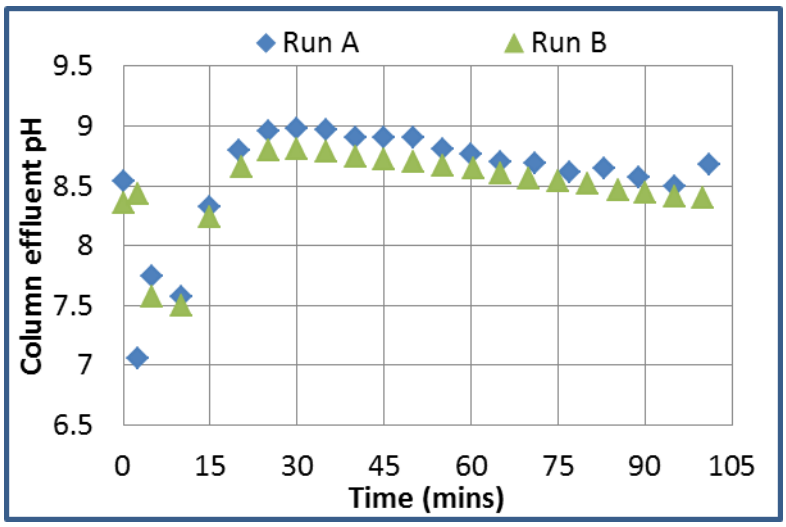

Figure 5.8. Column effluent pH for two WSA adsorption tests on 5 grams of GAC at 80°C and a constant WSA flow rate of 3 cc/min.

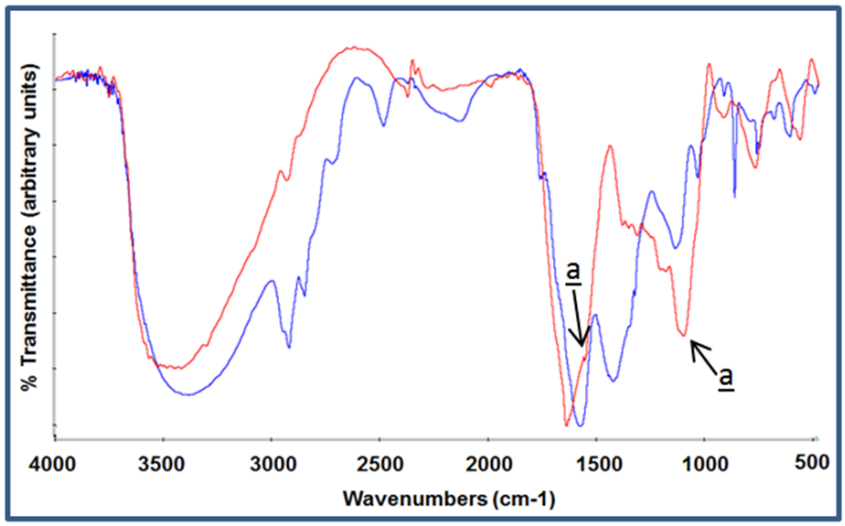

Figure 5.9. FTIR spectra of WSA (in blue) and adsorption column effluent (in red).

In Figure 5.9, WSA spectrum is represented by the blue line whereas the red line corresponds to the column effluent. The analyzed effluent is a sample withdrawn during the first 30 minutes of an adsorption test carried out at 80°C and pumping WSA at a flow rate of 3 cc/min.

Samples share some functionalities like the signals observed between 1580 $cm^{-1}$and 1630 cm^{-1}, corresponding to carboxylate anions. Sulfonic acids moieties are clearly

observed in both spectra, assigned to the peaks appearing at wavenumbers around 1200 cm^{-1}. Aromatics are evidenced in the blue and red curves at around 730 cm^{-1}. Nonetheless, other peaks are only existent in one of the samples. The effluent lacks of the alkyl functionalities present in the water soluble asphaltenes solution, as displayed in the 2900 cm^{-1} region and at 1480 cm^{-1}. An unknown peak vibrating at 2500 cm^{-1} is identified in the WSA solution but not in the suspended solids line. The zone comprised between 800 cm^{-1} and 1000 cm^{-1} highlight the fact that the spectra belong to different samples.

Another attempt was made to identify the nature of the powder collected from the outlet stream. Figure 5.10 shows the FTIR spectrum of insoluble material produced at preparing WSA solutions at 300°C and 3 hours of residence time (green line). The unknown powder spectrum is represented in red. Undoubtedly, suspended solids contrast in nature to unconverted asphaltenes recovered from the oxidation process. Alkyl functionalities produce a strong signal in the green spectrum but a weaker one for the effluent sample (2800-2900 cm^{-1} region). The two infrared bands at 1150 cm^{-1} and near 1500 cm^{-1} (denoted as a in the charts below) are typical of the single S=O bond, shown in the column effluent but undetectable in the unconverted asphaltenes spectrum. For these reasons, it can be concluded that column effluent does not resemble the insoluble material from WSA production processes.

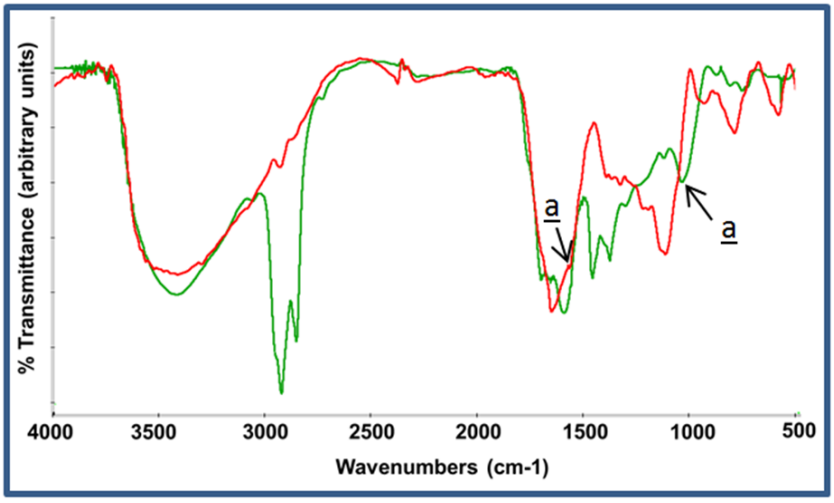

Figure 5.10. FTIR spectra of insoluble materials after an oxidation process (in green) and adsorption column effluent (in red).

Characterization of filtered solids was successful in terms of discarding hypotheses that seriously affect the sustainability of the process such as carbon attrition. For the purpose of this research, efforts made to describe the suspended solids were enough to analyze

possible causes and infer potential consequences. It is suspected that unidentified solids could be carboxylic acids precipitating from the WSA solution. Quantities of the unknown particles were not substantial, and did not contribute to pressure drops in the packed bed reactor or blockage of valves, but their buildup might cause problems in the long term. Further consideration of these aspects will need to be addressed for further development.

In relation to the chapter concerning lab-scale WSA adsorption in non-continuous operation, the highest concentration point in the isotherm for GAC (Figure 4.5, page 47) can be compared with results from the bench-scale dynamic adsorption experiments. The GAC isotherm was developed at room temperature and batch conditions, and for the highest concentration point (9,300 ppm TOC content, 4400 mg/L equilibrium concentration), the WSA uptake was 200 mg/g. The test carried out at the same temperature in the dynamic setup described in this chapter, resulted in a WSA uptake of 140 mg/g, utilizing a WSA solution with initial concentration around 9,000 ppm TOC content. Nevertheless, the lab-scale outcome was obtained after equilibrium conditions were reached (after 72 hours), which is not the case for the continuous operation experiments. Therefore, the differences in uptakes between the batch and continuous operation are expected as in the last one, the bed was not fully saturated and more time is required to fill available spots in the adsorbent surface.

6. HYDROPROCESSING OF ADSORBED WATER SOLUBLE ASPHALTENES

Hydroprocessing was without a doubt, the most critical phase of the project as it would demonstrate the feasibility of the proposed process. This step was linked to the dynamic adsorption stage described in the previous chapter, as the setup used for continuous adsorption experiments was the same one that carried out hydroprocessing tests. Findings on adsorption operating conditions were used to adsorb the WSA subjected to hydroprocessing. Characterization of virgin GAC (meaning activated carbon with no active phases) was compared to synthetized catalysts and important features were extrapolated to support conclusions derived from this chapter. Pages henceforth summarize conceived methodologies, catalysts synthesis and characterization, and gas and liquid products obtained from pre-adsorbed WSA hydroprocessing tests.

6.1 Hydroprocessing catalysts preparation methodology

Catalyst selection requires a detailed study for the specific application, but commonly, combinations of active species fall in the CoMo, NiMo and NiW families (Topsøe et al, 1996). This research was focused on hydroprocessing using an in-house impregnated NiMo catalyst supported on GAC. Its synthesis consisted in three steps: pretreatment of the support, impregnation, and activation of active species.

6.1.1 GAC pretreatment

GAC was oxidized with nitric acid to increase its acidity and to improve the dispersion of active metals due to the hydrophobic nature of the support. This a typical procedure applied to carbon-supported hydroprocessing catalysts before impregnation (Calafat et al, 1996; Marsh et al, 1997; Furimsky, 2008; Narayanasarma, 2011). Support oxidation consisted of drying a known amount of GAC, preparing a 5 M HNO_3 solution and mixed them together in a beaker using a ratio of 10 mL HNO_3/g GAC. Then, the solution was placed on a heating plate, the temperature was increased up to 60°C and the solution was held at this temperature for 2 hours at a stirring speed of 100 rpm. Then, the pretreated support was filtered and washed with abundant warm water (50 – 60°C). At the end, the solid was dried overnight in the oven at 100°C.

6.1.2 Impregnation

Incipient-wetness impregnation was the method employed to add Ni and Mo to the support. In this regard, the solid's pore volume, or the ratio of water volume required to saturate the solid per gram of GAC, was calculated as follows: 1.5 grams of HNO_3 treated GAC were equally distributed in three petri dishes. Water droplets were carefully added drop-by-drop to each petri dish until saturation was visible, utilizing a 5 mL volumetric burette. Finally, the ratio of water volume per gram of GAC was computed, resulting in an average pore volume of 1.69 mL/g.

Three nominal metal loads (2 wt%, 5 wt% and 8 wt%) were selected to impregnate the oxidized support. Ammonium heptamolybdate tetrahydrate ($[N_5H_{24}Mo_7O_{27} \bullet 4H_2O]$ and Nickel Acetate Tetrahydrate $[(C_2H_3O_2]_2Ni \bullet 4H_2O)$ were used to prepare the aqueous solutions, using the well-known molar ratio of Ni / (Ni + Mo) = 0.33 (Topsøe et al, 1996; Segawa, 2011; Schachtl et al, 2012). First, the treated carbon was impregnated with the molybdenum solution, and then dried overnight in an oven set at 100°C. Subsequently, the nickel solution was added drop by drop to the molybdenum-impregnated support and once again, the solid was dried overnight at 100°C.

6.1.3 Sulfidation

30 mL of a 10% by volume CS_2 in decaline solution was poured into a 100 mL batch reactor (Parr Instruments, Figure 6.1) containing 3.5 grams of dried catalyst. 200 psig of ultra-high purity hydrogen (99.999%, Praxair) was injected to the reactor. The mixture was heated up to 350°C at a constant stirring speed of 500 rpm, and dwelled for 6 hours. Once the reactor was cooled down, gases were safely vented in the fume hood and solids were vacuum filtered. Solids were extensively washed with toluene until the filtrate was color-free and posteriorly, the sulfided catalyst was stored in a capped glass vial with toluene.

6.2 Catalyst characterization

Prepared catalysts were characterized by Inductively Coupled Plasma (ICP) spectroscopy and X-ray Photoelectron Spectroscopy (XPS). BET surface areas and BJH pore volumes were measured after the nitric acid pretreatment, after impregnation and after reaction. X-ray Diffraction (XRD) analysis for virgin GAC was carried out to complement support characterization.

Figure 6.1. Sulfidation batch reactor.

6.2.1 Metal analysis

Exactly 1 gram of each catalyst was burnt in the oven in which the sample was held at 600°C for 12 hours under ambient atmosphere (air). Remaining ashes were accurately weighed, crushed and treated under the coning and quartering method (Skoog and West, 1976), in which each sample was piled into a cone, flattened, and divided into four quarters. Two opposing quarters were discarded and the other two remaining were piled, flattened and divided into quarters again, until approximately 50 mg of sample are left. Then, 2 mg of each catalyst was placed in digestion vessels and mixed with 10 mL of a 70 wt% HNO_3 solution, 1 mL of an 85 wt% H_3PO_4 solution and 23 mg of a 1,000 ppm cobalt standard solution. Next, vessels were placed inside the Microwave Accelerated Reaction System (MARS), where temperature was increased to 210°C and held for 50 minutes. Afterwards, vessels were cooled down to room temperature and their contents were diluted to 100 mL using deionized water, as discussed in section 3.1.3.4. Each catalyst sample was replicated four times and results are shown in Table 6.1.

Table 6.1. Metal analysis of prepared catalysts by Inductively Coupled Plasma.

Nominal load (wt%)	Measured metal content (wt%)				Ni /(Ni+Mo) Mass ratio
	Fe + K + Na	Ni	Mo	Ni+Mo	
0% NiMo	0.17 ± 0.03	0.00	0.00	0.00	-
2% NiMo	0.11 ± 0.07	0.51 ± 0.05	1.43 ± 0.12	1.94 ± 0.17	0.26
5% NiMo	0.17 ± 0.08	1.24 ± 0.05	3.99 ± 0.19	5.23 ± 0.24	0.24
8% NiMo	0.14 ± 0.06	2.03 ± 0.11	5.45 ± 0.48	7.48 ± 0.59	0.27

0 wt% NiMo sample corresponds to the virgin GAC, which clearly doesn't have nickel or molybdenum and its metal content is less than 0.2 wt%. The average mass ratio

Ni/(Ni+Mo) for all catalysts was 0.26. The molar ratio Ni/(Ni+Mo) = 0.33 corresponds to a theoretical mass ratio Ni/(Ni+Mo) = 0.23, which is remarkably similar to the values obtained in the previous table.

6.2.2 BET Surface Areas

Surface areas were monitored using a Micromeritics Surface Area and Porosity System Analyzer (model Tristar II 3020) using the procedure described in section 4.1.2. GAC, HNO_3 treated support and non-sulfided impregnated GAC were analyzed to track changes in their surface areas, summarized in Table 6.2.

Table 6.2. Surface areas of virgin, treated and non-sulfided impregnated granular activated carbon before reaction.

Sample	BET surface area m^2/g solid
GAC	615
HNO_3 treated GAC	607
2% NiMo (before reaction)	531
5% NiMo (before reaction)	430
8% NiMo (before reaction)	373

After the HNO_3 oxidation process, the BET surface area slightly declined with respect to the virgin GAC. On the other hand, surface areas were reduced with increasing metals load. The 2% non-sulfided catalyst has 84 m^2/g less than the virgin sample, but 101 m^2/g and 158 m^2/g more than the 5% and the 8% non-sulfided impregnated supports, respectively.

6.2.3 X-ray Photoelectron Spectroscopy (XPS)

The XPS technique is used in studies of the surface of solid samples, providing information about the composition of the surface, elemental quantification, and chemical environment of the elements in the sample. The sample is irradiated with x-rays and photoelectrons are emitted. An electron energy analyzer determines the kinetic energy of the photoelectrons, which is converted to binding energy; by studying the binding energy and intensity of a photoelectron peak, the elemental identity, chemical state, and quantity of an element are determined (Physical electronics, 2014).

Each sample was mounted and pumped down from atmospheric pressure to ultra-high vacuum in a Phi 5000 VersaProbe from Physical Electronics. A wide energy survey (0-1,400 eV) at a passing energy of 187 eV was performed in order to get the highest sensitivity and identify all elements in the sample. Then, a smaller energy window was

used on every sample (10-30 eV) with passing energy of 23 eV to get a high energy resolution at areas where elements were recognized; these conditions allow determining the oxidation state and chemical environment of the elements in the sample. Afterwards, a curve fitting was performed to obtain the atomic percentage of every element in the sample surface in a depth between 4 to 6 nm. Table 6.3 displays the elemental composition of the catalysts surfaces derived from the XPS analyses and Figure 6.2 presents the survey spectra for each sample.

Table 6.3. Elemental composition of virgin GAC and non-sulfided catalysts by XPS analyses.

Sample	Weight percentages								Ni + Mo wt%	Ni / (Ni+Mo) mass ratio
	C %	O%	N%	Si%	Na%	S%	Mo%	Ni%		
Virgin GAC	84.2	10.9	1.44	2.44	0.76	<0.25	0	0	0	0
2% NiMo	72.3	17.3	0.98	1.86	0.00	0.00	6.66	0.86	7.52	0.11
5% NiMo	78.0	14.5	1.32	2.16	0.00	0.00	10.9	1.36	12.3	0.11
8% NiMo	67.3	14.8	1.29	1.92	0.00	0.00	13.5	1.2	14.7	0.09

It is deemed necessary to clarify that nitrogen and molybdenum atomic percentages found in the 2%, 5% and 8% NiMo materials, don't correspond to the reported weight percent values from Table 6.3. The $Mo3p^3$ and N1s signals overlapped in the XPS survey, and a more detailed fitting was required to identify the area contribution for each species. Therefore, the atomic percentage assigned to nitrogen had to be adjusted by subtracting the molybdenum contribution (in that overlapping peak) from the nitrogen atomic percentage computed by the software. Likewise, the molybdenum contribution in the overlapping peak was added to the molybdenum percentage computed by the software.

The XPS apparatus detected sodium on the surface of virgin GAC, but is not seen in impregnated NiMo samples. This sodium loss was attributed to the HNO_3 pre-treatment of the support before impregnating the nickel acetate and ammonium heptamolybdate solutions. Other metals identified by the ICP technique (iron and potassium) were not seen on the support surface, so it is inferred that these species are part of the activated carbon bulk. As for silicon, it was identified in virgin GAC and catalysts surfaces and in larger amounts that nitrogen.

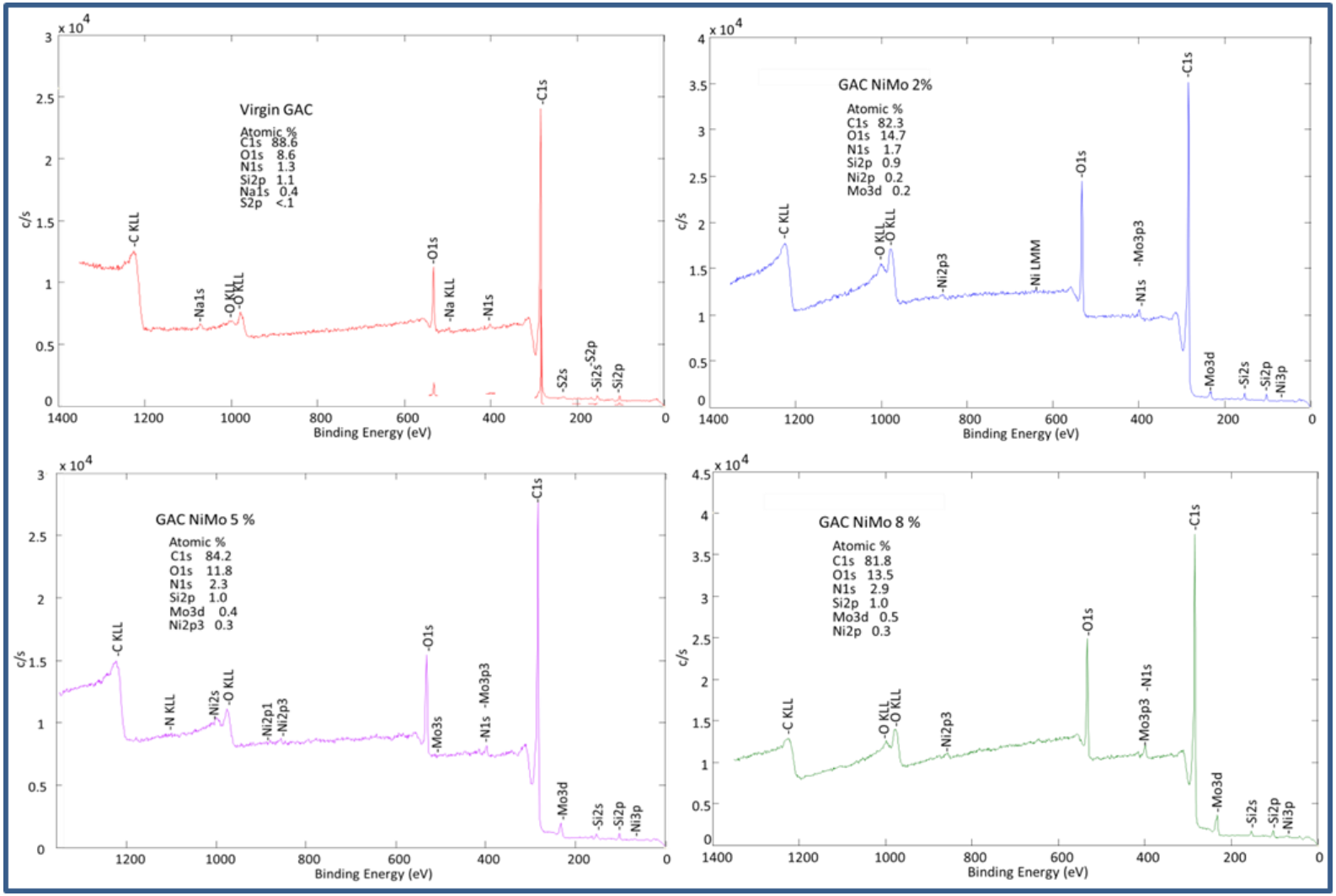

Figure 6.2. XPS surveys of virgin GAC (in red), 2% NiMo catalyst (in blue), 5% NiMo catalyst (in purple) and 8% NiMo catalyst (in green).

XPS results showed that summed Ni and Mo contributions in catalysts surfaces surpass the nominal metal load with which these solids were designed. Yet, the percentages coherently rise as the metal nominal load increases as well. These values could be understood as active species being successfully positioned on catalysts surfaces. Interestingly, Ni / (Ni + Mo) mass ratio declined to less than half of the design value (0.23), which can be interpreted as nickel being placed in deeper pores. Even though Mo was the first metal impregnated, Ni molecules are smaller and presumably, were able to access smaller pores in which molybdenum could not be placed; consequently, molybdenum could be more exposed to the catalyst surface in comparison to nickel atoms, resulting in a peripheral surface with lower Ni / (Ni +Mo) mass ratio values.

6.2.4 X-ray diffraction (XRD)

XRD is an analytical tool that allows characterization of the crystalline structure of materials. The X-ray analysis of virgin GAC was performed using a Rigaku ULTIMA III X-ray diffractometer with Cu K-alpha radiation as the X-ray source and with 40 kV and 44 mA. Scanning was carried out in the range of 3-70 2-theta using a 0.02 degree step and a counting time of 1.0 degree per minute for the detailed, full diffractogram. XRD patterns were referenced to powder diffraction files from the International Centre for Powder Diffraction PDF 2005, using the software JADE (Materials Data Inc.) for identification of crystalline phases.

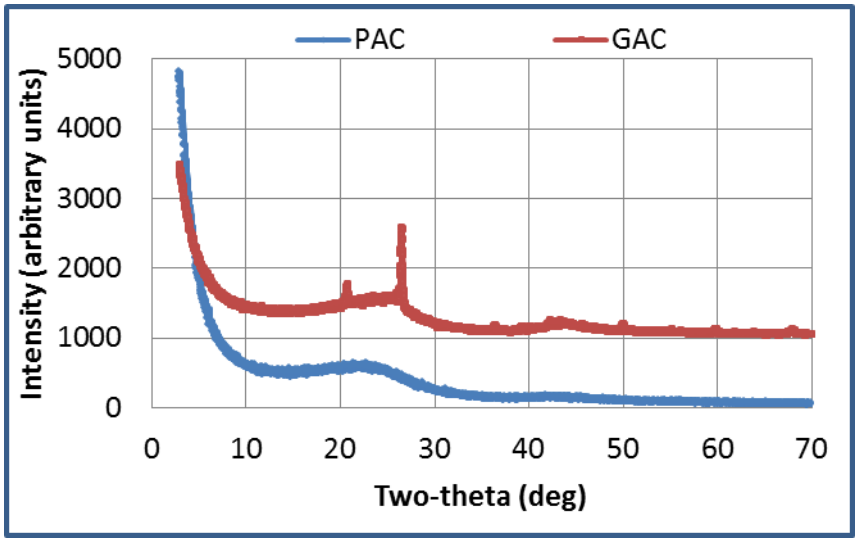

Figure 6.3. XRD scan of virgin GAC and PAC.

The diffractogram shown in Figure 6.3 corresponds to the analysis of virgin GAC (in red) and PAC (in blue). The red pattern evidences the noteworthy amount of quartz, or crystalline SiO_2, in the GAC structure. It is inferred that quartz is part of the non-

pyrolyzed material found in the TGA curves displayed in the previous chapter (Figure 5.3). Quartz content could also explain the reduction in surface area at comparing GAC (615 m^2/g) to PAC (about 1300 m^2/g), utilized in experiments described in Chapter 4. Porosity dropped down in a substantial extent with the presence of the crystalline material in the granular activated carbon.

6.3 Hydroprocessing experimental methodology

Hydroprocessing of pre-adsorbed WSA was evaluated by using catalysts with three concentrations of active species: 2 wt% NiMo / GAC, 5 wt% NiMo / GAC and 8 wt% NiMo / GAC. Sulfided catalysts, which were stored in toluene, were removed from the capped glass vials and dried in the vacuum oven (-25 mm Hg, 70°C) the night before the adsorption stage. Afterwards, approximately 6 grams of sulfided catalyst were packed in the reactor as indicated in the standard operating procedure (Appendix D). In this regard, it is important to clarify that once the GAC was treated with nitric acid, the solid gained weight due to incorporation of oxygen and other elements in its structure. If 5 grams of virgin GAC were intended to impregnate and activate, at the end of the oxidation treatment and sulfidation procedure, the solid weighed 6 grams instead. Therefore, the reactor capacity "increase" was due to the catalyst weight gain during its synthesis, and not because the reactor volume, that originally was able to contain 5 grams of virgin GAC, had changed.

Once the reactor was packed, a nitrogen purge at 120°C was carried out by flowing inert gas for about 3 hours, constantly monitoring the stream passing through the reactor by gas chromatography analysis. Next, the reactor was pressurized with nitrogen at 30-40 psig and allowed to cool down to 80°C. In the meantime, a WSA solution of around 9,000 mg organic carbon/L was loaded in the pump. Adsorption was carried out at target conditions of 80°C, WSA flow rate of 3 cc/min, and 90 minutes. These conditions were chosen based on the experiments described in Chapter 5, as these values resulted in the largest WSA uptake under the studied range of conditions. As soon as the experiment finished, the system was cooled down to room temperature but was kept pressurized with nitrogen to avoid catalyst deactivation. Then, the packed bed was quickly removed and dried overnight in the vacuum oven at -25 mm Hg and 70°C. On the other hand, liquid aliquots collected during the adsorption test were assessed in the TOC analyzer and their pH was recorded.

The next day, the catalyst with pre-adsorbed asphaltenes was rapidly packed again and the system was pressurized with hydrogen at 550 psig. The hydrogen mass flow

controller was set to deliver 5 SCCM and temperature was increased to 350°C. Hydroprocessing was carried out for 4.5 hours at this temperature for each catalyst, injecting produced gases in the GC for online analyses and constantly monitoring pressures, flow rates and temperatures. At the end of the experiment, produced liquids were retrieved and analyzed via High Temperature Simulated Distillation (HTSD). The unpacked bed was dried in a furnace and weighed the next day.

Three thermal runs were performed using pre-adsorbed asphaltenes on virgin GAC (denoted as 0 wt%) at 250°C, 300°C and 350°C. Since these solids were not HNO_3 pre-treated, impregnated or sulfided, 5 grams of virgin GAC plus the amount of asphaltenes adsorbed were packed and hydroprocessed using the same conditions as those used during catalytic runs (550 psig, 5 SCCM, 4.5 hours). The experimental plan for pre-adsorbed WSA hydroprocessing is shown in Table 6.4.

Table 6.4. Experimental plan for pre-adsorbed WSA hydroprocessing at 550 psig, H_2 flow rate of 5 SCCM and 4.5 hours.

Hydroprocessing temperatures	**NiMo load (wt%)**			
	0%	**2%**	**5%**	**8%**
250°C	X			
300°C	X			
350°C	X	X	X	X

6.3.1 Hydroprocessing products characterization

Gases were monitored through an SRI gas chromatograph model 8610, equipped with a Flame Photometric Detector (FPD) and a Thermal Conductivity Detector (TCD). The FPD analyzes the spectrum of light emitted by compounds as they luminesce in the flame, and is very sensitive to sulfurous and phosphorous compounds. The TCD is the most universal detector which measures the difference in thermal conductivity in the carrier gas flow and the sample peaks (SRI Instruments, 2014). The GC was able to quantify hydrocarbons ($<C_5$), CO, CO_2 and nitrogen using the TCD filament, and H_2S and SO_2 contents were examined through the FPD detector by use of calibration curves.

Liquid products were characterized by High Temperature Simulated Distillation (HTSD). In this technique, liquid hydrocarbons are volatilized, then separated by a capillary column as function of their boiling points and analyzed with a flame ionization detector. The analytical tool provides accurate results with standard deviations less than 0.5 wt%. An Agilent Gas Chromatograph Model 6890N with capillary columns P/N SS-112-02-01 from Separation Systems, was used for the analysis. Sample solutions are normally prepared in CS_2 using the standard ASTM-D7169-2005 procedure (about 0.15 g sample /

20 mL solvent), however modifications had to be made because the liquid sample size at the end of the hydroprocessing experiments was small.

In this research, 4 mL of CS_2 were added to products recovered from runs utilizing 2% NiMo and 8% NiMo catalysts, and 8 mL were mixed with liquids collected after the 5% NiMo experiment. Two phases were seen as depicted in Figure 6.4a, in which an organic phase (soluble in CS_2) and a CS_2 insoluble phase were clearly formed. The CS_2 soluble phase (Figure 6.4b) was extracted from the bottom of the two-phase mixture and analyzed in the HTSD apparatus.

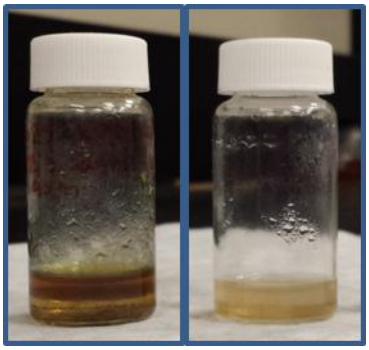

Figure 6.4. CS_2 addition to hydroprocessing liquid samples for simulated distillation analyses: a) formation of two phases, and b) CS_2 soluble phase.

The HTSD system summed peaks areas from C_5 to C_{100}, which were matched to hydrocarbon mass in the sample by the calibration curve plotted in Figure 6.5. This curve was created by mixing known quantities of naphtha, atmospheric gas oil and vacuum gas oil (or vacuum residue), diluting them to 25 mL of CS_2, and correlating measured areas with hydrocarbons concentration.

6.4 WSA Adsorption on prepared catalysts results

Breakthrough curves were obtained by plotting normalized TOC concentrations (C/Co) versus time. Normalized concentrations were computed by dividing the TOC content of the aliquot at a given time (C) over the initial TOC content of the WSA solution (Co ≈ 9,000 mg/L). Average TOC values were reported by the TOC apparatus, with resultant standard deviations lesser than 2% of TC content. It is worth mentioning that IC content was negligible and TOC composition was taken as the sample TC composition.

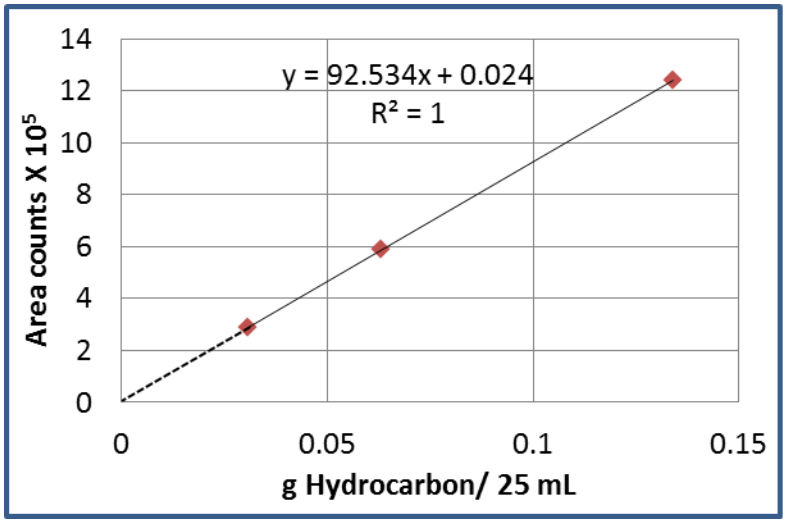

Figure 6.5. High temperature simulated distillation calibration curve.

As in previous adsorption tests, aliquots had to be filtered with hydrophilic nylon syringe filters (0.45 µm, Whatman) to remove fine powders suspended in the samples. Mass balances closed at an average of 97.9% ± 3.3%. Organic carbon uptake (in milligrams) was computed by the following equation:

(Equation 6.1) $$TOC\ uptake\ = \sum_{t=0}^{t=90} Aliquot\ volume\ (t) \times (Co - C(t))$$

In the previous equation, the aliquot volume is given in liters, Co is the initial concentration of the WSA solution and C(t) represents the TOC content of the sample at time t, in mg/L. Asphaltenes uptake was quantified by dividing the previous value by the weight of catalyst packed at the beginning of the adsorption test, and results are presented in Table 6.5.

Asphaltenes uptake is quantified in terms of mg of carbon per gram of solid, and as mg of carbon divided by the BET surface area of each catalyst. Areas of spent catalysts (i.e. after hydroprocessing experiments) were measured after solids were thoroughly washed with toluene, dried overnight at the vacuum oven at 70°C and -25 mm Hg, and degasified as explained in section 4.1.2. Figure 6.6 relates asphaltenes uptake (in mg C/g adsorbent) to metal load, breakthrough curves are illustrated in Figure 6.7, and effluent pH is plotted in Figure 6.8.

Asphaltenes uptake declined as active metals were impregnated on the support. Using the same conditions, the WSA uptake on virgin GAC was 88 mg/g higher than the one obtained by the 2% NiMo catalyst. In relation to the adsorption capacity of virgin activated carbon, the percentage of adsorbed asphaltenes decreased by around 60% using the 5 wt% and 8 wt% NiMo catalysts. The trend presented in Figure 6.6 shows a

non-linear relationship between asphaltenes uptake and metal load. Of notice, asphaltenes uptake was practically identical for the 5% and the 8% NiMo catalysts. The relation of WSA uptake with respect to the catalyst surface area was kept constant for the three catalysts, but lower in comparison to that of virgin GAC.

Table 6.5. Asphaltenes uptakes after dynamic adsorption on NiMo / GAC catalysts.

NiMo load	Asphaltenes uptake (mg/m^2 adsorbent)	Asphaltenes uptake (mg/g)
0 wt%	0.33	202
2 wt%	0.21	114
5 wt%	0.21	80
8 wt%	0.19	78

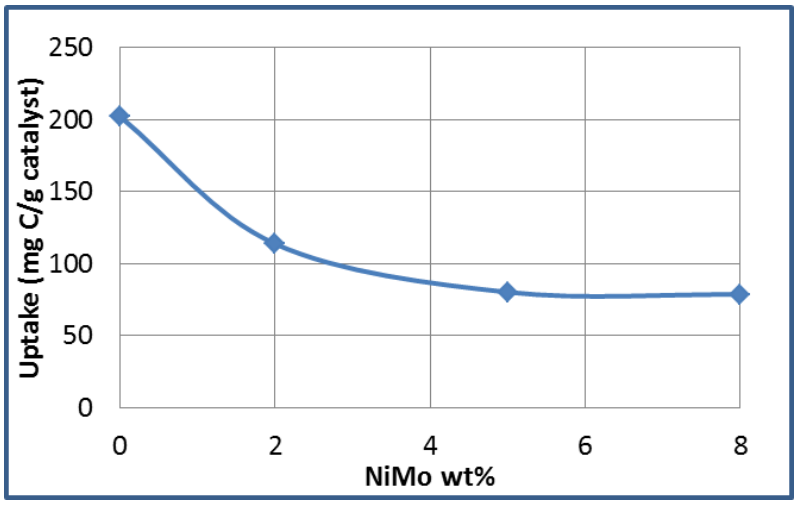

Figure 6.6. WSA uptake vs. metal load on catalyst.

Previous results are coherent with findings on surface area, in which less area matched with lower asphaltenes uptake. It is not surprising that NiMo catalysts retain less WSA on their surfaces, as the active species occupied pores that were originally destined for asphaltenes adsorption. The decrease in adsorption capacities could also be explained by changes in the nature of solids. As catalysts were packed in the reactor after sulfidation, sulfur compounds were introduced to catalysts surfaces that were not on the virgin GAC. It is known that H_2S competitively adsorbs with oxygenated compounds (i.e. WSA) on $NiMo/Al_2O_3$ catalysts (Deutsch and Shanks, 2012), so it was possible that H_2S, still trapped on the surface of the catalysts, inhibited WSA adsorption.

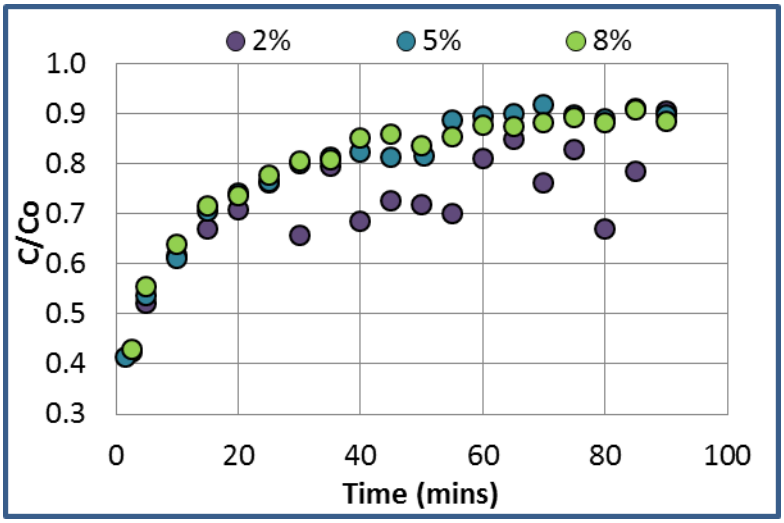

Figure 6.7. WSA adsorption on 6 grams of NiMo / GAC catalysts at 80°C, 30-40 psig, at a constant WSA flow rate of 3 cc/min.

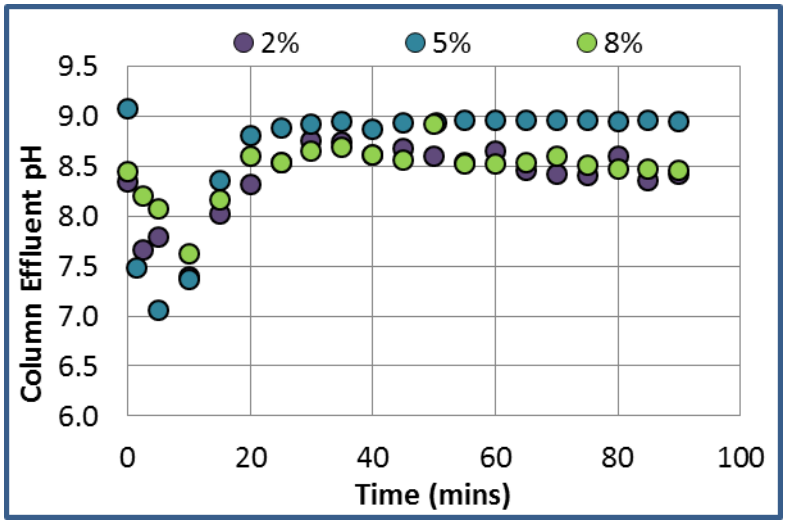

Figure 6.8. Column effluent pH for WSA adsorption on 6 grams of NiMo / GAC catalysts at 80°C, 30-40 psig, at a constant WSA flow rate of 3 cc/min.

Aliquots retrieved during the first adsorption test on the catalyst had a strong, recognizable sulfur smell, which indicated that some sulfur compounds of the catalyst surface were being "carried away" by the WSA effluent. Therefore, a nitrogen purge at 120°C was implemented and with the aid of gas chromatography analyses, H_2S and SO_2 were identified in the purged stream. Even though the nitrogen pre-treatment of the sulfided bed was executed, there was a chance that these or other species were competitively adsorbing on the catalysts, hence, reducing the overall uptake. The nitrogen pre-treatment stopped when the gas chromatograph no longer detected sulfur

peaks on the purged stream; regardless, collected adsorption samples still had a sulfurous smell, although less strong.

On the other hand, there were some similarities found with adsorption outcomes using virgin GAC. Breakthrough curves of virgin GAC and catalysts indicated that the column length was not long enough to reach C/Co = 1. For every catalyst, C/Co ratio reached 0.90 at the end of the experiment, whereas for virgin GAC this value was higher at the same operating conditions (80°C, 3 cc/min, 90 minutes). Regardless, it was demonstrated that the contact time between the catalysts and WSA was not sufficient to fully exhaust the bed, and therefore, longer adsorption times would be required to achieve an effluent with a TOC concentration ratio larger than 0.95.

The breakthrough curve developed for the 2 wt% NiMo catalyst presents an odd shape, in particular at points plotted when t = 55 min, t = 80 min and t=85 min, attributed to experimental errors. The other two catalysts presented overlapping breakthrough curves, which translates into practically the same asphaltenes uptake in terms of TOC content.

Effluent pH also jumped down during the first 15 minutes as evidenced during dynamic adsorption runs on virgin GAC; once more, these variations suggest that ionic interactions between WSA and the packed bed occurred while adsorbing on NiMo catalysts. It is important to mention that the 5% catalyst run was performed a few months after the 2% and 8% experiments, and in consequence, the somewhat increased basicity in the effluent pH was attributed to changes occurring during this time frame. First, the WSA solution in the 5% run was a little bit more concentrated as water might have evaporated, directly affecting the WSA solution pH and TOC content. Furthermore, the 5% catalyst was prepared utilizing a different HNO_3 GAC treated batch that the one used for the 2% and 8% NiMo catalysts, which might have led to a slightly different support surface. In order to reduce the pH of the effluent, the OH^- ions must adsorb on the catalyst or adsorbent. An aged basic solution usually forms carbonates with the acid CO_2 from air which reduces the pH, i.e., increasing its acidity. This doesn't seem to have happened as the sample was well preserved.

6.5 Pre-adsorbed WSA hydroprocessing results

Hydroprocessing results were summarized in diverse charts representing hydrocarbons (and other gases) evolution in the gas stream. Distillation curves were created to evaluate the quality of the liquid product, and for overall assessment, conversion and selectivities were defined as follows:

(Equation 6.2) $$Carbon\ conversion\ (\%) = \frac{Cgas+Cliquids}{Cinitial} \times 100\%$$

(Equation 6.3) $$Liquid\ Selectivity\ (\%) = \frac{Cliquids}{Cgas+Cliquids} \times 100\%$$

(Equation 6.4) $$Gas\ Selectivity\ (\%) = \frac{Cgas}{Cgas+Cliquids} \times 100\%$$

In the previous equations, Cgas represents the carbon mass (in grams) obtained in the gas stream, Cliquids relates to the carbon mass (in grams) quantified in the liquid phase and Cinitial corresponds to the amount of organic carbon initially adsorbed on the catalyst (in grams).

The amount of carbon in the gas stream was calculated considering carbon monoxide, carbon dioxide, methane, ethane, ethylene, propane, propylene, isobutene, 1-butene, n-butane and isopentane contributions. Each composition given at time t (given in volumetric percentage by the GC analyzer), was multiplied by the volumetric flow rate measured at time t, and then converted to carbon mass by stoichiometry and the ideal gas law. The sum of mass contributions by each species throughout the hydroprocessing run gave the total gaseous carbon for every test.

Carbon in the liquid stream was quantified by means of data provided by the HTSD apparatus, as described in section 6.3.1. The carbon mass was computed under the assumption that 82% by weight of the hydrocarbonaceous sample relates to carbon.

6.5.1 Thermal runs

Thermal runs were carried out using pre-adsorbed WSA on virgin activated carbon (0 wt% NiMo) at 250°C, 300°C and 350°C, injecting 5 SCCM of H_2 for 4.5 hours, at 550 psig. Overall results are displayed in Table 6.6, from which is obvious that only gas products were recovered as the liquid selectivity was zero in all thermal cases. Figures 6.9 to 6.11 show hydrogen consumption, H_2S generation and hydrocarbons evolution in time.

Table 6.6. Results of thermal runs at 250°C, 300°C and 350°C on virgin GAC.

Temperature (°C)	Reaction time (mins)	C initial (g)	Carbon liquid selectivity (%)	Carbon conversion (%)
250	285	0.627	0	1.3
300	285	0.629	0	2.3
350	295	0.710	0	3.0

Achieving barely acceptable mass balances for thermal runs was a difficult task. The amount of carbon that was not converted was impossible to calculate by weighing the sample at the end of the run because any grain loss represented a considerable sample size in the packed bed. Moreover, weight changes not related to carbon (i.e, sulfur losses during catalyst pre-treatment) added difficulty to calculating carbon mass balances by gravimetric analyses. Therefore, only carbon conversion and carbon selectivities were quantified, both for thermal runs and catalytic experiments. Even so, results were coherent and reproducible as blanks were repeated twice at each condition, in which hydrocarbons production in gas streams mimicked at all tested temperatures.

Figures below show a continuous decrease of hydrogen in the gas stream as time went by. However, the decline of hydrogen composition is not linked to its consumption; in the first hour of reaction, this decrease was caused by early CO_2 production at temperatures between 250°C and 300°C, as a result of the decarboxylation of adsorbed WSA. Methane production was evidenced at t = 100 minutes and t = 140 minutes at 350°C and 300°C, respectively, yet it was not detected at lower temperatures. CH_4 was the main hydrocarbon product as it reached around 2% molar at the end of the test run at 350°C, and at 300°C this value was around 0.5% molar. C_2 and C_3 were produced later in time in comparison to CH_4, and their quantities were almost negligible, and correspondingly lower than methane amounts. In regards to carbon dioxide, it is clear that it was the main product as its percentage was the highest in all cases, and it was generated even at the lowest temperature. At 250°C, CO_2 was the only carbon source in the gas stream.

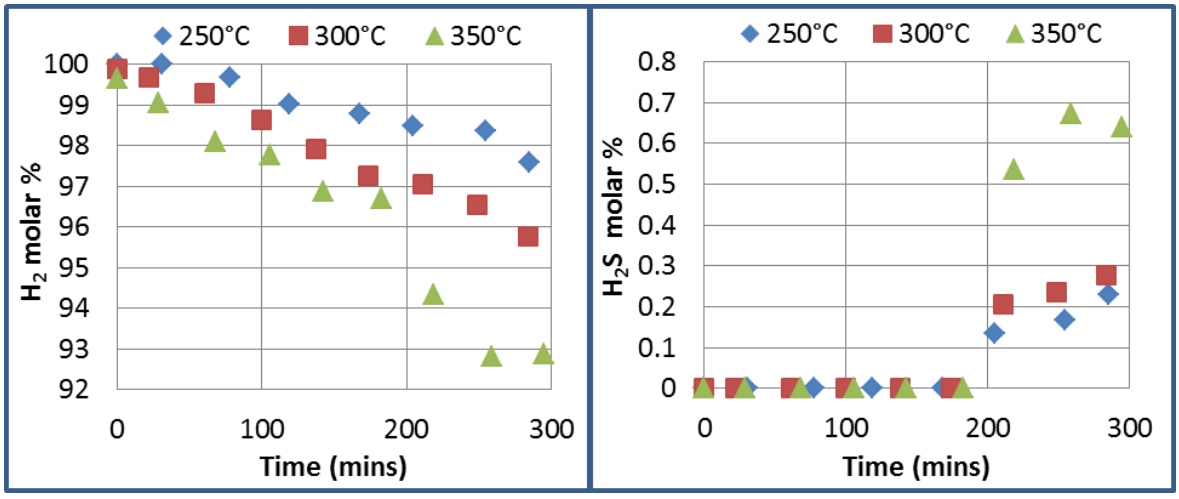

Figure 6.9. Hydrogen and H_2S composition in the outlet gas stream during thermal runs at 250°C, 300°C and 350°C, 5 sccm H_2, 550 psig and 300 minutes.

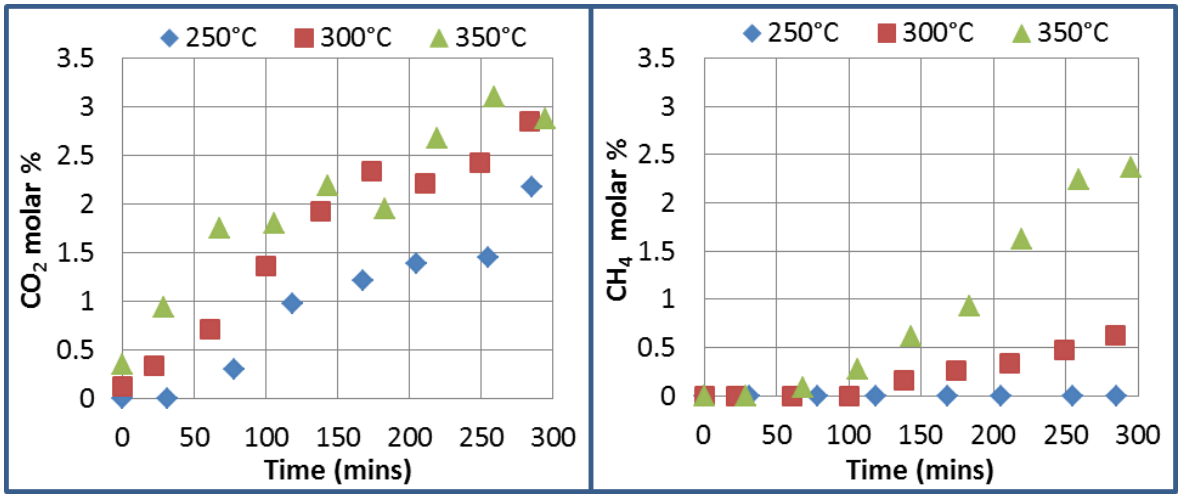

Figure 6.10. Carbon dioxide and methane composition in the outlet gas stream during thermal runs at 250°C, 300°C and 350°C, 5 sccm H_2, 550 psig and 300 minutes.

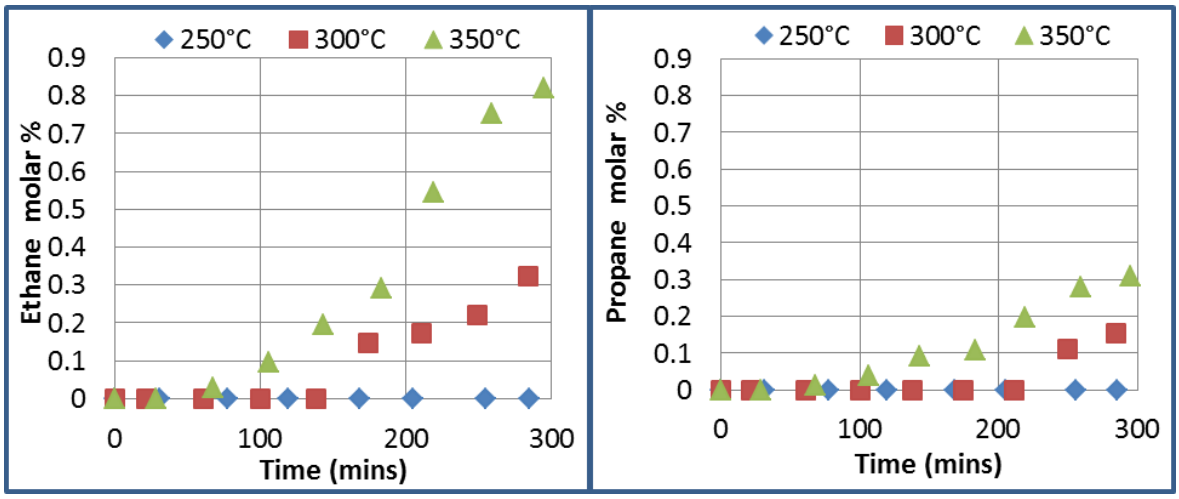

Figure 6.11. Ethane and propane composition in the outlet gas stream during thermal runs at 250°C, 300°C and 350°C, 5 sccm H_2, 550 psig and 300 minutes.

Hydrogen was consumed after three hours of reaction as evidenced in the H_2S chart, as production of light hydrocarbons, seen at earlier stages of the process, come from WSA thermal cracking. H_2S was identified only after 3 hours of reaction yet it was identified at all tested temperatures. These results are in agreement with reviewed literature, in which it is reported that decomposition of all saturated sulfur compounds in hydrocarbons (with just a few exceptions) is thermodynamically favored at temperatures below 425°C; in fact, substantial decomposition of thiols can occur at temperatures lower than 300°C if hydrogen is present in stoichiometric quantities (Speight, 1999).

At the most severe conditions, carbon conversion was 3%, and the percentage was consistently reduced at lower operating temperatures. Results at 350°C were taken as the blank or baseline for comparison with GAC catalysts, addressed in the next section.

6.5.2 Catalytic runs

Hydroprocessing of previously adsorbed asphaltenes was performed at nearly 350°C, injecting hydrogen at 5 SCCM for 4.5 hours, and keeping the system pressure at 550 psig. Summarized results for catalytic runs are displayed in Table 6.7. In addition, BET surface areas of catalysts after hydroprocessing tests were measured to determine any changes in this textural property. Spent catalysts were thoroughly washed with dichloromethane and placed overnight in the vacuum oven (-25 mm Hg, 70°C). Then, degasification of the sample and subsequent procedures for monitoring textural properties, as explained in previous chapters. Surface areas are shown in Table 6.8.

Table 6.7. Results of hydroprocessing runs on NiMo/GAC catalysts.

Metal load (wt%)	Temperature (°C)	Reaction time (mins)	C initial (g)	Carbon liquid selectivity (%)	Carbon conversion (%)
2% NiMo	346	285	0.669	34.0	42.2
5% NiMo	346	290	0.473	29.0	57.5
8% NiMo	343	290	0.487	7.73	53.4

Table 6.8. BET surface areas of NiMo catalysts measured after hydroprocessing experiments.

Sample	BET surface area m^2/g solid	Percentage of surface area reduction
2% NiMo (after reaction)	405	24%
5% NiMo (after reaction)	325	24%
8% NiMo (after reaction)	275	26%

Overall results proved the catalytic effect of metallic species on GAC as they yielded liquid hydrocarbons and carbon conversions went considerably up in comparison to thermal runs. Liquid selectivity achieved by the 2% NiMo was remarkable higher than the 8% catalyst, in which only 7.73% of converted carbon was found in the liquid stream. It is suspected that better dispersion was achieved with the 2% NiMo catalyst, which led to an increase in selectivity for liquid products in comparison to the other catalysts. Similarly, results suggest that selectivity to gases increases as the metal load is increased.

As shown in Table 6.7, the highest conversion was reached in the 5% NiMo experiment, which was 15% and 4% higher than the 2% and 8% catalytic tests, respectively. Of note,

the temperature in the 8% NiMo test was 3°C lower than reaction temperatures in other catalytic experiments due to operational problems during the run. It is suspected that if 346°C were achieved, probably conversion would have increased to a value closer to (or above) the maximum computed conversion.

Spent catalysts areas were reduced after reaction, although it is important to keep in mind that sulfidation contributed to this diminishment. The percentage of surface area reduction, presented in the previous table, relates the difference of this property before and after reaction, to the area measured before reaction. Ongoing studies on hydroprocessing of asphaltenes, carried out in a batch reactor and a $NiMo/Al_2O_3$ catalyst at slightly more severe conditions (800 psig, 380°C, 6 hours), showed a decrease of 68% in surface area with respect to the catalyst before reaction (Isquierdo et al, 2014). The loss was accredited to coke deposition on the support (1 wt%), demonstrated with TGA curves; however, feedstock quantities in the referred investigation were far higher than the available amounts in this research. In the present study, computed percentages of surface area reduction suggest that they are not critical as these values might only represent losses derived from the catalyst sulfidation procedure.

6.5.2.1 Gas stream

Evolution of gases is plotted in subsequent figures, in which purple dots represent gases composition obtained using the 2% NiMo catalyst, 5% NiMo data correspond to blue dots and green dots relate to results utilizing the 8% catalyst. Summed contributions of isobutene, n-butane, 1-butene and isopentane never exceeded 1% at any moment in any of the catalytic runs and they are not illustrated in the figures below.

Hydrogen charts displayed a minimum composition at around 150 minutes of reaction, which is the specular image of all other compounds measured in the gas stream. The lowest hydrogen composition quantified for the volatile products was around 70% (molar) and during thermal runs, neither the trend nor the lowest hydrogen composition (94% molar) match these outcomes. H_2S production seemed to reach a maximum at the same time, and its generation declines after this point. In relation to thermal runs, this gas was produced only after 180 minutes of reaction utilizing the non-impregnated GAC. Results showed an apparent favouring of H_2S generation employing the 2% NiMo catalyst, although it is important to clarify that H_2S composition for the 5% NiMo experiment could not be measured during the first stages of the reaction due to operational problems.

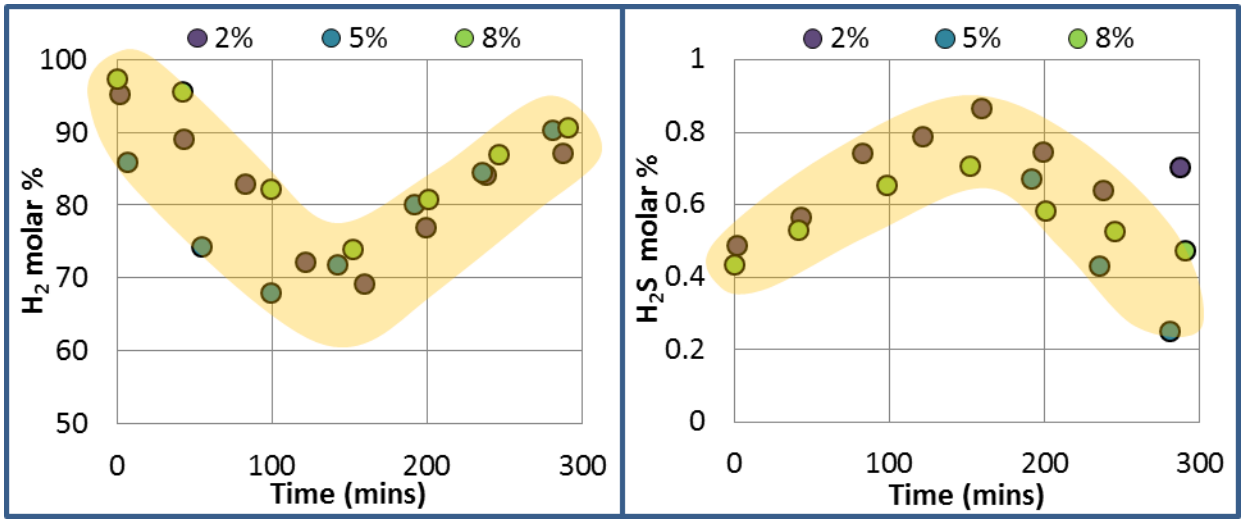

Figure 6.12. Hydrogen and H_2S composition in the outlet gas stream during catalytic runs at 350°C, 550 psig, 5 sccm H_2 and 4.5 hours, using 2%, 5% and 8% NiMo / GAC catalysts.

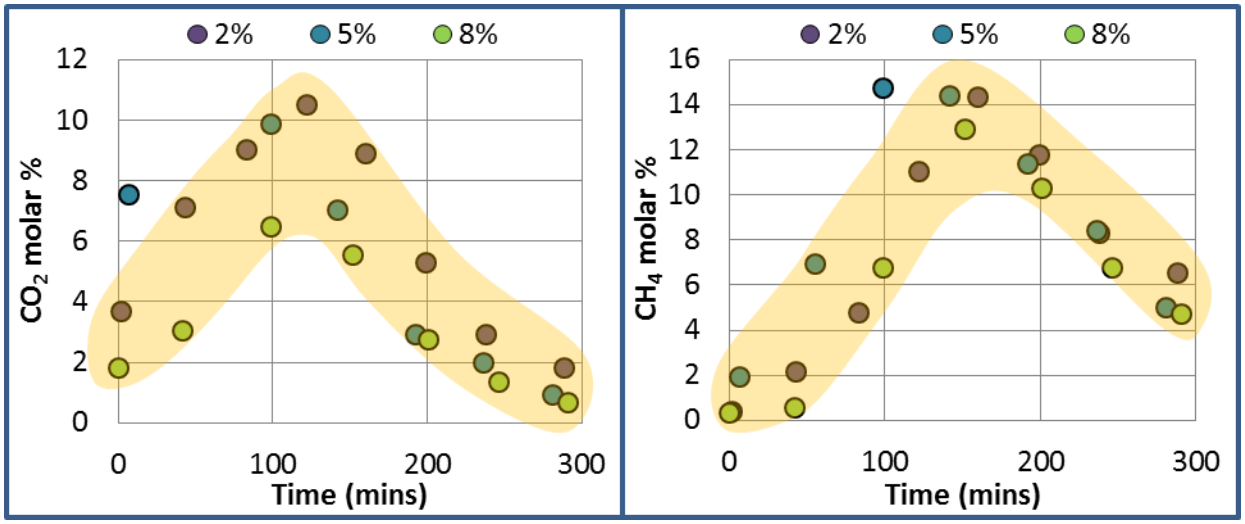

Figure 6.13. Carbon dioxide and methane composition in the outlet gas stream during hydroprocessing catalytic runs at 350°C, 550 psig, 5 sccm H_2 and 4.5 hours, using 2%, 5% and 8% NiMo / GAC catalysts.

Figure 6.13 shows carbon dioxide and methane molar compositions in the gas stream versus time of reaction. The evolution trend is specular in regards to hydrogen consumption and differs from results obtained with virgin GAC. The fact that methane maximum composition was larger than that of CO_2 is noteworthy. Evidently, catalysts enhanced methane production, presumably via CO_2 methanation, as the blank run showed a maximum amount of 2.4% (molar) during the same time frame, which was slightly below the maximum obtained for CO_2 (3% molar).

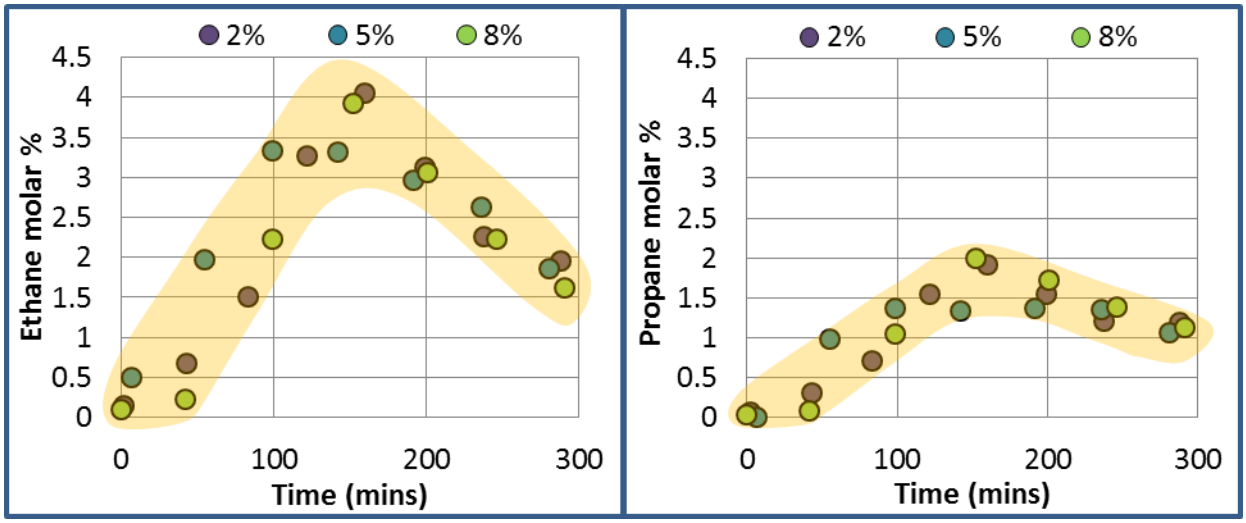

Figure 6.14. Ethane and propane composition in the outlet gas stream during catalytic runs at 350°C, 550 psig, 5 sccm H_2 and 4.5 hours, using 2%, 5% and 8% NiMo / GAC catalysts.

Impregnated solids proved their catalytic activity by promoting water soluble asphaltenes dealkylation, as supported by data reported in Figure 6.14. As seen in previous charts, there is a tendency of obtaining a maximum of volatile hydrocarbons composition that corresponds to the maximum hydrogen consumption (minimum hydrogen composition). Ethane and propane production was remarkable in comparison to the thermal run, and these gases were generated from the beginning of the experiment. Yet, CO_2 production was more pronounced than that of C_2 and C_3.

Overall results showed a slight difference between catalysts metal loads in regards to gas composition in the last 100 minutes of reaction; molar percentages of hydrogen, methane, ethane and propane practically overlapped within this region. The 2% NiMo catalyst, in comparison to the other catalysts, seemed to promote CO_2 from the maximum hydrogen consumption point to the end of the experiment, though this difference was somewhat reduced in the last half an hour. Interestingly, the maximum CO_2 content obtained by the 2% and the 5% catalysts were very close one another, although the 5% curve seems to be slightly shifted to the left. This was also the case with CH_4 during the 2% and 5% runs. In regards to H_2S content, it is not clear how much of this gas could be attributed to asphaltenes desulfurization and how much is related to sulfur species coming from the activation procedure, adsorbed on the surface of the solid and detaching during hydroprocessing.

6.5.2.2 Liquid stream

Liquid products were analyzed via HTSD and major findings are presented in the following figures.

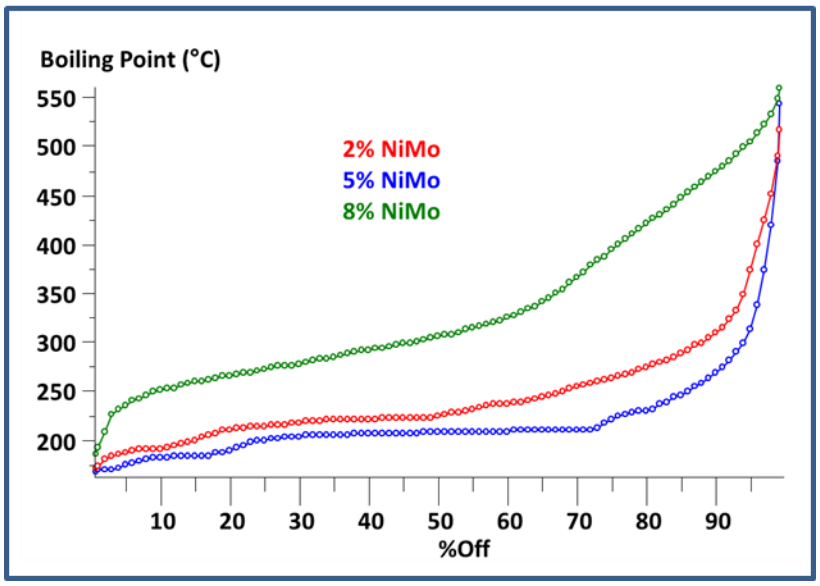

Figure 6.15. Distillation curve of liquid products from hydroprocessing runs carried out at 350°C, 550 psig, 5 sccm H_2 and 4.5 hours, using 2%, 5% and 8% NiMo / GAC catalysts.

Liquids retrieved from the 8% catalyst test showed a remarkable heavier quality, confirmed by the curve shift to the upper side of the boiling point chart. 1.8% of the liquid products were in the naphtha range (<200°C, <C_{12}), around 17% was kero quality (200°C- 260°C, C_{12}-C_{14}), approximately 46.6% designated diesel amounts (260-340°C, C_{14}-C_{20}) and 20.3% was light vacuum gas oil (340-450°C, C_{20}-C_{30}), for a total amount of distillates of 85.6%. In the case of the 2% NiMo catalyst, naphtha, kero, diesel and light vacuum gas oil percentages were 17.4%, 57.9%, 18.3% and 4.4% respectively. The total percentage of distillates, with respect to the total amount of liquid products, was 98%. The lightest product was obtained in the 5% NiMo test, in which 34% of liquids were considered as naphtha, 55% were identified as kerosene, 7.3% fell in the diesel region and 2.1% were in the light vacuum gas oil range. In this case, conversion to distillates was 98.5% from the total amount of liquid products.

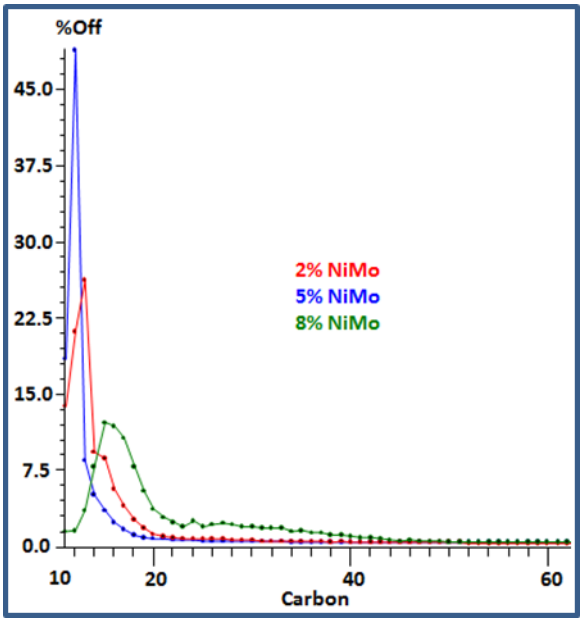

Figure 6.16. Carbon chain length distribution of liquid products from hydroprocessing runs carried out at 350°C, 550 psig, 5 sccm H_2 and 4.5 hours, using 2%, 5% and 8% NiMo / GAC catalysts.

Figure 6.16 shows that liquids streams didn't show significant amounts of hydrocarbons heavier than C_{50}, and the two catalysts with lowest NiMo loads practically truncated carbon chain lengths above C_{24}. The liquid product from the 8% NiMo catalyst had the largest proportion of diesel and hydrocarbons in the range between C_{22} and C_{40}, which were not recognized as majority products from other catalytic experiments.

6.6 WSA Adsorption and post adsorption hydroprocessing assessment

The alternative path proposed in this project consists in adsorption and hydroprocessing stages for water solubilized asphaltenes processing. Therefore, the necessity of evaluating combined results is imperative as it would validate the feasibility of further studying this path.

Current CNOOC-Nexen's practices in the Long Lake upgrader project provide a comprehensive comparison to the technology studied in this research. As mentioned in the first chapter of the document, CNOOC-Nexen's patented technology OrCrude™ consists in the gasification of asphaltenes removed prior to thermal cracking, generating hydrogen for the hydrocracker unit, and excess syngas for steam generation and power. This facility is also capable of sending precipitated asphaltenes to a delayed coking unit in which asphaltenes are converted to coke and other products. Predicted yields for

delayed coking of pitch would result in 12.4 wt% to gases, 36.4 wt% to distillates and 12.4 wt% to coke (Pereira, 2012).

Figure 6.17 summarizes the carbon route in the highest conversion scenario, achieved by the 5% NiMo catalyst. Carbon yields to liquid products (in wt%) and distillates (in wt%) were calculated based on the amount of carbon adsorbed on the catalyst. The weight percentages of adsorbed carbon were computed in relation to the amount of carbon available in a WSA solution of around 9,000 ppm TOC content. The carbon yield to WSA (in wt%) refers to the amount of solubilized carbon with respect to the parent nC_5 asphaltenes. Of note, the distillates cut was defined as the liquid products in the range of naphtha and light vacuum gas oil (<450°C).

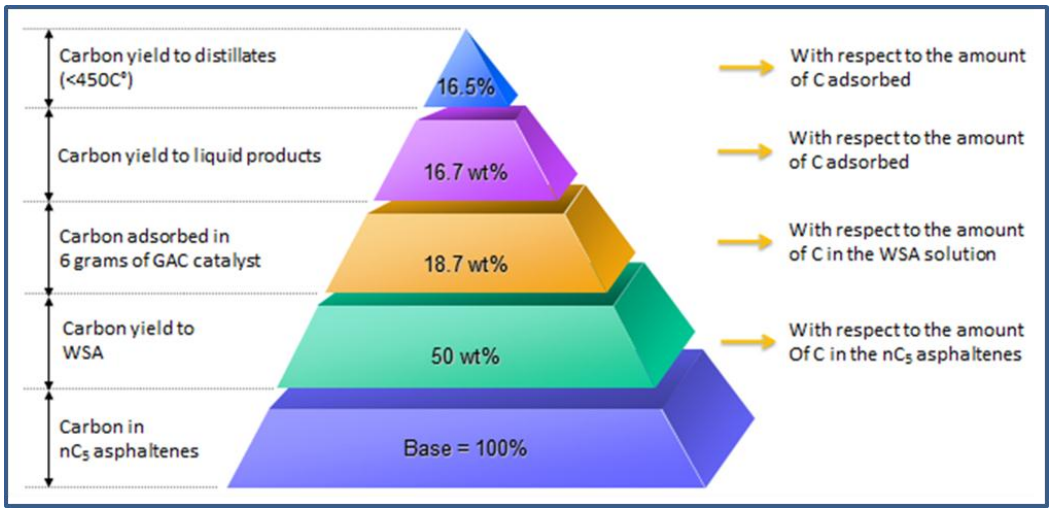

Figure 6.17. Carbon map of the complete WSA adsorption-hydroprocessing route using 6 grams of 5% NiMo catalysts in a packed bed reactor.

Values in Figure 6.17 show that the adsorption stage has room for improvement. In comparison to the carbon available in the WSA, less than 20% in weight is adsorbed using a 9,000 ppm solution. If a solid has a better affinity towards WSA than that exhibited on impregnated GAC, the overall process would seem more promising. However, it is important to remember than these results are for only one bed of catalyst and the larger scale process would consider a battery of packed beds in series. This type of operation would represent an advantage as the less concentrated WSA solution would lower its TOC content as it passes through a fresh bed of catalyst, retaining more asphaltenes available for posterior conversion. Furthermore, the battery would help clean the water until its TOC limits are low enough for disposing or for reuse in the oxisolubilization process.

In relation to delayed coking, yield percentages to distillates are 36.4 wt% for pitch (Pereira, 2012). Using the combined adsorption-hydroprocessing unit, the cumulated yield value is around 15 wt% in terms of carbon, considering the feedstock as nC_5 asphaltenes from Athabasca Vacuum Residue; yet, carbon conversions reached 50%. These outcomes indicate that catalyst formulation plays an important role in the success of the proposed pathway, as for the moment selectivity to gases doubles the selectivity to liquids. Manipulating catalyst formulations could represent larger yields to distillates and ensure the feasibility of the proposed pathway in a larger scale. Once again, all these numbers were calculated based on a single bed of NiMo/GAC catalyst, therefore products and reagents amounts would have to be analyzed to assess the scheme unit using multiple beds, including full assessment of regeneration of these beds.

Overall outcomes demonstrated that the project needs further studies to ensure its viability on a commercial level. Conditions and materials described in this document resulted in yield and selectivity values that are not promising enough to implement the two step process of adsorption/hydroprocessing to a larger scale by implementing a single bed unit. Nevertheless, key areas such as adsorbent affinity, oxisolubilization conditions and catalyst formulation may play an important role in improving these. A configuration of multiple packed bed reactors in series has to be considered. A compromise between metal load and WSA adsorption is made when increasing the amount of active species on the surface. Energy requirements need to be determined if this technology is going to be weighed against delayed coking, the alternative process in hand. Consequently, a more comprehensive assessment will determine if at some specific conditions, results would be favorable enough to scale-up the process.

7. FINAL REMARKS

7.1 Summary and conclusions

This project studied an new procedure attempting to provide better utilization of residual fractions (asphaltenes) and yield valuable light products. This pioneering process consisted in three basic steps: asphaltenes solubilization in water, adsorption and post-adsorption hydroprocessing. This new concept was evaluated utilizing different analytical techniques, varying operating conditions and testing various materials aiming to prove the feasibility of the whole process.

Water soluble asphaltenes were successfully produced for numerous experiments carried out throughout this project. Product quality and reaction conditions were studied under a certain range of operating parameters. It was found that oxidation temperature and residence time have a pronounced effect on CO_2 production. An optimum set of operating conditions, under the studied range of variables, was found at 230°C and 3 hours of residence time. At these conditions, the aqueous solution had the largest TOC content with less than 1% of IC concentration in the final product.

The selective adsorption of water soluble asphaltenes was investigated on a number of solids, assessing asphaltenes uptake in both qualitative and quantitative terms. Experiments carried out at static conditions and room temperature demonstrated that activated carbon had a strong affinity towards water soluble asphaltenes. The iron-silicate material (OMM-20) was the best ranked in comparison to other in-house adsorbents. Developed isotherms for ordered mesoporous materials and PAC showed multilayer adsorption of WSA.

A packed bed reaction setup was successfully built and implemented to adsorb water soluble asphaltenes in continuous mode at diverse operating conditions, showing reproducible results. The adsorption process on granular activated carbon was relatively fast as the effluent concentration stabilized after just 300 minutes at the lowest flow rate (1 cc/min). A slight adsorption enhancement was found at high temperatures but the bed was not fully saturated at these conditions, probably because the column was too short and the mass transfer zone was not long enough to completely exhaust the adsorbent.

Granular activated carbon was effectively impregnated with metals at concentrations of 2%, 5% and 8% by weight. ICP spectroscopy and XPS evidenced the presence of nickel and molybdenum in prepared catalysts. WSA adsorption on catalysts declined due to the reduction of surface area caused by metals addition to the solid. Furthermore, these outcomes were attributed to adsorption of sulfur species coming from the catalyst activation step, reducing the availability of pores for WSA retention.

The catalytic effect of metals in the reaction process was demonstrated as liquid hydrocarbons were yielded, carbon conversions were significantly improved and amounts of light hydrocarbons in gas streams increased in comparison to thermal runs.

Thermal cracking of pre-adsorbed WSA occurred at temperatures between 250°C and 300°C, in which decarboxylation reactions took place and CO_2 was generated at early stages of the process. Small traces of methane and ethane were produced at thermal runs carried out at 300°C and 350°C, and H_2S was formed only after 3 hours of reaction, yet in negligible amounts.

Hydroprocessing runs showed that NiMo catalysts favored methane over CO_2 production, presumably via CO_2 methanation. A maximum of volatile hydrocarbons generation was found at around 150 minutes of reaction, corresponding to the maximum hydrogen consumption evidenced by gas chromatography analyses. H_2S reaches a maximum composition at the lowest hydrogen percentage reported for the 2% NiMo and 8% NiMo catalysts.

Liquid hydrocarbons of <450°C boiling temperature were evidenced by the HTSD technique, and the lightest products were obtained using the 5% NiMo catalyst. The 8% NiMo impregnated solid yielded the heaviest products, yet distillable, and the 2% NiMo catalyst product quality was in between. Liquids selectivity was found to be 34%, 29% and 8% for the 2%, 5% and 8% metal loads, respectively.

The overall WSA adsorption-hydroprocessing practice was assessed using only one packed bed and not a battery of reactors arranged in series, as conceived for the larger-scale design. At the moment, by implementing a single reactor acceptable amounts of liquid hydrocarbons were not produced. Hydroprocessing reaction conditions were achieved, yet quantities of valuables were barely enough to analyze them. From the carbon route map, it was possible to identify that the adsorbent selection was the factor that presumably led to these outcomes.

7.2 Future work

The amount of adsorbed asphaltenes was crucial to determine the success of the proposed chemical pathway for heavy oil upgrading. More adsorbent-catalyst combinations are worth exploring to recognize if there is one most able to adsorb the totality of WSA using a reasonable amount of solid and highly concentrated solutions.

The overall process needs to be further assessed in terms of implementing a battery of packed beds to increase the amount of adsorbed carbon and to clean the water at a proper level for reutilization. Hydrogen requirements for the full battery and energy balances are necessary in order to compare the project at a larger scale with the delayed coking technology.

Characterization of filtered solids during adsorption runs is fundamental to understand all implications of the combined process. Although efforts were made to identify the collected material, other techniques must be employed to categorize unknown solids; process operating conditions and/or setup has to be modified in order to avoid these suspended solids that could lead to additional processing stages.

Higher temperatures, different reaction times and other hydrogen pressures are recommended to be tested with the purpose of providing further insight on WSA hydroprocessing. Some mechanical alterations could be made to the setup to guarantee a proper operation in much longer runs, such as more powerful data acquisition systems and the installation of a profile probe thermocouple inside the reactor; the last one would enable the user to read more temperatures inside the packed bed, allowing more accurate controlling and monitoring during adsorption and hydroprocessing experiments.

As part of the integral process, conditions for oxisolubilization of asphaltenes in water need to be explored in detail, targeting minimization of water/asphaltenes ratio while increasing asphaltenes concentration in the solution without compromising the stability of the product (i.e., precipitation).

REFERENCES

Ackelson, D. *UOP Unicracking Process for Hydrocracking* in *Handbook of Petroleum Refining Processes*. 3rd Ed, 2004: digital edition. McGraw-Hill Education.

Alberta Energy Resources Conservation Board. *Alberta's Energy Reserves 2012 and Supply-Demand Outlook 2013-2022*. ST98-2013, 2013 [retrieved January 2014], available online from http://www.aer.ca/documents/sts/ST98/ST98-2013.pdf.

American Society for Testing and Materials. *D-7169 Standard test method for boiling point distribution of samples with resid such as crude oils and atmospheric resids by high temperature gas chromatography*. 2005.

Allen, E. *Process water treatment in Canada's oil sands industry: II. A Review of emerging technologies*. Journal of Environmental Engineering and Science, 2008 (7): p. 499-524.

Ancheyta, J., Rana, M., and Furimsky, E. *Hydroprocessing of heavy petroleum feeds: Tutorial*. Catalysis today, 2005 (109): p. 3-15.

Ancheyta, J. and Speight, J. *Hydroprocessing of heavy oils and residua*. 1st ed, 2007: Boca Raton, United States of America. CRC Press/Taylor & Francis group.

Aprile, C., Corma, A. and Garcia, H. *Enhancement of the photocatalytic activity of TiO_2 through spatial structuring and particle size control: from subnanometric to submillimetric length scale*. Physical Chemistry Chemical Physics, 2008 (10): p. 769-783.

Asuha, S., Gao, Y. W., Deligeer, W., Yu, M., Sulaya, B. and Zhao, S. *Adsorptive removal of methyl orange using mesoporous maghemite*. Journal of Porous Materials, 2011 (18): p. 581-587.

Bridge, A. G. and Hamilton, G. L. *Hydrogen Processing* in *Handbook of Petroleum Refining Processes*. 3rd Ed, 2004: digital edition. McGraw-Hill Education.

Byambajav, E. and Ohtsuka, Y. *Cracking behavior of asphaltenes in the presence of iron catalysts supported on mesoporous molecular sieve with different pore diameters*. Fuel, 2003 (82): p. 1571-1577.

Calafat, A., Laine, J. and López-Agudo, A. *Hydrodenitrogenation of pyridine over activated carbon-supported sulfide Mo and NiMo catalysts. Effects of hydrogen sulfide and oxidation of the support.* Catalysis letter, 1996 (40): p. 229-234.

Carbognani, L. Technical report, 1992, Intevep S. A. Caracas, Venezuela.

Carbognani, L. *Literature review on oxidative processes, water solubilization of petroleum heavy fractions/asphaltenes, characterization of solubilized hydrocarbons and production of light ends from solubilized asphaltenes*. Technical report, 2012, NSERC/NEXEN/Alberta Innovates Energy and Environment Solutions Industrial Research Chair in Catalysis for Bitumen Upgrading. Calgary, Canada.

Carbognani, L., Roa-Fuentes, L. C., López-Linares, F., Vasquez., A., Pereira-Almao, P., Haghighat, P., Maini, B. B. and Spencer, R. J. *Monitoring Bitumen Upgrading, Bitumen Recovery and Characterization of Core Extracts by Hydrocarbon Group-type SARA Analysis*. Petroleum Science and Technology, 2010 (28): p. 632-645.

Chadwick, D., Oen, A. and Siewe, C. *Influence of water and ammonia on hydrotreating catalysts and activity for tetralin hydrogenation*. Catalysis today, 1996 (29): p. 229-233.

Choi, J. W., Chung, S. G., Hong, S. W., Kim, D. J. and Lee, S. H. *Development of adsorbent for the simultaneous removal of organic and inorganic contaminants from aqueous solution*. Water Science & Technology, 2011 (64): p. 1821-1827.

Choo, K. and Kang, S. *Removal of residual organic matter from secondary effluent by iron oxides adsorption*. Desalination, 2003 (154): p. 139-146.

Cooper, C. and Burch, R. *Mesoporous materials for water treatment processes.* Water Research, 1999 (33): p. 3689-3694.

Curtis, C. W., Jeom, Y. W. and Clapp, D. J. *Adsorption of asphalt functionalities and oxidized asphalts on aggregate surfaces*. Fuel Science and Technology International, 1989 (7): p. 1225-1268.

Das, D., Gaur, V. and Verma, N. *Removal of volatile organic compound by activated carbon fiber*. Carbon, 2004 (42): p. 2949-2962.

Davies, G., Fataftah, A., Cherkasskiy, A., Ghabbour, E. A., Radwan, A., Jansen, S. A., Kolla, S., Paciolla, M. D., Sein Jr., L. T., Buermann, W., Balasubramanian, M., Budnick, J. and Xing, B. *Tight metal bindings by humic acids and its role in biomineralisation*. Journal of the Chemical Society, Dalton Transactions, 1997: p. 4047-4060.

Debellefontaine, H., Chakchouk, M., Foussar, J. N., Tissot, D. and Striolo, P. *Treatment of organic aqueous wastes: Wet air oxidation and wet peroxide oxidation.* Environmental Pollution, 1996 (92): p. 155-164.

Deutsch, K. L. and Shanks, B. H. *Hydrodeoxygenation of lignin model compounds over a copper chromite catalyst*. Applied Catalysis A: General, 2012 (447-448): p. 144-150.

Doyle, D. H. and Brown, A. B. *Produced Water treatment and hydrocarbon removal with organoclay*. Proceedings: SPE Annual Technical Conference and Exhibition. Dallas, October 1-4, 2000. SPE 63100.

Duyvesteyn, W. and Morley, R. L. *Oxidation of asphaltenes*. United States Patent application number 2020100320118 (published in 2010).

Eldood, A., Scott, C. and Pereira, P. *Wet Oxidation of Asphaltenes Annual Report.* Technical report, Laricina Energy Ltd*,* 2010. Calgary, Canada.

European Virtual Institute for Speciation Analysis (EVISA). *Instrument Database: Antek – Model 9000 Nitrogen/Sulfur Analyzer*. 2010 [retrieved in May 2014], available online from http://www.speciation.net/Database/Instruments/Antek/MODEL-9000-NitrogenSulfur -Analyzer-;i2248

Fahim, M. A., Al-Sahhaf, T. A. and Elkilani, A. S. *Fundamentals of Petroleum Refining*. 1st ed, 2010: Oxford, United Kingdom. Elservier.

Fettig, J. *Removal of Humic Substances by Adsorption/Ion Exchange*. Water Science and Technolgy, 1999 (40): p.173-182.

Filimonova, T. A., Yertakova, L. D., Yeliseyev, V. S. and Kryazhev, Yu. G. *Ozonolysis of asphaltenes*. Petroleum Chemistry U.S.S.R., 1976 (16): p. 180-185.

Furimsky, E. *Carbons and Carbon-supported Catalysts in Hydroprocessing*. 1st Ed, 2008: Cambridge, United Kingdom. RSC Publishing.

Furimsky, E. *Catalyst for Upgrading Heavy Petroleum Feeds*. 1st Ed, 2007: Oxford, United Kingdom. Elsevier Science.

Furimsky, E. *Hydroprocessing in Aqueous Phase*. Industrial & Engineering Chemistry Research, 2013 (52): p. 17695-17713.

Gary, J. and Handwerk, G. *Petroleum Refining*. 4th Ed, 2001: New York, United States of America. Marcel Dekker, Inc.

Goswamil, J., Kakadiya, J. and Shah, N. *Development and validation of Q-absorbance ratio method for simultaneous estimation of ambroxol hydrochloride and cepfodoxime proxetile in combined tablet dosage form. International.* Journal of Pharmascholars, 2012 (1): p. 56-61.

Grant, T. and King, J. *Mechanism of Irreversible Adsorption of Phenolic Compounds by Activated Carbons*. Industrial and Engineering Chemical Research, 1990 (29): p. 264-271.

Green car congress. *Mascoma announces feedstock processing and lignin supply agreement with Chevron technology ventures; Chevron working on converting lignin to hydrocarbon fuel components*. 2009 [retrieved in February 2014], available online from http://www.greencarcongress.com/2009/09/mascoma-chevron.html.

Groot, C., de Beer, V. H. J. and Prins, R. *Comparative study of alumina and carbon-supported catalysts for hydrogenolysis and hydrogenation of model compounds and coal-derived liquids.* Industrial & Engineering Chemistry Product Research and Development, 1986 (25): p. 522-530.

Gupta, S. and Babu, B. V. *Experimental investigations and Theoretical Modeling Aspects in Column Studies for Removal of Cr(VI) from Aqueous Solutions Using Activated Tamarind Seeds*. Journal or Water Resource and Protection, 2010 (2): p. 706-716.

Gupta, V. K., Carrott, P. J. M., Ribeiro Carrott, M. M. L. and SUHAS. *Low-Cost Adsorbents: Growing Approach to Wastewater Treatment – a Review*. Critical Reviews in Environmental Science and Technology, 2009 (39): p. 789-842.

Güvenir, Ö. *Synthesis and characterization of clinoptilolite*. Master of Science Thesis, 2005: Middle East Technical University, Ankara, Turkey.

Hansen, B. R. and Davies, S. R. H. *Review of potential technologies for the removal of dissolved components from produced water*. Transactions of the Institution of Chemical Engineers, 1994 (72): p. 176-188.

Heinemann, H., Somorjai, G. A., Pereira, P. and Carrazza, J. *Catalytic Gasification of Graphite and Chars.* Journal Preparation Paper – American Chemical Society, Division Fuel Chemistry, 1989 (34): p. 121-129.

Higman, C. and van der Burgt, M. *Gasification*. 2nd Ed, 2008: Burlington, United States of America. Elsevier.

Hillerová, E. and Zdražil, M. *High activity Ni-Mo/C hydrodesulfurization catalyst: comparison with commercial Ni-Mo/Al_2O_3 catalyst at increased hydrogen pressure.* Catalysis Letters, 1991 (8): p. 215-220.

Hillerová, E., Zdražil, Shkuropat, M. S. A., Bogdanets, E. N. and Startsev, A. N. *Comparison of carbon and alumina supported-nickel-molybdenum sulfide catalysts in parallel hydrodenitrogenation and hydrodesulfurisation*. Applied Catalysis, 1991 (67): p. 231-236.

Hong, A. *Fragmentation of heavy hydrocarbons using an ozone-containing fragmentation fluid*. United States Patent application number 2006/0163117 A1 (published in 2006).

Hood, W. *Activated Carbon used to treat produced water at gas storage field*. Proceedings: Rocky Mountain Symposium on Environmental Issues in Oil and Gas Operations. Golden, July 14-15, 1997, Colorado School of Mines.

Hosseini, N. and Fatemi, S. *Experimental study and adsorption modeling of COD reduction by activated carbon for wastewater treatment of oil refinery.* Iranian Journal of chemistry and chemical engineering, 2013 (32): p. 81-89.

Hsu, C. S. and Robinson, O. R. *Practical advances in Petroleum Processing.* 1st Ed, 2006: New York, United States of America. Springer.

Humic Consortium for Carbon Sequestration. *Why use Humic Substances for Carbon Sequestration*. 2008 [retrieved in October 2013], available online from http://ihccs.org/humic.htm.

Institute of Petroleum. *Standard IP 143/90. Asphaltene (Helptane Insolubles) in Petroleum Products* in *Standards for Petroleum and Its Products.* 1985: London, United Kingdom. John Wiley and Sons.

Isquierdo, F. , Pereira-Almao, P., Vitale, G. and Scott, C. E. *Asphaltene hydroprocessing*. Preprint paper for the 248th ACS National Meeting & Exposition, San Francisco in August 10-14, 2014.

Janssens, J. P., Elst, G., Schrikkema, E. G., van Langeveld, A. D., Sie, S. T. and Moulijn, J. A. *Development of a mechanistic picture of the hydrodemetallization reaction of metallo-tetraphenylporphyrin on a molecular level*. Recueil des Travaux Chimiques des Pays-Bas, 1996 (115): p. 465-473.

Jiang, J. and Ashekuzzaman, S. M. *Development of novel inorganic adsorbent for water treatment*. Current opinion in Chemical Engineering, 2012 (1): p. 1-9.

Kindpac, T. *Bentonite introduction.* 2012 [retrieved May 2014], available online from http://en.kindpac.com/index.php?module-news-view-9.html

Koubaissy, B., Toufaily, J., Kafrouny, L., Joly, G., Magnoux, P. and Hamieh, T. *Industrial water treatment, by adsorption, using organized mesoporous materials*. Physics Procedia, 2011 (21): 228-233.

Kudo, S., Hachiyama, Y., Takashima, Y., Tahara, J., Idesh, S., Norinaga, K. and Hayashi, J. *Catalytic hydrothermal reforming of lignin in aqueous alkaline medium*. Energy & Fuels, 2011 (28): p. 76-85

Kuehler, C. W. *Hydroprocessing carbonaceous feedstocks containing asphaltenes*. United States Patent number 4381987, 1983.

Lapinas, A. T., Klein, M. T., Gates, B. D., Macris, A. and Lyons, J. E. *Catalytic hydrogenation and hydrocracking of fluorene: reaction pathways, kinetics and mechanisms*. Industrial and Engineering Chemical Research, 1991 (30): 42-50.

Le Page, J. F., Chatila, S. G. and Davidson, M. *Resid and heavy oil processing*. 1st ed, 1992: Paris, France. Éditions Technip.

Leckel, D. *Catalytic hydroprocessing of coal-derived gasification residues to fuel blending stocks: effect of reaction variables and catalyst on hydrodeoxygenation (HDO), hydrodenitrogenation (HDN), and hydrodesulfurization (HDS)*. Energy & Fuels, 2006 (20): p. 1761-1766.

Manrique, A., López-Linares, F., Carbognani-Ortega, L. and Pereira-Almao, P. *Adsorption of water solubilized asphaltenes*. Presented at the 2013 Heavy Oil Latin America Conference & Exhibition, Puerto Vallarta in September 24-26, 2013. Paper HOLA13-116.

Marczewski, A. and Szymula, M. *Adsorption of asphaltenes from toluene on mineral surface*. Colloids and Surfaces A: Physicochemical and Engineering Aspects, 2002 (208): p. 259-266.

Marsh, H., Heintz, E. A. and Rodríguez-Reinoso, F. *Introduction to Carbon Technologies*. 1st Ed, 1997: Alicante, Spain. Publicaciones de la Universidad de Alicante.

McKay, G., Otterburn, M. S. and Aga, J. A. *Fullers earth and fired clay as adsorbents for dyestuffs – equilibrium and rate studies*. Water Air Soil Pollution, 1985 (24): p. 307-322.

Meynen, V., Cool, P. and Vansant, E. F. *Verified syntheses of mesoporous materials.* Microporous and Mesoporous Materials, 2009 (125): p. 170-223.

Mochizuki, T., Chen, S., Toba, M. and Yoshimura, Y. *Deoxygenation of guaiacol and woody tar over reduced catalysts*. Applied Catalysis B: Environmental, 2014 (146): p. 237-243.

Morel, F. and Peries, J. P. *Residue Hydroconversion*, in *Petroleum Refining 3. Conversion Processes.* 2001: France. Institute Français du Pétrole Publications.

Moschopedis, S. E. and Speight, J. G. *Water-soluble derivatives of Athabasca asphaltenes*. Fuel, 1971 (50): p. 34-40.

Narayanasarma, P. *Mesoporous Carbon Supported NiMo Catalyst for the Hydrotreating of Coker Gas Oil.* Master of Science Thesis, 2011: University of Saskatchewan, Saskatoon, Canada.

Nassar, N., Hassan, A. and Pereira-Almao, P. *Metal Oxide Nanoparticles for Asphaltene Adsorption and Oxidation*. Energy & Fuels, 2011 (25): p. 1017-1023.

Nimmanwudipong, T., Runnebaum, R. C., Brodwater, K., Heelan, J., Block, D. E. and Gates, B. C. *Design of a high-pressure flow reactor system for catalytic hydrodeoxygenation: guaiacol conversion catalyzed by platinum supported on MgO.* Energy & Fuels, 2014 (28): p. 1090-1096.

Nomura, M., Rahimi, P. M. and Koseoglu, O. R. *Heavy Hydrocarbon Resources: Characterization, Upgrading and Utilization*. ACS Symposium Series, 2005 (895) p: 1-18.

Oliveira, R. C., Palmieri, M. C. and Garcia Jr, O. *Biosorption of Metals: State of the Art, General Features, and Potential Applications for Environmental and Technological Processes*, in *Progress in Biomass and Bioenergy Production*. 2011 [retrieved in March 2014], available online from http://cdn.intechopen.com/pdfs-wm/16643.pdf.

Ouki, S. K. and Kavannagh, M. *Performance of natural zeolites for the treatment of mixed metal-contaminated effluents*. Waste Management & Research, 1997 (15): p. 383-394.

Penrose, C., Wallace, P. S., Kasbaum, J. L., Anderson, M. K. and Preston, W. E. *Enhancing refinery profitability by gasification, hydroprocessing and power generation*. Presented at the Gasification Technologies Conference, San Francisco in October 17-20, 1999.

Peña-Méndez, E., Havel, J. and Patočka, J. *Humic substances – compounds of still unknown structure: applications in agriculture, industry, environment, and biomedicine*. Journal of applied biomedicine, 2005 (3): p. 13-24.

Pereira, P., Somorjai, G. A. and Heinemann, H. *Catalytic Steam Gasification of Coals*. Energy & Fuels, 1992 (6): p. 407-410.

Pereira, P. *Delayed Coking*. 2012, Class notes for the course *ENGG 503 Upgrading and Refining Technology*. University of Calgary.

Physical Electronics. *XPS: X-ray photoelectron spectroscopy and ESCA: Electron Spectroscopy for Chemical Analysis.* 2014 [retrieved in April 2014], available online from https://www.phi.com/surface-analysis-techniques/xps.html.

Qader, S. A. and McOmber, D. B. *Conversion of Complex Aromatic Structures to Alkyl Benzenes*. ACS Symposium Series, 1975 (20): 82-98.

Rana, M.S., Sámano, V., Ancheyta, J. and Diaz, J. A. I. *A review of recent advances on processing technologies for upgrading of heavy oils and residua.* Fuel, 2007 (86): p. 1216-1234.

Rao, P., Lo, I. M. C., Yin, K. and Tang, S. C. N. *Removal of natural organic matter by cationic hydrogel with magnetic properties*. Journal of Environmental Management, 2011 (92): p. 1690-1695.

Rase, H. F. *Chemical reactor design for process plants. Volume one: Principles and Techniques.* 1st ed, 1977: New York, United States of America. John Wiley & Sons.

Rivera-Utrilla, J., Sánchez-Polo, M., Gómez-Serrano, V., Álvarez, P. M., Alvim-Ferraz, M. C. M. and Dias, J. M. *Activated carbon modifications to enhance its water treatment applications. An overview.* Journal of Hazardous materials, 2011 (187): p. 1-23.

Sadeghbeigi, R. *Fluid catalytic cracking handbook: An Expert Guide to the Practical Operation, Design and Optimization of FCC Units*. 3rd Ed, 2012: Waltham, United States of America. Elsevier.

Salmani, M. H., Vakili, M. and Ehrampoush, M. H. *A comparative study of copper (ii) removal on iron oxide, aluminum oxide and activated carbon by continuous down flow method*. Journal of Toxicology and Environmental Health Sciences, 2013 (5): p. 150-155.

Schachtl, E., Wuttke, E., Gutiérrez, O. Y. and Lercher, J. A. *Effect of Ni on the characteristics and hydrogenation activity of sulfide Mo/ γ -Al_2O_3.* Presented at the Reducing the Carbon Footprint of Fuels and Petrochemicals DGMK Conference, Berlin, in October 8–10, 2012.

J. Scherzer and A. J. Gruia. *Hydrocracking Science and Technology*. 1st Ed, 1996: New York, United States of America. Marcel Dekker, Inc.

Segawa, K. *Catalyst developments for the production of sulfur free flues: Effect of Ni promoter and chelating reagent on Ni-MoS2 HDS catalysts.* Presented at the 21st Saudi Arabia-Japan Joint Symposium, Dhahran, in November 27-28, 2011.

Seifi, L., Torabian, A., Kazemian, H., Bidhendi, G. N., Azimi, A. A. and Charkhi, A. *Adsorption of Petroleum Monoaromatics from Aqueous Solutions Using Granulated Surface modified Natural Nanozeolites: Systematic Study of Equilibrium Isotherms.* Water Air Soil Pollution, 2011 (217): 611-625.

Serna-Guerrero, R. and Sayari, A. *Applications of Pore-Expanded Mesoporous Silica. 7. Adsorption of Volatile Organic Compounds*. Environmental Science and Technology, 2007 (41): 4761-4766.

Shabtai, J. S. and Zmierczak, W. W. *Process for conversion of lignin to reformulated hydrocarbon gasoline*. United States Patent number US5959167, 1999.

Shabtai, J. S. and Zmierczak, Chornet, E. and Johnson, D. *Process for converting lignins into a high octane blending component*. United States Patent number US20030115792, 2003.

Sharma, E. A. and Shah, N. J. *Development and validation of Q-absorbance ratio method for simultaneous estimation of ambroxol and desloratadine in combined tablet dosage form.* International journal of pharmaceutical and chemical sciences, 2012 (1): p. 773-778.

Shen, Y. *Removal of phenol from water by adsorption-flocculation using organobentonite*. Water research, 2002 (36): p. 1107-1114.

Shimadzu. *TOC-VCPH/CPN Total Organic Carbon Analyzer. User's Manual*. 2011

Shon, H. K., Vigneswaran, S. and Snyder, S. A. *Effluent Organic Matter (EfOM) in Wastewater: Constituents, Effects and Treatment*. Critical Reviews in Environmental Science and Technology, 2006 (36): p. 327-374.

Skoog, D. A. and West, D. N. *Fundamentals of analytical chemistry*. 3rd Ed, 1976: New York, United States of America. Holt, Rinehart and Winston.

Sosa, C., Gonzalez, M. F., Carbognani, L., Perez-Zurita, M. J., López-Linares, F., Moore, R. G., Husein, M. and Pereira, P. *Visbreaking based integrated process for bitumen upgrading and hydrogen Production.* Presented at the Canada International Petroleum Conference, Calgary in June 13-15, 2006. Paper 2006-074.

Speight, J. *New approaches to hydroprocessing*. Catalysis Today, 2004 (98): p. 55-60.

Speight, J. *Refinery of the future*. 1st ed, 2011: Oxford, United Kingdom. Elsevier Inc.

Speight, J. *The chemistry and technology of petroleum*. 4th ed, 2007: Boca Raton, United States of America. CRC Press/Taylor & Francis group.

Speight, J. *The desulfurization of heavy oils and residua*. 2nd ed, 1999: New York, United States of America. Marcel Dekker, Inc.

SRI Instruments. *Gas Chromatograph User's Manual*. 2014 [retrieved in April 2014], available online from http://www.srigc.com/MG2.pdf

Stevenson, F. J. *Humus Chemistry Genesis, Composition, Reactions*. 1st Ed, 1982: New York, United States of America. Willey Interscience.

Suzuki, T., Itoh, M., Takegami, Y. and Watanabe, Y. *Chemical structure of tar-sand bitumens by 13C and 1H NMR spectroscopic methods*. Fuel, 1982 (61): p. 402-410.

Tan, K. *Humic matter in Soil and the Environment Principles and Controversies*. 1st ed, 2003: New York, United States of America. Marcel Dekker, Inc.

Teermann, I. and Jekel, M. *Adsorption of humic substances onto B-FeOOH and its chemical regeneration*. Water Science and Technolgy, 1999 (40): p.199-206.

Topsøe, H., Clausen, B. S. and Massoth, F. E. *Hydrotreating Catalysis: Science and Technology* in *Catalysis, Science and Technology*. 1st ed, 1996: New York, United States of America. Springer – Verlag Berlin Heidelberg.

Toufaily, J., Koubaissy, B., Kafrouny, L., Hamad, H., Magnoux, P., Ghannam, L., Karout, A., Hazimeh, H., Nemra, G., Hamieh, M., Ajouz, N. and Hamieh, T. *Functionalization of SBA-15 materials for the adsorption of phenols from aqueous solution*. Central European Journal of Engineering, 2013 (3): p. 126-134.

United States Geological Survey. *Mineral Commodity Summaries 2013*. 2013 [retrieved in January 2014], available online from http://minerals.usgs.gov/minerals/pubs/mcs/2013/mcs2013.pdf

Vit, Z. and Zdražil, M. *Simultaneous hydrodenitrogenation of pyridine and hydrodesulfurization of thiophene over carbon-supported platinum metal sulfides*. Journal of Catalysis, 1989 (119): p. 1-7.

Wang, H., Male, J. and Wang, Y. *Recent advances in hydrotreating of pyrolysis bio-oil and its oxygen-containing model compounds*. ACS Catalysis, 2013 (3): p. 1047-1070.

Wennerberg, A. N. and Frazier, A. W. *Hydrotreatment of fossil fuels*. United States Patent number US3812028, 1974

Yahaya, N. K., Abustan, I., Latiff, M. F., Bello, O. S. and Ahmad, M. Z. *Fixed-bed column study for Cu (II) removal from aqueous solutions using rice husk based activated carbón.* International Journal of Engineering & Technology, 2011 (11): p. 186-190.

Zeinali, F., Ghoreyshi, A. A. and Najafpour, G. D. *Adsorption of dichloromethane from aqueous phase using granular activated carbon: isotherm and breakthrough curve Measurements*. Middle-East Journal of Scientific Research, 2010 (4): p. 191-198.

Zhang, K. *Mesostructured porous materials: pore and surface engineering towards bio-inspired synthesis of heterogeneous copper catalysts.* Doctoral Thesis, 2008: Université de Lyon, Lyon, France.

Zhang, Y., Qiao, Z., Li, Y., Liu, Y. and Huo, Q. *Cooperative adsorbent based on mesoporous SiO_2 for organic pollutants in water*. Journal of Materials Chemistry, 2011 (21): p. 17283-17289.

Zhang, S., Shao, T. and Karanfil, T. *The correlation between structural characteristics of activated carbons and their adsorption of organic solutes from aqueous solutions*. Adsorption, 2012 (18): p. 229-238.

Zhao, D., Huo, Q., Feng, J., Chmelka, B. and Stucky, G. *Nonionic Triblock and Star Diblock Copolymer and Oligomeric Surfactant Syntheses of Highly Ordered, Hydrothermally Stable, Mesoporous Silica Structures*. Journal of the American Chemical Society, 1998 (120): p. 6024-6036.

Zhao, X. S., Ma, Q. and Lu, G. Q. *VOC Removal: Comparison of MCM-41 with Hydrophobic Zeolites and Activated Carbon*. Energy & Fuels, 1998 (12): p. 1051-1054.

Zhu, L., Tian, S. and Shi, Y. *Adsorption of volatile organic compounds onto porous clay heterostructures based on spend organobentonites*. Clays and clay minerals, 2005 (53): 123-136.

APPENDIX A. BJH DESORPTION CURVES OF SCREENED ADSORBENTS

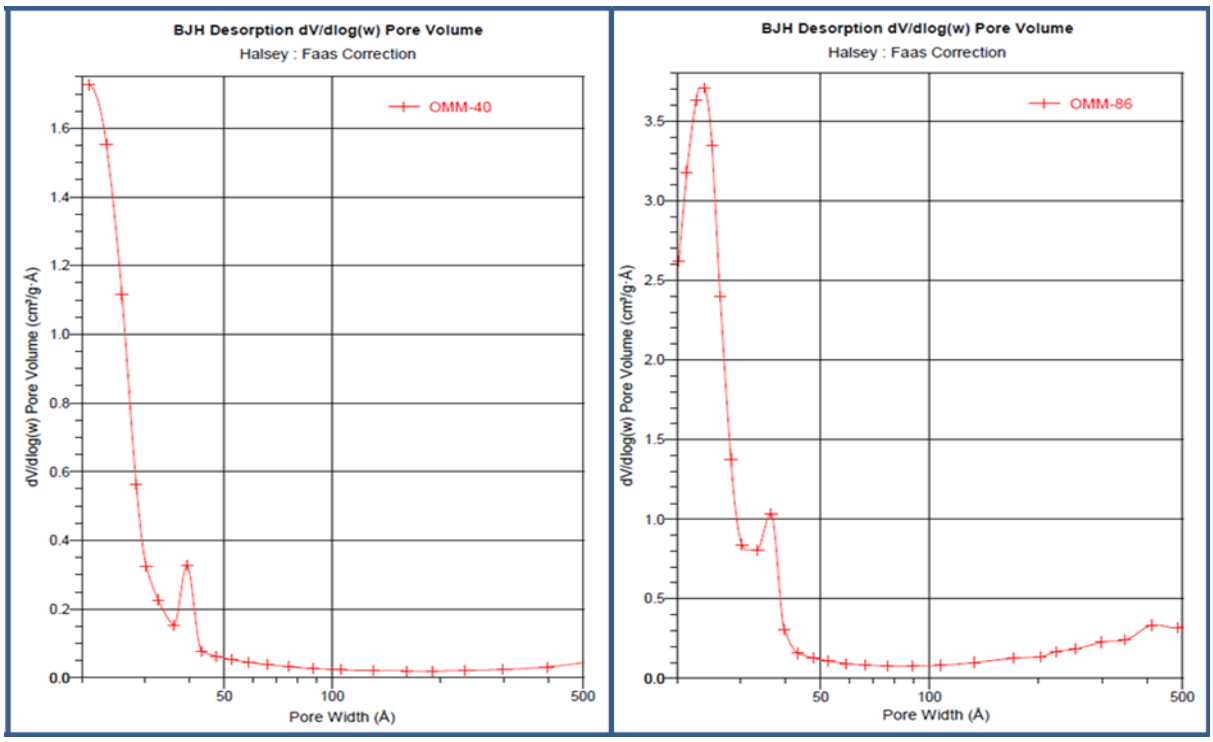

Figure A.1. Pore distribution charts of SiO_4 based adsorbents: OMM-40 and OMM-86.

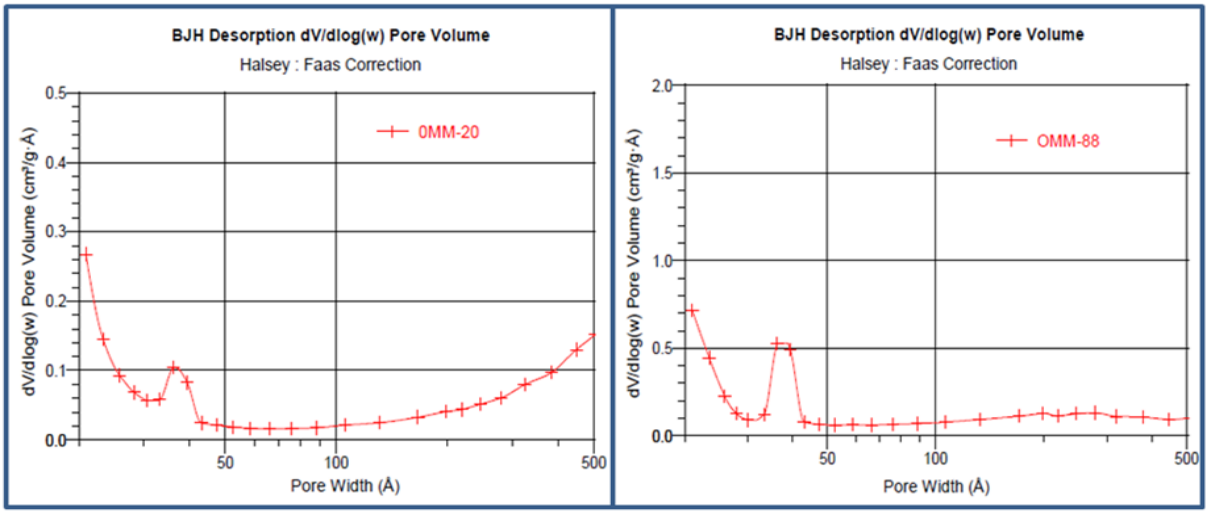

Figure A.2. Pore distribution charts of Fe–SiO_4 based adsorbents: OMM-20 and OMM-88.

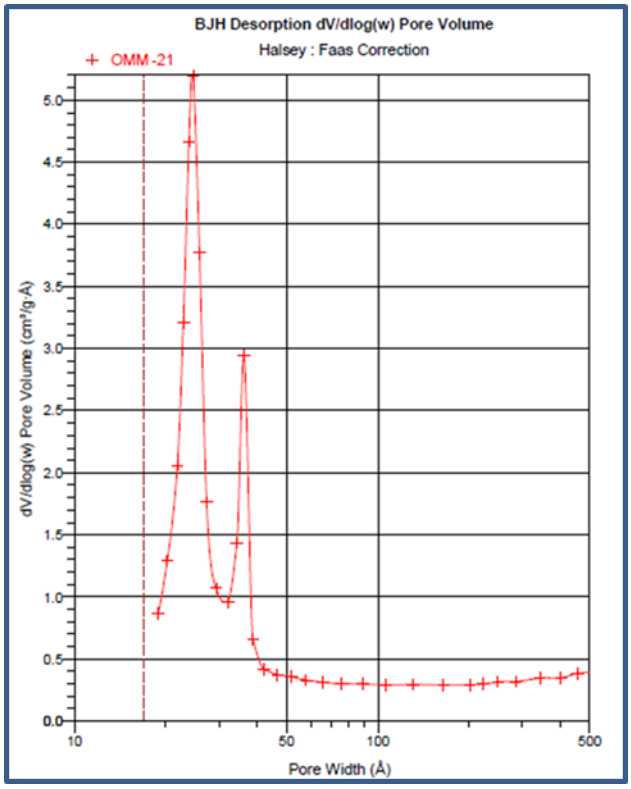

Figure A.3. Pore distribution chart of OMM-21 (Cu-SiO_4 based).

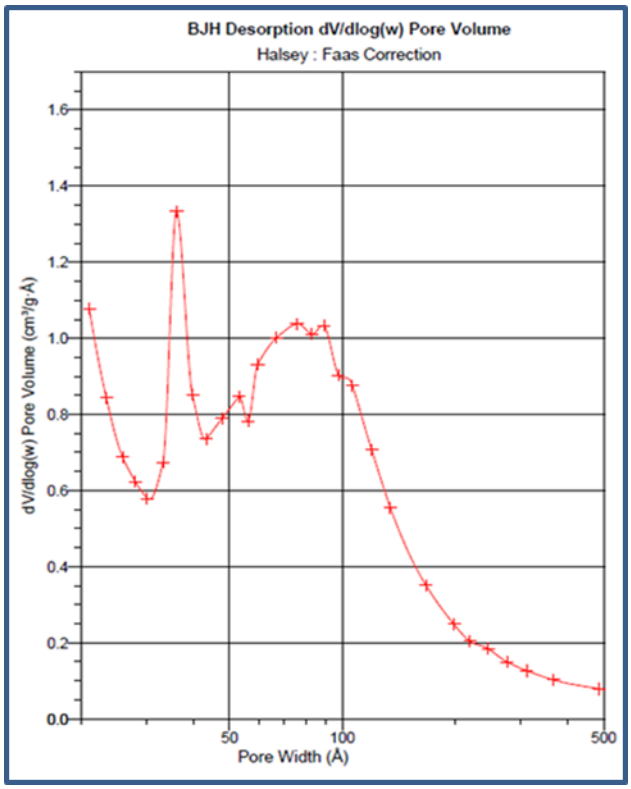

Figure A.4. Pore distribution chart of PAC.

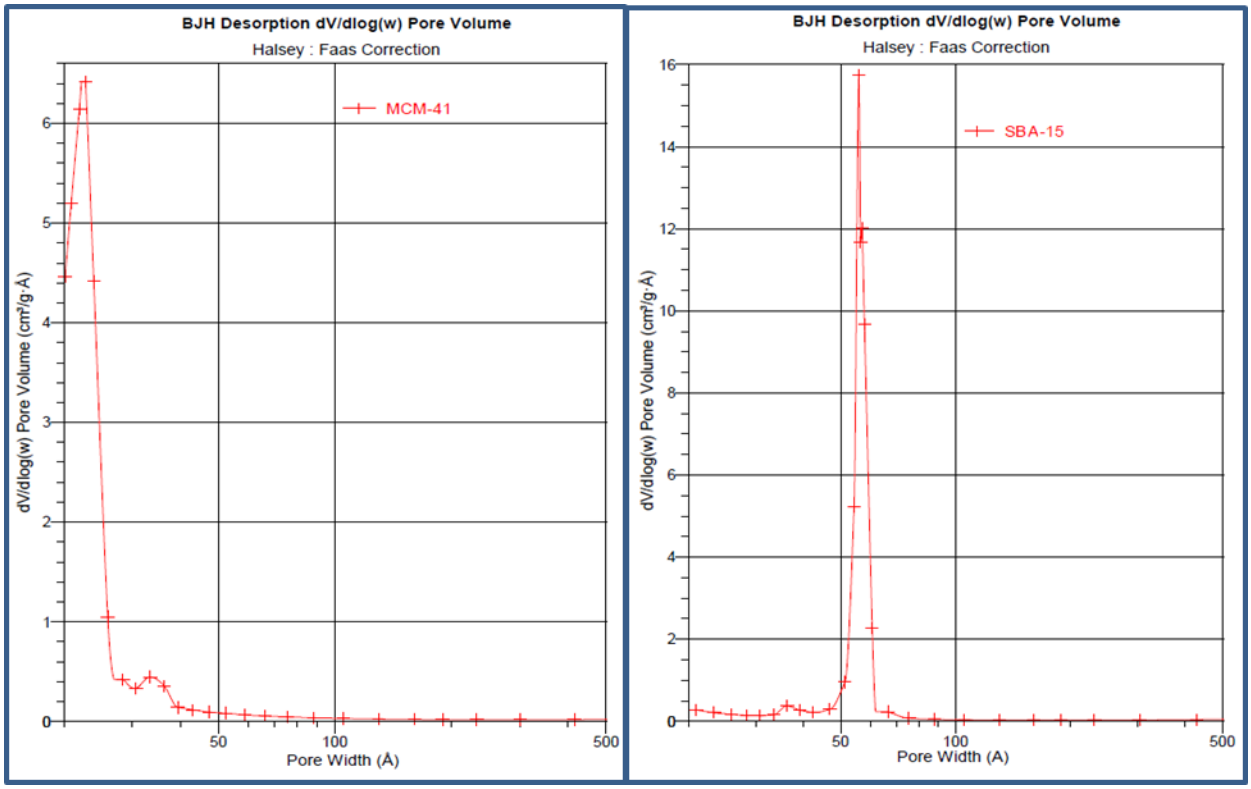

Figure A.5. Pore distribution charts of benchmark materials: MCM-41 and SBA-15.

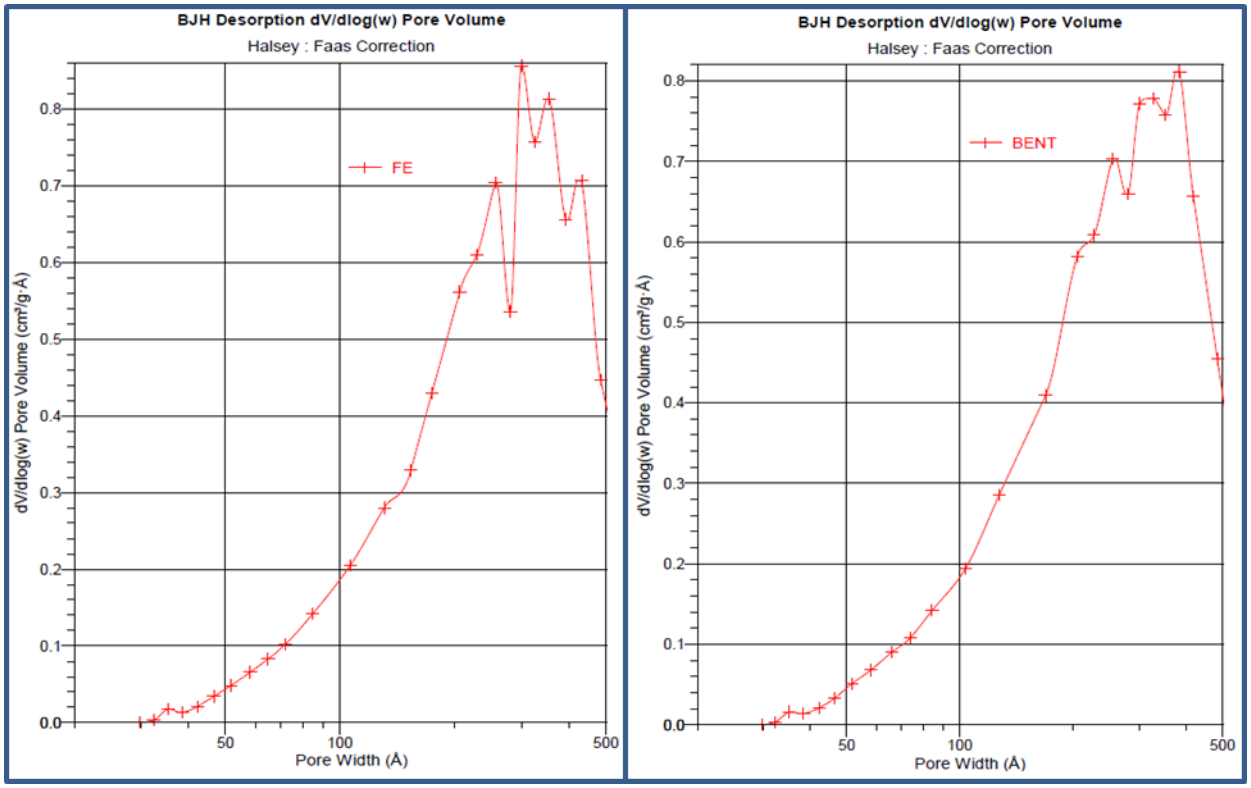

Figure A.6. Pore distribution charts of clays: Fuller's Earth (FE) and Bentonite (BENT).

APPENDIX B. PIPING AND INSTRUMENTATION DIAGRAM OF THE BUILT ADSORPTION / HYDROPROCESSING UNIT

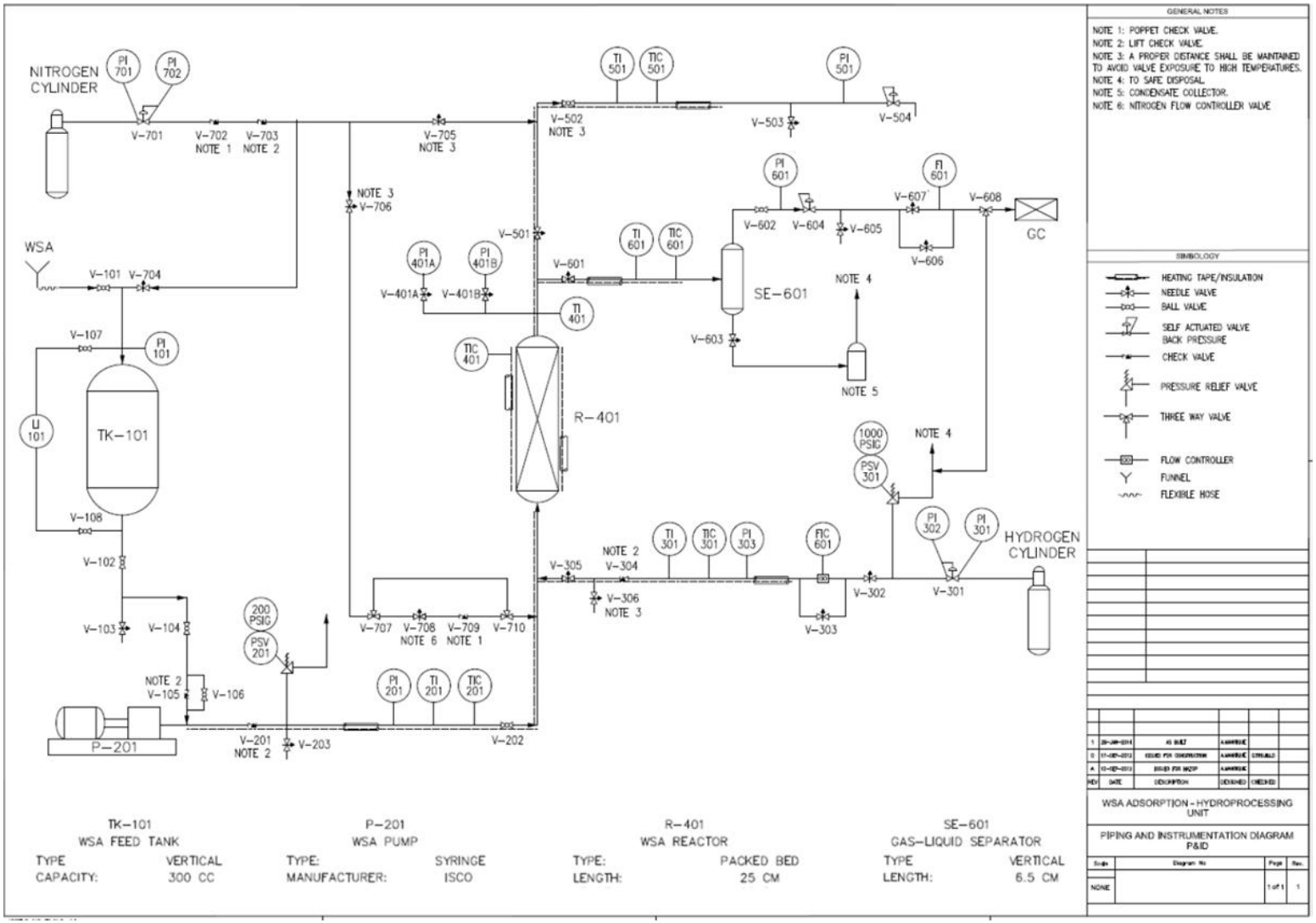

APPENDIX C. HAZOP STUDY

The Hazop study was developed at the University of Calgary on September 12, 2012, in presence of 1 chemist and 6 engineers, 3 with professional experience in oil and gas design. Nodes breakdown is shown in Figure C.1., the risk assessment matrix employed is presented in Figure C.2., and the final report is attached within the next pages of the document.

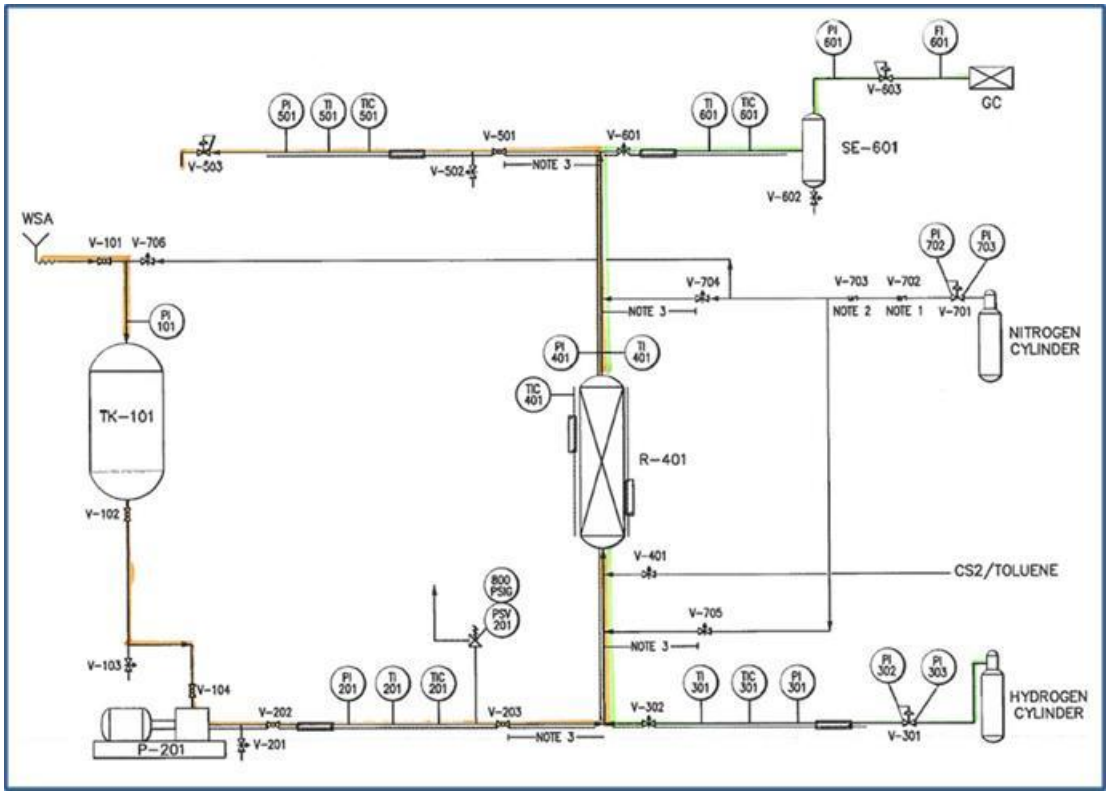

Figure C.1. Piping and instrumentation diagrams for HAZOP. Node 1 in green, Node 2 in orange.

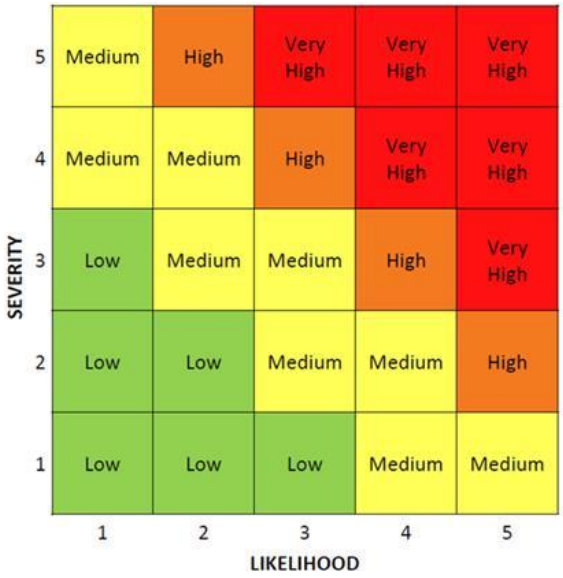

Figure C.2. Risk Assessment matrix for HAZOP study.

HAZOP STUDY					
Date of Analysis:	September 12, 2012	Location:	CCIT 026 UofC	Unit:	
Node/Section:	1	Node Description:	Hydrotreatment column		
P&ID Title:	WSA ADSORPTION - HYDROTREATMENT SMALL UNIT		P&ID No. 1	P&ID Rev	A
Design Intention:	Hydrotreatment: T = 325°C, P = 600 psig Sulfidation: T = 400°C, P= 15 psia				

Guideword	Deviation	Possible Causes	Potential Consequences	Safeguards	S	L	R	Recommendations	Remarks
Flow	Reverse	V-302 left open or failure	Liquids in the hydrogen line, liquid loss	None	1	3	L	Install lift check valve in the cold side of the hydrogen line and a drain valve close to V-302 (make sure to leave enough space to not heat up the drain valve)	Check if flow controller is needed
Flow	High	Not found	Not significant						
Flow	High	Not found	Not significant						
Pressure	High	Wrong operation or failure of V-301	Possible damage in the instrumentation and reactor bed, leaks	PIs along the the plant	2	2	L	Install a PSV on the hydrogen line, lock the regulator.	Put a sign "please don't touch the regulator, experiment in progress"
Pressure	Low	Wrong operation or failure of V-301, run out of gas in the cylinder, V-603/V-602 failure or wrong operation. Leaks.	Coke formation in the reactor. Explosive atmosphere.	PIs along the the plant. Leak test performed before starting experiments.	2	1	L	Lock the regulator. Include in the SOP to check the H_2 cylinder pressure. Register the pressure during the experiments.	Put a sign "please don't touch the regulator, experiment in progress"
Temperature	High	TIC and heating tape failure, wrong operation	Coke formation in the reactor. Equipment damage. Personal injuries.	TIs along the plant. Alarms in the control system. Heating tape, controller test	4	4	H	Install the control system in a PC. Install accesible electric breaker.	

HAZOP STUDY									
Date of Analysis:	September 12, 2012	Location:	CCIT 026 UofC				Unit:		
Node/Section:	1	Node Description:	Hydrotreatment column						
P&ID Title:	WSA ADSORPTION - HYDROTREATMENT SMALL UNIT				P&ID No.	1	P&ID Rev	A	
Design Intention:	Hydrotreatment: T = 325°C, P = 600 psig Sulfidation: T = 400°C, P= 15 psia								

Guideword	Deviation	Possible Causes	Potential Consequences	Safeguards	S	L	R	Recommendations	Remarks
Temperature	Low	TIC and heating tape failure, wrong operation	Not significant						
Level	High	Not found	Not significant						
Level	Low	Not found	Not significant						
Concentration									Not applicable
Electrical Power									Electrical power failure was indirectly analyzed with previous guidewords.

Figure C.3. HAZOP report for Node 1: Hydrogen injection zone, reactor and hydroprocessing products separation section.

HAZOP STUDY					
Date of Analysis:	September 12, 2012	Location: CCIT 026 UofC		Unit:	
Node/Section:	2	Node Description: Adsorption column			
P&ID Title:	WSA ADSORPTION - HYDROTREATMENT SMALL UNIT		P&ID No. 1	P&ID Rev	A
Design Intention:	Adsorption: Room < T < 150°C, 10 psig < P < 50 psig				

Guideword	Deviation	Possible Causes	Potential Consequences	Safeguards	S	L	R	Recommendations	Remarks
Flow	Reverse	V-202 and V-104 left open when P-201 is pumping or failure of V-103	No liquid through reactor, feed tank refilled	None	1	4	L	Install lift check at both suction and discharge. Install recirculation line for bypassing the check at the pump suction	
Flow	High	Wrong operation of pump flow controller	Loss of feedstock and adsorbent	None	2	2	L	Set alarm in pump controller for high flow	Include in SOP the proper operation of suction and discharge valves
Flow	Low	Wrong operation of pump flow controller	Not significant						
Pressure	High	Wrong operation of any valve	Possible damage in the instrumentation, leaks	PSV-201, PIs, pump inherent controller	2	2	L	Change the PSV-201 set point to a lower value. Move PSV-201 upstream V-202.	
Pressure	Low	Wrong operation or fail of any valve, leaks.	Not significant						
Temperature	High	TIC and heating tape failure, wrong operation	Coke formation in the reactor. Plugging by coke formation. Equipment damage. Personal injuries.	TIs along the plant. Alarms in the control system. Heating tape, controller test	4	4	H	Install the control system in a PC. Install accesible electric breaker.	

HAZOP STUDY					
Date of Analysis:	September 12, 2012	Location: CCIT 026 UofC		Unit:	
Node/Section:	2	Node Description: Adsorption column			
P&ID Title:	WSA ADSORPTION - HYDROTREATMENT SMALL UNIT		P&ID No. 1	P&ID Rev	A
Design Intention:	Adsorption: Room < T < 150°C, 10 psig < P < 50 psig				

Guideword	Deviation	Possible Causes	Potential Consequences	Safeguards	S	L	R	Recommendations	Remarks
Temperature	Low	TIC and heating tape failure, wrong operation	Not significant						
Level	High	Not found	Not significant						
Level	Low	Wrong operation of valves at suction / discharge operations	Pump cylinder filled with gas. Not enough feestock for the run and therefore, loss of adsorbent	None	2	2	L	Install a level meter in the feed tank. Include in the SOP a procedure to check if the pump cylinder is totally filled with liquid when discharging, and afterwards, check for sufficient feedstock for the run.	
Concentration									Not applicable
Electrical Power									Electrical power failure was indirectly analyzed with previous guidewords.

Figure C.4. HAZOP report for Node 2: WSA feed zone, reactor and liquids pressurization and sampling section.

University of Calgary *HEALTH, SAFETY AND ENVIRONMENTAL*		
STANDARD OPERATING PROCEDURE FOR: WSA ADSORPTION AND HYDROPROCESSING UNIT	***Issued:***	***Alejandra Manrique***
	Revised:	***G. Trujillo/A. Coy***
	Reviewed:	***1***
	Pages	***17***

1. PURPOSE/BACKGROUND

The WSA Adsorption and Hydroprocessing (AHP) unit was designed and built to evaluate the adsorption of Asphaltenes solubilized in water -Wet Solubilized Asphaltenes, or WSA, followed by hydroprocessing of the adsorbed molecules under a wide range of variables and conditions.

This procedure is written to comply with all of the UofC HS&E regulatory requirements, and to teach new users, the standard operative protocols of the WSA AHP Unit.

2. SCOPE

This procedure is intended for all those workers and/or students/interns working in the Upgrading and Refining laboratory that will be operating the WSA AHP Unit. The procedure covers specifics about starting up of the unit, pressurization, warming up, adsorption procedures, hydroprocessing procedures, shut-down and learning experiences.

3. PRE-REQUISITES AND SAFETY ISSUES

Specific information related to the feed to be processed, catalytic formulation, operational conditions, and test length among others, have to be provided in the experimental plan. Standard machine shop tools are required in case of any repair, change or adjustment in the system.

Successful completion of the University of Calgary generic WHIMS course and H_2S Alive course are mandatory.

Protocol:

- Do not work alone in the laboratory, sign up to the University of Calgary procedures for working alone.
- Be aware of the inherent risks associated to, and the nature of, the processes, materials and chemicals used in the laboratory. This is not limited to the risks and

hazards in one own equipment, but extended to include those of every other person in the laboratory. Please refer to MSDS for all chemical used in the process

- Wear appropriate laboratory personal protective equipment (lab coat, safety glasses, and closed shoes).
- Maintain a neat and organized working environment.
- If leaving an experiment unattended, ensure that an identification tag is placed visible in order to make others aware, including an emergency shutdown protocol to inform how to proceed. Main telephone number as well as experiment responsible is required.
- Dispose of waste in a safe and environmentally friendly manner.

Hazard Identification (Hazardous Chemicals or Processes):

Hazardous chemical products and by-products expected from the system are:

- Nitrogen and hydrogen compressed gases
- Light liquid hydrocarbons
- Hydrocarbon gases
- H_2S in concentrations lower than 100 ppm

Hazardous processes involved:

- Light liquid hydrocarbons and hydrocarbon gases flowing under moderate pressures and temperatures.

Hazard Assessment:

Products:

Hydrogen leaks demand high ventilated environment. Hydroprocessing gaseous products are sweetened in a KOH solution at the outlet stream. Personnel must wear personal protective equipment (PPE) all the time when working in the unit.

Processes:

Heat insulation is used in all process lines under high temperature conditions. Pressure relief devices are located in the hydrogen feed line and the pump outlet line, aiming to protect the system in the case of an overpressure caused by plugging of process line.

Engineering/Ventilation Controls:

The WSA AHP unit was built inside of an enclosure provided with an extraction system, especially designed to suit the needs of the process. All venting lines (release and exhaust gas lines form the unit) are disposed to the extractor.

Personal Protective Equipment:

Personal protective equipment (PPE) required for this SOP includes, but is not limited to:

Nitrile gloves, safety glasses and laboratory coats are standard safety equipment for all employees, students and interns in the lab. Respirators with adequate filters/cartridges when cleaning any oil or emulsion spill from the plant using any type of solvent like toluene, acetone, etc. Quartz fiber gloves are needed for handling high temperature objects.

4. PROCEDURES

4.1 REACTOR PACKING

1. Dry the adsorbent-catalyst to be loaded at least for one day before packing the reactor.
2. Create seals or washers (refer to **Figure**.) using an appropriate mesh size for the adsorbent-catalyst to be used.
3. Place washers at the edges of the reactor and construct the fittings with the washers inside. This procedure guarantees that the fittings will close properly.
4. Weigh the reactor without adsorbent-catalyst but including the washers and the plugs at the bottom and top of the reactor. This value is denoted as *Reactor weight.*
5. Accurately weigh the initial amount of carborundum (or glass beads) required to provide additional support to the packed bed. The quantity of the inert material has to be calculated considering the desired level of inert package, and the bulk density of the material (either carborundum or glass beads). This value is called as *Inert weight*.
6. Place the reactor in a secure location for the adsorbent-catalyst addition, and put the bottom washer at position.
7. Using a funnel, slowly add approximately half of the initial amount of inert at the bottom of the reactor. If glass beads are used, make sure the bigger beads are placed at the bottom and the smaller ones on top. While filling the bed, hammer the reactor wall and stop every 5-10 minutes to allow the material to settle. Add more material after 5 minutes, and repeat until the desired level of inert packing is reached.
8. Using a funnel, slowly add the desired amount of adsorbent-catalyst while hammering the reactor wall. Stop every 5-10 minutes to allow the material to settle. Add more catalyst after 5 minutes, and repeat until all catalyst is placed.
9. Using a funnel, slowly add the remaining inert material at the top of the reactor. If glass beads are used, make sure that smaller beads are placed right on top of the carbon packing, and the bigger ones over the smaller ones. While filling the bed, hammer the reactor wall and stop every 5-10 minutes to allow the material to settle. Add more inert material after 5 minutes, and repeat until the reactor is filled.

10. Carefully put both top washer and plug. Weigh the reactor, and calculate the amount of catalyst by using the following equation:

$$Catalyst\ weight\ (g) = Reactor\ weight\ (g) - Inert\ weight(g)$$

Figure 1. Washers (Mott Porous Metal and Mesh-300 rings).

4.2 GENERAL PROCEDURES

4.2.1 Primary Inspection

1. Verify that the plant is not energized by checking the electrical box light bulb (**Figure 2**). At the beginning of each week or after a long period of time without running, all switches must be turned off.
2. Make sure all valves are closed, except V-401B.
3. Check pressure gauges PI-101/201/303/401B/501 and the pressure indicator in the pump controller, and confirm there is no pressure in the plant. If any of the readings is above 2 psig, carefully open the corresponding drain valve of the pressurized section.
4. Check the nitrogen cylinder pressure gauge PI-701, the reading should be above 550 psig. Adjust the nitrogen regulator V-701 to deliver the desired pressure by reading the gauge PI-702.
5. Check the hydrogen cylinder pressure gauge PI-301, the reading should be above 650 psig. Adjust the hydrogen regulator V-301 to deliver 610 psig downstream by reading the gauge PI-302.
6. Check the gas chromatograph gases cylinders (hydrogen, air, and helium). The cylinders outlet pressure has to be at least 80 psig, 25 psig and 50 psig for hydrogen, air and helium, respectively.
7. Energize the plant by turning on the switch in the power supply box.

4.2.2 Plant depressurization/Drainage

During the operation of the WSA AHP unit, depressurization of some sections of the plant is often required. Instructions for pressure depletion in all sections of the unit are listed below.

Figure 2. Electrical panel and switches turned on.

Depressurization of the Gas-Liquid Separator SE-601 and gas stream section

Maximum operating pressure of the separator was set to 600 psi, hence, special care must be taken when the vessel is going to be drained, or the gas sampling system needs to be depressurized.

1. Align the three way valve V-608 towards the PSV-301 discharge/vent, manipulating the valve handle as indicated in **Figure 3**.
2. Check that V-601, V-603, V-605 and V-607 are closed.
3. Open V-606, and slowly open V-604 to the maximum until PI-601 readings are zero.
4. Close V-606 and align three way valve V-608 to the off position.

Figure 3. Three way valve, a) aligned to gas chromatograph, b) closed, c) aligned to vent.

Depressurization of other sections of the WSA AHP Plant

1. Identify the drain valve to be opened by locating the pressure gauge related to each zone and reading suggestions provided in **Table 1**.
2. Read the temperature of the zone to be drained and place a suitable flask/plastic bottle on the available trays built for this purpose.
3. Carefully, open the needle valve and allow the system to deplete its pressure. This procedure should be carried out slowly.

4. Close the valve once the desired pressure is reached.
5. If needed, inject nitrogen to drag liquids trapped in the unit walls.

Table 1. Pressure gauges and related drain valves

Section	Instrument	Drain valve
WSA Feed tank	PI-101	V-103
Pump discharge/Reactor	PI-201	V-203
Hydrogen Feed	PI-303	V-306
Liquids sampling	PI-501	V-502

4.3 ADSORPTION EXPERIMENTS

4.3.1 Pump loading

1. Follow all instructions described in section 4.2.1 for a primary inspection of the unit.
2. Turn the pump on and check the filling status. If the display and the piston indicator show the cylinder is completely empty, skip to step 9. Otherwise, go to step 3.
3. Place a suitable flask/plastic bottle on the tray below valve V-203. Check that valves V-202 and V-106 are closed.
4. Open V-203, and set the pump controller to a discharge flow of 10 cc/min.
5. Press the “RUN” button in the pump controller and press "STOP” when liquid no longer flows through the valve and the pump indicator show the cylinder is empty.
6. Make sure that V-101, V-107, V-108 and V-103 are closed.
7. Open V-102, V-104 and V-704 to flush the system with nitrogen for a couple of minutes.
8. Close V-704, V-102, V-104 and V-203.
9. Open valve V-101 and insert the funnel tubing to the mark. Open V-107 and V-108.
10. Pour the desired amount of WSA –maximum 300 cc- into the tank TK-101. While filling the tank, check the LI-101 to avoid over-filling and spilling.
11. Once the WSA solution is in the feed tank, remove the funnel and close V-101. Check V-202/V-106 are closed and open valves V-102 and V-104.
12. Pressurize the feed tank to 5 psig by opening V-704. Never exceed 50 psig in the feed tank when V-107 and V-108 are open.
13. In the pump controller, input a recommended suction flow of 10 cc/min. Press the “REFILL” button to start suctioning. Keep track of the tank level by checking LI-101 while loading the pump.
14. Once the liquid is loaded, press “STOP”. Take into account dead volume between the pump cylinder and the tank outlet. Close V-102 and V-104.

15. In case that more than 300 cc must be pumped through the reactor, repeat steps 9 to 14. Don't forget the pump cylinder capacity is 0.5 L.
16. Drain the pump discharge line for mass balance purposes and write down the loaded volume in the pump.

4.3.2 Continuous adsorption operation

1. Once the pump is loaded, check that V-106, V-202 and V-203 are closed.
2. Read pressures in the pump display and in the gauge PI-201 and ensure that the system is not pressurized in this zone.
3. Open V-401A for more accurate pressure readings, however, V-401B could be left open or closed.
4. Open V-501, V-502, and V-504. Check **Table 2** for recommended pressures relative to the operating temperature.

Table 2. Minimum recommended pressure values for different adsorption test temperatures

Temperature	Minimum recommended pressures
60-70 °C	5 psig
80 °C	10 psig
90 °C	20 psig
100 °C	35 psig
120 °C	50 psig

5. Slowly open V-705 and pressurize the system to the desire value by checking the pressure gauges PI-501 and PI-401A/B and by manipulating V-504.
6. Close V-705, open V-202 and corroborate the desired pressure in the instrument PI-201 and the pump display. Allow some time for stabilization.
7. Place a proper flask/vial for collecting the liquid samplings on the tray below V-503.
8. Open the temperature controller software by clicking the icon shown in **Figure 4**.
9. Click the "Run" button to access the main menu window. Hit "Set setpoints", disable Channel 1 by clicking the "1" button and check if the "Set Point" and "Temperature" fields are shaded.
10. Write in channels 2, 4 and 5 the desired temperature for the adsorption test, taking into consideration the ramps recommended in **Table 3**. Once the set points are defined, click on "Load Change" and "Return/Run" to update the changes and view the main menu window (**Figure 5**).
11. Wait until the temperature is stable by checking the local temperature indicators TI-201, TI-401 and TI-501.

12. In the pump controller, configure the pump discharge to the desired flow rate. Before hitting “RUN”, make sure V-106 is closed and valves V-202/V-501/V502 are open.
13. Click “RUN” and stay alert for drastic changes in pressure or temperature. If temperature is going too high/too low, modify the input parameters using the temperature controller software. If pressure is rapidly increasing, manipulate V-504 to stabilize the unit. Record temperature profiles and times as required.

Table 3. Recommended heating ramps

Temperature Range [˚C]	Recommended Heating Ramp
0 – 80 (adsorption runs)	20 °C / 4 min
80 – 120 (adsorption runs)	10 °C / 4 min
0 – 320 (hydroprocessing runs)	20 °C / 4 min
320 – 400	10 °C / 4 min

Figure 4. Temperature controller icon as shown in the WSA AHP laptop.

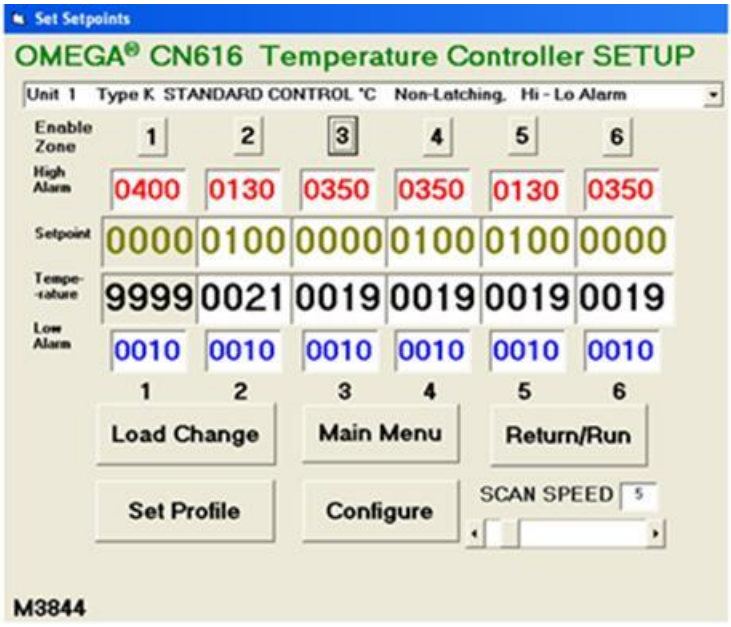

Figure 5. Set points input for adsorption experiments at 100°C

4.3.3 Adsorption shut down

1. After all liquid is pumped, or a determined volume is collected, press “STOP” in the pump controller.
2. Cool down the unit by following steps 10 and 11 described in section 4.3.2. Check temperature indicators located in the pump discharge (TI-201), reactor (TI-401) liquids sampling line (TI-501).
3. Depressurize the unit as indicated in section 4.2.2.
4. Align V-707 and V-710 to bypass valves V-708 and V-709 (refer to **Figure 6a**).
5. Open V-501, V-502 and V-706. Slowly open V-503 and collect any liquid trapped in the reactor. Let the system purge with nitrogen for about 5 minutes. Close V-706 and then V-502.
6. Open V-202 and check that valves V-104, V-106 and V-502 remain closed. Open V-705 and slowly, open V-203 to collect any liquid trapped in the reactor or connecting lines. Let the system purge with nitrogen for about 5 minutes. Close V-705 and then, V-202, V-203 and V-501.

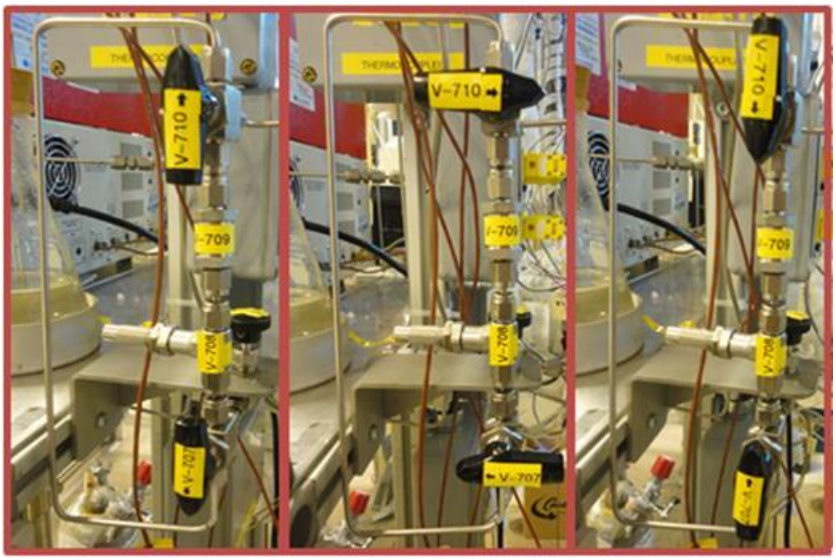

Figure 6. Three way valves V-707 and V-710, a) aligned to system pressurization, b) closed, c) aligned to hydroprocessing flow control.

4.4 ADSORPTION EXPERIMENTS

Prior to commencing hydroprocessing reactions, it is fundamental to ensure that the Gas Chromatograph -GC- is calibrated for the expected gases and its readings are within desired accuracy. A gas standard must be measured before each test and if required, V-708 (nitrogen flow controller valve) must be set to the desired value.

This procedure is conceived under the premise that WSA adsorption has already taken place and that after shut down, all valves are closed (except V-401B), the unit is depressurized, lines have been properly drained and the system is at room temperature.

Additionally, the user must calibrate the mass flow controller (FIC-601) taking into account that the instrument needs a minimum pressure gradient of 50 psig between the inlet pressure (provided by the hydrogen cylinder) and the outlet pressure (reactor pressure). In order to do so, choose an inlet pressure that is at least 50 psig above the desired operating pressure. Then, calibrate the mass flow controller with this pressure drop and for posterior hydroprocessing experiments, remember to use the same pressure drop as the one established for calibration.

4.4.1 Hydroprocessing continuous operation

1. Follow the procedure for primary inspection described in section 4.2.1.
2. Adjust V-301 to deliver a maximum of 600 psig.
3. Check that valves V-202, V-302, V-306, V-401A, V-501 and V-603 are closed. Then, open V-303, V-305, V-601, V-602 and V-604.
4. Align V-608 to the vent (refer to **Figure 3c**) and bypass the flow meter FI-601 by opening V-606 and closing V-607
5. Slowly open V-302 to inject hydrogen to the system and manipulate V-604 to set the back pressure to the chosen value, utilizing PI-601 and PI-401B as guides.
6. Close V-303 and V-302. Adjust the hydrogen regulator valve to deliver the required controller inlet pressure, according to the instrument calibration previously performed.
7. Close V-606 and open V-607. Align V-608 to the GC as shown in **Figure 3a**.
8. Turn the mass flow controller FIC-601 on and set the flow rate to the desired value. Open V-302 and allow stabilizing for 10 minutes.
9. Turn the local flow indicator FI-601 on and open the flow meter software in the main computer. Create a new log file and flow measurements will be directly recorded in the computer.
10. Open the temperature controller software by clicking the icon shown in **Figure 4**.
11. Click the “Run” button to access the main menu window. Hit “Set setpoints”, disable Channel 1 by clicking the “1” button and check if the “Set Point” and “Temperature” fields are shaded.
12. Setup the desired hydroprocessing test temperatures in channels 3, 4 and 6, taking into consideration recommended ramps (**Table 3)**. Once the set points are defined, click on “Load Change” and “Return/Run” to update the changes and view the main menu window (**Figure 5**).
13. Wait until the temperature is stable by checking the local temperature indicators TI-301, TI-401 and TI-601.
14. Inject gas samples in the GC periodically and record temperature, pressure and mass flow controller flow rates.

4.4.2 Hydroprocessing shut down

1. Turn the mass flow controller off and close V-302.
2. Cool down the unit by following steps 11 and 12 described in section 4.4.1.
3. Close V-305 and V-601. Remove the lid of the condensate collector and place a suitable flask to drain the liquids accumulated in the separator SE-601.
4. Using appropriate respirator masks and gloves, carefully open V-603 until no liquids flow through the valve.
7. Close V-603. Put the lid back on the condensate collector and open V-601.
8. Depressurize the gas stream section and separator as indicated in section 4.2.2. Both PI-601 and PI-401B must display 0 psig.
9. Open V-605 and collect any condensates accumulated in the trap. Close V-605.
10. Check that V-305 is close and depressurize the hydrogen injection lines by opening V-306 until no pressure is seen in PI-303.
11. Check that V-601 is open and close V-602. Remove the lid from the condensate collector and place a suitable flask under V-603.
12. Align V-707 and V-710 to bypass valves V-708 and V-709 (refer to **Figure 6a**).
13. Open V-706. Slowly open V-603 and collect any liquids trapped in the reactor. Let the system purge with nitrogen for about 5 minutes. Close V-706 and then, V-603.
14. Put the lid back on the condensate collector and close V-601

4.5 EMERGENCY SHUT DOWN

If any emergency situation is presented and immediate shut down is required, follow the next procedure:

1. Turn off the pump pressing the turn off button, and set all unit temperatures to 0.
2. Turn off the breakers of the electrical box (Figure 1). It will de-energize all heating tapes.
3. Pull down the power supply switch located next to the hydrogen cylinder. This will shut down the entire enclosure.

5. ROLES AND RESPONSIBILITIES

Key Personnel
Main operator and responsible of the system: Alejandra Manrique – 403-210-9587
Alternate operators: Luis Coy–403-210-9781

6. TRAINING

It is recommended that any person operating the WSA Adsorption-and Hydroprocessing Unit is educated or pursuing studies in the area of chemical or petroleum engineering and/or chemistry.

Any new operator of the WSA AHP Unit has to follow an operational training conducted by either the main operator or alternate operator. The operational training would be no shorter than three whole experimental runs which include previous preparation of the unit, adsorption experiments, hydroprocessing experiments, mass balances and shutting down of the plant.

As per the pre-requisites of entering the lab, The Upgrading and Refining Lab Generic WHIMS and H_2S alive course must be successfully completed.

7. MONITORING REQUIREMENTS

Not applicable

8. RECORD MANAGEMENT

Each SOP shall be reviewed within 12 months of the date of issuance or date of last review to ensure the SOP is up-to-date.
This first SOP for the WSA AHP unit, including only the methodology for adsorption experiments, has been submitted on January 29, 2013

9. REFERENCES

Not applicable.

10. DEFINITIONS

Other abbreviations as stated in the SOP.

11. EMERGENCY

Contact 911
University Emergency: 403 220-5333
Immediately supervisors: Luis Alejandro Coy 403-210-9781
Principal Investigator: Dr. Pedro Pereira-Almao 403-220-4799

12. UNIVERSITY NOTIFICATION

Indicate if there are any concerns that EH&S should be made aware of prior to the start of a particularly hazardous protocol, such as a disruption to a water source, loss of power, loss of gas detection systems etc.

Signed:_____ Date:_____

Principal Investigator/Manager Signature